# Different functions played by centrosomal protein CEP135 and centriolar satellite proteins SSX2IP and WDR8

**Dissertation**

zur

Erlangung des Doktorgrades (Dr. rer. nat)

der

Mathematisch-Naturwissenschaftlichen Fakultät

der

Rheinischen Friedrich-Wilhelms-Universität Bonn

vorgelegt von

**Zhenzhen Chu**

aus

Shandong, P.R. China

Bonn ( December 2021)

Angefertigt mit Genehmigung der Mathematisch-Naturwissenschaftlichen Fakultät der Rheinischen Friedrich-Wilhelms-Universität Bonn

1.Gutachter: Oliver Gruss

2.Gutachter: Walter Witke

Tag der Promotion: 10.03.2022

Erscheinungsjahr: 2022

## Summary

The centrosome of animal cells is a crucial organelle that regulates cell division, cell migration, ciliogenesis, intracellular transportation and polar determination with microtubule organizing center as its primary function. Misfunction of centrosome associated proteins can lead to ciliopathies, microcephalies and cancers. In recent years, novel proteins which locate within or surrounding the centrosomes have been discovered every year. The detailed roles of these proteins and how they contribute to centrosome functions are, however, often still unclear. Our lab previously discovered two centriolar satellite proteins WDR8 and SSX2IP, that can interact with each other as well as with the centrosomal protein CEP135. The dependency and inter-regulations of these three proteins and how much they can affect cell division and ciliogenesis are not fully understood. Therefore, my project aims at further understanding their interactions and functions in performing the centrosomes' duties.

Previously, WDR8 and SSX2IP were shown to be the centriolar satellite proteins that facilitate the targeting of ciliary membrane versicles to the basal body. ssx2ip depletion affects bipolar spindle formation in *Xenopus* egg extract. Moreover, maternal Wdr8 is very important for early embryonic development in Medaka fish.

To achieve my aim, I firstly checked their presence and interaction in *Xenopus* oocytes and eggs. I exploited the large amount of proteins accumulated in eggs to survey the interctome of wdr8 using immunoprecipitation and observed a tight interaction of cep135, wdr8 and ssx2ip. I also show different subpopulations of cep135 by immunoprecipitation in *Xenopus* with different cep135 antibodies. I further demonstrate that ssx2ip' expression level is slowly increased during oocyte growth and maturation and that cep135 only expresses after egg maturation. Both ssx2ip and cep135's expression in oocytes and eggs are under the regulation of CPEB. Consistent with previous results on ssx2ip, cep135 depletion also affected bipolar spindle formation in *Xenopus* egg extract.

Secondly, I checked the functions of SSX2IP, CEP135 and WDR8 in human somatic cells. I generated CRISPR knockouts using human RPE-1 cells. While *wdr8* and *ssx2ip* knockout cells show growth abnormalities, *cep135* knockout proliferated normally although none of

the knockouts of did show any defects in cell division and ciliogenesis. The protein expression and centrosomal localizations of SSX2IP and WDR8 are dependent on each other and on CEP135. However, Cep135's centrosomal localization is not affected in *wdr8* and *ssx2ip* knockout cells. Importantly, *cep135* knockout cells show premature centrosome splitting.

Thirdly, I further analyzed premature centrosome splitting caused by the loss of CEP135. Premature centrosome splitting in *cep135* knockout cells is associated with diminished pericentriolar material as exemplified by reduced levels of γ-tubulin and CDK5RAP2. The imbalanced distribution of CDK5RAP2 between mother and daughter centrioles showed that splitting happens without the completion of centriole to centrosome conversion. The different aster patterns formed in a MT regrowth assay in *cep135* knockout cells showed a diminishment and scattering of pericentriolar material. Lastly, I provide evidence for regulation of satellite proteins and centrosomal proteins by phase separation.

In conclusion, I further explored the functions of CEP135, WDR8 and SSX2IP. Loss of satellite proteins WDR8 or SSX2IP affected their interacting proteins but centrosome's functions were not obviously compromised. Cep135, in turn, turned out to have a very important and uncompensated role in maintaining stable organization of interphase PCM.

Table of Contents

# 1 Introduction

The basic knowledge of science is important, however, the way science develops is also crucial, especially for cultivating scientific thinking. In here, I give this introduction in three chapters: chapter one focuses on the milestones of historic exploration and how scientists form the ideas based on their limited tools (from the discovery of microscope to 20th century); chapter two describes recent progresses; chapter three focuses mainly about the proteins I interested: CEP135, WDR8 and SSX2IP.

## 1.1 From the historical timeline to view great discoveries in cell division and cilia areas

**The science world before cells were discovered** 1.9 million years ago, six thousand years after they stood erect, Homo ergaster learned how to use fire. From 5800 BC to 2500 BC, the ancient empire countries were established. The culture of human being is on the stage ever after. Human beings are intellectual species that could observe and conclude their life and explore the intrinsic rules and invented theories. The prototypes of medicine, mathematics, chemistry, astronomy, construction, alchemy and water conservancy appeared. This knowledge communicated and promoted each other, ancient Greece was the hot spot then. The ideas dating back then still effect today's world, e.g. that the world is made up of atoms. From 14 AC to 16 AC, Europe went through the Renaissance Period, accelerating the development of science. The modern science revolution lifted its curtain as Nicolaus Copernicus published his *De Revolutionibus Orbium Coelestium* in 1543. From this time point on, only around five hundred years passed, however, the world (appearance and civilization) has experienced an enormous change comparing to the one accumulated through five thousand years before science explosion. Although China has a five thousand years' history, it lags behind in modern science development. To catch up with leading countries in modern science, the People's Republic of China directly civilized its citizens with knowledge diverted from western world. As a result, the bond is weaken between Chinese and Chinese culture. Lots of people feel lost with the abrupt interruption between ancient and modern China and cannot relate to the process of science explosion. Luckily, I have the opportunity to study in Germany to feel the cultural and scientific atmosphere which promotes the formation of modern science.

**The birth of microscope and the naming of "cell"** As people knew more about light, refraction and reflection, in 1590, Hans Janssen and his son invented the first compound microscope with two convex lenses. Microscopes were soon popular in medicine and scientific laboratory (Hajdu, 2002). In 1664, Robert Hooke (1635–1702), with the compound microscope, observed the dead cell wall of the plant cells (cork) and gave the structure a name as "cell". Antonie von Leeuwenhoek (1632-1723), inspired by Robert's book *Micrographia*, began to hand craft lenses and constructed some simple microscopes, which had a higher magnification than Robert Hooke's compound microscope. Leeuwenhoek's observation was ahead of his peers in many aspects: seeds, nerves, muscles, bacteria, sperm and ciliated protozoa (J. Hardy, 2016). With the invention of the light microscope, many scientists were looking into the world around them with a much higher resolution than the naked eyes.

**The Cell Theory** Although the cell was known already (1600s), its underlying dogma - The Cell Theory - was concluded only two centuries later (1800s) (Mazzarello, 1999). It was the invention of achromatic lenses (1823) that gave scientists the ability to see structures of ca. 1μm and to see the real scenario inside a cell. In 1831, the Scottish botanist Robert Brown (1773-1858) discovered and named the nucleus and proposed that the nucleus is an essential component of a cell. With the development of achromatic microscopes, the nucleus was found basically in all kinds of tissues, giving the hints that cells may be the unit of all living organisms. In 1838, the botanist Matthias Jakob Schleiden (1804-1881) and zoologist Theodor Schwann (1810-1882) concluded separately that all plants and animals are made of cells. In Schwann's words, "the tissues of animals are formed of cells. The globules of lymph, pus and mucus are cells with their walls distinct and isolated from each other. Horny (squamous) tissues are cells with distinct walls, but united into coherent tissues; bone and cartilage are formed of cells whose walls have coalesced; fibrous tissue and tendon are cells which have split into fibers; and muscle, nerves and capillary vessels are cells of which both the walls and cavities have coalesced" (Schwann, 1993). For life continuity, Aristotelian's spontaneous generation was still dominating the world then: everything was composed of water, air, fire and earth with variant ratios. Although Schleiden disagreed with the "spontaneous generation", he thought the cell was generated by an intracellular substance, by enlargement to become a new cell. Soon, in 1858, Rudolf Virchow (1817-1905) influenced by Robert Remark, found that cells are formed through scission of pre-existing cells (Wilson, 1947). As a result, the fact that all new cells come from the pre-existing cells

became a very important part of the Cell Theory. During these discoveries, the neuronal system was an exception. The Golgi staining made the neuron structure visible, however, it was until the appliances of electron microscopy (1950s), which could recognize the synapses between neurons, the Cell Theory finally dominated the whole scientific world (Glickstein, 2006).

**Science acceleration in the 19th century** Soon after Virchow brought up the idea that cells come from pre-existing cells, in 1859, Charles Darwin (1809-1882) concluded the origin of species in his book *On the Origin of the Species by Means of Natural Selection*. In 1860 Louis Pasteur (1822-1895) proved that non-living material cannot give rise to life. Lister (1827-1912) developed the aseptic surgery. At this time, Mendel already started his garden pea breeding experiments. Not only biology went through a prosperous period, physics and chemistry also made big leaps. The law of conservation of energy (1840s) and the periodic table (1860s) set the basic line of natural science. Researches about light and electricity were progressing.

**The sample-preparing skills of microscope in the late 19th century** After the microscope was invented for more than 200 years, the way of samples preparation also improved. In 1840s, the standard procedures with standard-sized slides, thin coverslips and mounting balsam appeared, which was as important as the development of the microscope itself. However, none of the sample was stained. The scientists tried to make the slice as thin as possible to make it transparent for visualization. Different kinds of microtomes were invented. Some preservative liquids such as formaldehyde were used as fixative in 1892. In 1889, dry freezing was introduced by Altmann to harden the objects. At that time, the microscope, although without aberration, did not have the ability to generate contrast. Therefore, many people were trying every stain they could get from natural plants and the textile industry. Some dyes could also be used as medicine. In 1770, Hill first used cochineal as a stain. In 1867, heamatoxylin was becoming popular. In 1884, Gram published his staining method to distinguish between different bacteria. In 1876, Wissowzyky introduced the still-in-use haematoxylin and eosin stain combination. In 1886, Golgi developed the silver Golgi staining, promoting the discovery of the neural system. (For more details, see Brian Bracegirdle's review (Bracegirdle, 1989)).

**Chromatin, mitosis and centrosome** After unmasking of The Cell Theory, the development of synthetic stain made the transparent cell sample more visible. The high

numerical aperture condenser (1875) and oil immersion lenses (1878) gave the microscope a resolution of around 0.2 μm, increasing the ability for observing tiny cellular structures (Mazzarello, 1999). In 1835, Remak recognized the appearance and disappearance of the nucleus during cell division and the concept of direct binary fission was brought up. In 1866, Haeckel suggested that nucleus maybe responsible for heredity.

In 1872, Walther Flemming (1843-1905) began his study on cell division. Through observing the wounds and scars, he confirmed that tissue growth was achieved by increasing the cell number (cell division). Flemming used the acid aniline to stain the basic material in the nucleus, which was much clearer than any other stains at that time. With fire salamanders and sea urchins he made lots of critical discoveries with the acid fixation and adapted basophilic staining. He named chromatin because of its easy-to-dye character. In 1882, Flemming named somatic cell division as "mitosis" and also its different stages as "prophase, metaphase and anaphase" and published lots of beautiful drawings of progressing mitosis. The spindle-shaped structure, symmetrically arranged at the two sides of nuclear threads and will be departed evenly to two daughter cells, is referred to bipolar spindle. According to Flemming, mitosis referred to "nuclear threads", which formed in the nucleus in prophase (Paweletz, 2001). With chromatic aberrations, Flemming failed to prove that chromatin in intephase is the same thing of nuclear threads in metaphase.

The research of cell division achieved great improvements with Theodor Boveri (1862-1915). In 1887, just two years after he switched from nerve fibers to cell division, this young postdoc made lots of important discoveries. He found there is a structure located at the spindle pole which is not described by Flemming. Boveri named this structure in different destain stages as "centrosome" and "centriole" by checking the cell division of early embryos of the nematode *Ascaris megalocephala* (Scheer, 2014). He found that the centrosome was not a transient object which can only form in cell division but that it was a permanent organelle which can replicate, handling to next offspring. He predicted that the centrosome has an important function in cell division. After Flemming, researchers were trying to figure out the relationship between chromatin and the "chromatic element" as Boveri called it. In 1888, considering the importance of this chromatic body, Wilhelm Waldeyer named it as "chromosome". Boveri observed the continuity of chromatin and chromosome by the existence of chromosome territories both in interphase and metaphase (Cremer & Cremer, 2010). Later on, in 1909, Boveri proved the individuality of the

chromosome in the nucleus. He used di-spermic eggs of sea urchins to see tripolar or tetrapolar spindles of the embryo of *pluteus* larva. With multipolar spindle and asymmetric chromosome separation, he observed one with exactly one-third lack of skeleton in its body, proving each chromosome bearing different traits (Baltzer, 1964). With the rediscovery of Mendel's experiments in 1902, Boveri and Walter Sutton (1877-1916), separately and simultaneously proposed that chromosomes are the hereditary factor in accordance with Mendel's Law, knowing as Boveri-Sutton Chromosome Theory. Except these, Boveri also recognized the diminution of chromosome in gametes, the inequality of cytoplasm in fertilization and the loss of centrosomes in gamete formation. In 1905, "meiosis" was introduced by J.B. Farmer and J.E.S. Moore.

People interested in this area tended to divide into two branches. One was focusing on chromosome condensation, structure and the heredity mechanism. The other was focusing on whole events happening during cell division (nuclear envelope disappearance, spindle formation, chromosome segregation and centrosome's functions).

**The journey to double helix chromosome** The first person to discover nucleic acid (nuclein) was Friedrich Miescher (1844-1895). In 1869, with the leukocytes from fresh bandages, after isolating the nuclei, he found there was flocculent precipitate after he added acid to it. Upon re-addition of alkaline, the precipitate dissolved. This precipitation was different from protein and lipid - high level of phosphorus, no sulphur, resistance to protease digestion - resulting in the naming "nuclein" by Miescher or "nucleic acid" by Altman Richard (Dahm, 2008). In 1909, Wilhelm Johannsen, a Danish biologist, proposed the basic terminology for genetics: the gene was the particulate unit of heredity; genotypes were defined as genetic constitution of an organism; and the phenotypes were an organism's inherited characteristics. In 1910, Thomas Hunt Morgan (1866-1945) established the chromosomal theory of heredity. He proved that the genes which control traits, located on chromosome, and he also developed a method to measure the distance between two genes. In 1927, Hermann J. Muller (1890-1967) demonstrated that X rays can induce mutations in Drosophila, further proving the relationship between gene, genotype and phenotype. Griffith's Transformation Experiment (1928) and Avery, MacLeod and McCarty's Experiment (1944) proved the DNA was the genetic material. In 1952, Rosalind Franklin got the X-ray diffraction image of the DNA. James Watson and Francis Crick (1953) built the model of the double helix. The Genetic central dogma formed in 1958. The protein

codons were deciphered in 1965. Sanger developed the dideoxyribonucleotide chain termination method for DNA sequencing in 1977. The polymerase chain reaction was established in 1983.

**The cell culture methods** In 1907, Harrison established a cell culture method in a hanging drop for maintaining frog embryo nerve fibers in vitro. Harrison's method, although adapted from microbiological techniques (invented by Robert Koch in the 1880s), was contaminated by bacteria. Then he introduced the aseptic methods. In 1916, Rous and Jones worked out trypsinization and subculture methods. In 1962, Richard G. Ham and Theodore T. Puck developed colonial growth of single mammalian cells, facilitating genetic experiments in cell culture (Puck, 1962). Animal cell culture became a common technique in the 1970s (Jedrzejczak-Silicka, 2017).

**Doubts on the existence of the spindle** Although Flemming's drawing had shown the existence of spindles, Spindle fibers were questionable then since they were only seen in fixed cells. And fixatives were known could cause the formation of asters-like structure in egg white and gelatin solution (1899). Observation of spindles in live cell in diatoms was achieved in 1896 and the microneedle manipulation of spindle was shown in eggs in 1917. In 1935, phase contrast microscopy invented by Zernike made the colorless structure more visible. More living spindles were observed by scientists. When the birefringent phenomena and polarized microscopy were discovered in physics, many biologists also used this in Biology with the strong birefringent material such as hair, muscle and neuron. Others also tested it on weak birefringent material, such as fixed mitotic eggs slides and cultured cells (A. Huges, 1948; Schmidt, 1939). They pointed out that in the egg of sea Urchins, chromosomes and the spindle are all birefringent (Fig. 1A). With the clear image of a spindle both in animal and plant species and the manipulation with micro needles, no one cast any doubts about the existence of spindle fibers any more. Shinya Inoué made lots observations of cell division in plant and animals with polarized light microscope. The dynamic change of the spindle during cell division was thoroughly recorded by the changes of birefringence in different conditions: low temperature, colchicine and alkaloid treatment (Inoué, 1953). Inoue proposed that the spindle fibers can generate force to move chromosome to two opposite poles.

**Electron microscopopy and microtubules, dynein and the kinetochore** The flagellum

was observed more than 300 years ago by Leuweenhoek in protemoazoen and sperm. Motile multicilia were then found in special organs, such as the respiratory tract, middle ear and lungs. The motile cilia and flagella always caught people's attentions. With the invention of electron microscopopy and glutaraldehyde (1963) fixative, the cytoplasmic microtubules (Fig. 1B) were seen, the fine structure of the cytoskeleton confirmed, the fine structure of the axoneme in flagella was observed. Ledbetter and Porter unified the structures of neuron axones, mitotic spindles, interphase filaments, cilia and flagella, naming it as " microtubule" (MT) (Ledbetter & Porter, 1963; Wells, 2005). They found most MTs compose of 13 filaments, but may change from 11 to 15 according different organisms and experimental conditions of assembly.

Flagella are composed of nine outer MT doublets, one center MT doublet and linking arms. Large observations were made on the axoneme with electron microscope. Gibbson confirmed the outer and inner arms of the doublet MT in flagella axonemes, suggesting a sliding mechanism for movement, which was inspired by the striated muscle system. However, the molecular components of the axoneme remained unknown. After axonemes were been successfully isolated (Watson & Hopkins, 1962), its arm was found has the ATPase activity. Gibbson improved the axoneme isolation methods with digitonin and $MgSO_4$ buffer to remove the ciliary membrane. Then he dialysed the demembranated axonemes in low-salt buffer without magnesium, which could dissolve the axoneme arm part that was responsible for ATPase activity, leaving the doublet structure untouched. The 30S peak protein confirmed by sucrose gradient sedimentation was the native whole axoneme arm protein, which could be disassociated to 4S and 14S (Gibbons, 2012). This axoneme arm protein complex was coined as "dynein". Cytoplasmic dynein, which was discovered in 1987, has multiple roles: transportation of cargo in the cytoplasm, maintaining centrosome integrity and spindle assembly (Paschal, Shpetner, & Vallee, 1987). Another motor protein was discovered in 1985 (Brady T, 1985). To find how the signal transmitted in neurons, Vale and his colleagues found the soluble protein Kinesin from AMP-PNP stabilized MT interactors in axoplasm of squid, which could move purified MT on coverslips.

The powerful electron microscope also promoted the discovery of the kinetochore in 1965 (Luykx, 1965). However, the first protein characterized in kinetochores was found only in 1984. Naomi Rothfield and his colleague took advantages of sera from scleroderma spectrum patients to get a staining of speckles in the interphase nucleus and the kinetochore in mitotic phase. Affinity purification displayed three proteins with molecular weight of 17,

80 and 140kDa (Earnshaw & Rothfield, 1985). A German scientist also recognized Cenp A from the autoimmune serum of scleroderma patients, publishing a little bit earlier than Rothfield (Guldner, Lakomek, & Bautz, 1984).

**Isolation of the spindle** The labile spindle apparatus (MA) is more difficult to isolate than the stable flagellum, cilium and neuron axon. In 1905, Foot used dissecting microscope to prick eggs in the ovaries of *Allolobophora fatide*, allowing the cytoplasm, as well as spindle, to come out of the eggs. The materials were so quickly dried that they could be well preserved after fixation (Foot & Strobell, 1905). In 1950, a large scale spindle preparation method was discovered with the sea urchins eggs stored in 30% cold ethanol to stabilize the metaphase status. The free spindles could be obtained either by mechanical way using a syringe to pass through or with detergent (H202, Iodine and ferricyanide) to dissolve the surrounding membranes. Then the mitotic apparatus was collected by centrifugation (Mazia, Chaffee, & Iverson, 1961). However, the spindle isolated could not perform the nuclear division process. With a new buffer containing 1M sucrose, 0.001M EDTA and 0.15M dithiogiglycol, MA could be more easily gained, washed and collected. The MA was confirmed to contain ATPase activity (Mazia et al., 1961). R. E. Kane found that chemicals did not have specific stabilization effect to spindles, just normal effects to all the proteins and what mattered was the pH and solvent concentration (KANE, 1965). The importance of the calcium concentration was discovered by Inoue, Salmon and Jenkins and Weisenberg around 1978.

**Tubulin** The anti-mitotic chemical colchicine had been studied in cells and tissues since 1950s. Colchicine could block cell division by some unknown mechanisms. When the mitotic apparatus was isolated, many scientists wanted to know what were the components of this complicated structure. Gary Borisy, with radiolabelled colchicine, found that this chemical could binds to the isolated mitotic apparatus of egg and egg extract (Borisy & Taylor, 1967a, 1967b). At that time, colchicine was thought to only affect spindles in dividing cell, so researchers uses brain material as a negative control. Much to their surprise, the brain had a high enriched colchicine binding protein, as well as sperm tail (Shelanski & Taylor, 1967; Weisenberg, Borisy, & Taylor, 1968). Mohri gave this colchicine binding protein the widely used name - “tubulin” (Mohri, 1968). The 6S sub-unit of MT discovered by Taylor could bind GTP (Weisenberg et al., 1968) and it containes two different

proteins (α- and a β-tubulin) with 1:1 ratio (Fine, 1971). Different modifications on tubulin were also found (ARCE, RODRIGUEZ, BARRA, & CAPUTTO, 1975).

Weisenberg's DEAE-Sephadex column method of MT purification was improved by using the polymerization and depolymerization nature of tubulin, a protocol that is still in use (Shelanski, Gaskin, & Cantor, 1973). Weisenberg also found the sensitivity of tubulin assembly to calcium, the importance of GTP and temperature-dependent nucleation. He invented a novel way to polymerize tubulin in vitro (Weisenberg, 1972). He showed that tubulin can self assemble, independent of any enzymes. Unlike isolating the whole spindle apparatus which was unresponsive to any treatment, the purified tubulin could de/polymerize in vitro. In 1979, the stabilization function of taxol to MT was discovered (Schiff, Fant, & Horwitz, 1979). The purification of MT with taxol stabilization was developed in 1982 (Vallee, 1982), leading to the discovery of microtubule associated protein MAP1 and MAP2. Except for taxol, vinblastine, podophyllotoxin and nocodazole were also discovered or synthesised at this time (Jordan, Thrower, & Wilson, 1992).

**Microtubule dynamic instability** With polarized microscope, scientists already found the dynamics of the spindle under different temperatures and drug treatments. With the observation of incorporation of free tubulin dimers into steady MT, they proposed the MT treadmilling model, which was proved in actin (one end showing assembly, the other end disassembly). In 1984, Mitchison and Kirschner proposed the MT dynamic instability model (Mitchison & Kirschner, 1984). They used centrosomes to nucleate MT seeds in a nucleating promoting buffer, then changed it to low tubulin concentration buffer. Although the total MT number was decreased, the length of single microtubule was never constant, some MTs still prolonged their length. Individual microtubule could randomly grow or shrink back and forth and the coexistence of growing and shrinking at the plus ends of microtubule was called dynamic instability (Fig.1C). Direct visualization of microtubule dynamic instability was achieved later (Hayden, Bowser, & Rieder, 1990; Rieder & Alexander, 1990). MTs are typically composed of 13 protofilaments in vivo and each protofilament composed of polarized α/β tubulin dimers. This dimer can bind two molecule of GTP. GTP bound to α-tubulin is unchangeable. When the dimer is incorporated into MT, the GTP bound to β-tubulin will stochastically hydrolyse to GDP. When MT goes through depolymerization, the MT will peel apart like a banana, which we call "catastrophe", contrasting the "rescue" during the polymerisation process. The α-tubulin side, often capped by proteins, was called minus end. The β-tubulin side, which is highly dynamic, was called plus end (Desai &

Mitchison, 1997). The dynamic instability enables MT to explore all the cytoplasmic space, and motor proteins can quickly transport material in any directions within it. Minus ends stabilized by the cortex can facilitate asymmetry of the MT network and cell polar movement. The dynamic microtubules can easily search chromosomes and drive them to the spindle poles. The search and capture model was proposed in 1986 (Kirschner & Mitchison, 1986).

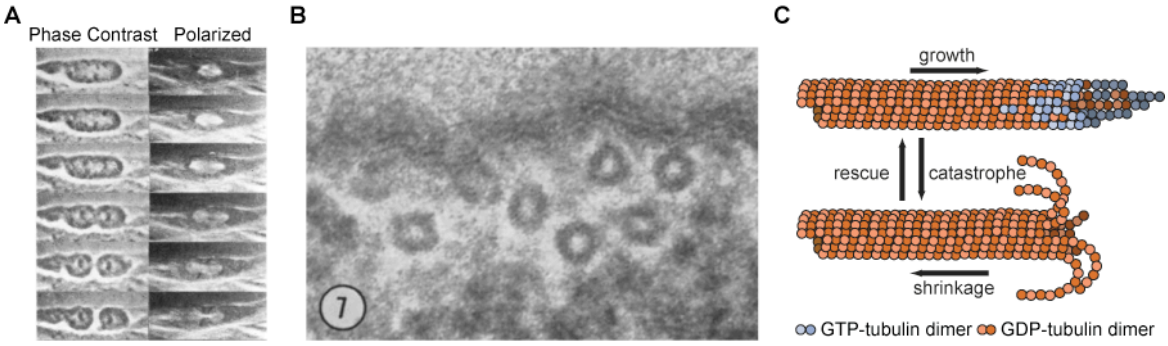


Fig. 1. The structure of microtubules: string-shaped in polarized light microscope and tube-shaped in electron microscope.

(A) Biframe record of osteoblasts in division; left-hand is phase contrast images, right-hand is polarized light microscope images. Each image in one series has an interval time of 1min (adapted from A. Huges, 1948).

(B) EM images of cross-sections of tubulins found in the cortex of a Phleum cell (adapted from Ledbetter & Porter, 1963).

(C) Microtubule dynamic instability (adapted from Bowne-Anderson, Zanic, Kauer, & Howard, 2013). MT can switch from growth and shrinkage periods stochastically. When the GTP capped MT end is lost, MTs begin its catastrophe process like a peeling banana. With newly incorporated GTP-tubulin, MTs can change to a rescue process.

**γ-Tubulin and γ-Tubulin Ring Complex (γ-TuRC)** When the centrosome was discovered, its microtubule nucleating function was soon following up. However, the molecular mechanisms of microtubule nucleation remained in mystery till the discovery of γ-TuRC. γ-Tubulin was first discovered in 1989. Early in 1950s , through chemical induced random mutations, scientists had screened many temperature sensitive mutants, which grew normally under permissive temperatures but could not grow under non-permissive temperatures. Most of the genes screened with temperature sensitive mutants were crucial genes, functioning in vital pathways. In *Aspergillus nidulans*, *benA33* was a heat-sensitive mutant of β -tubulin while *mipA* was extragenic suppressor of *benA33*. Through sequencing, *mipA* was found to be a member of the tubulin family and named γ-Tubulin (C. Elizabeth Oakley, 1989). Then γ-Tubulin was proved to be ubiquitously expressed in different species and different tissues and could localise to the centrosome. The first γ-Tubulin complex (γ-

TuRC) was purified from *Xenopus* egg extracts with sucrose gradient sedimentation and gel filtration in 1995 and observed with electron microscope (Trans et al., 1995). Sperm centrioles or salt stripped Drosophila centrosomes required γ-TuRC to become competent for MT nucleation (Moritz, Zheng, Alberts, & Oegema, 1998). In 1999, in *Drosophila* embryo extract, γ-Tubulin was found to exist both in big and small complexes (Oegema et al., 1999). In 1996, Mohammed purified γ-Tubulin from cytoplasm that already get rid of centrosomes, realizing that at least 80% of γ-Tubulin in the cytoplasm (Moudjou, Bordes, Paintrand, & Bornens, 1996). These discoveries laid foundations to following progress.

**IFT and ciliopathies** The striated muscle tissue was first observed by Lenweenhoek, its basic components myosin and actin were found in 1940s. The existence of actin in non motile contractile cell was facilitated by the use of antibodies and indirect immunofluorescence in 1974. The ubiquitous existence of interphase microtubules owed to the electron microscope and glutaraldehyde fixitives. In later 20$^{th}$ century, the existence of the primary cilium was also proven in almost all cells.

Motile multicilia originally were found in special organs, such as respiratory tracts, middle ears and lungs. At that time, researchers thought the main purpose of the cilium was motion. In 1898, the primary cilium was first observed by Zimmerman and first named by Sergei Sorokin (1968). Until the late 1990s, the primary cilium was found in all cells. In 1993, Rosenbaum and his colleagures observed a novel form of flagellar motility in *Chlamydomonas* -the introflagellar transport (IFT) (Kozminski, Johnson, Forscher, & Rosenbaum, 1993). The kinesin-like protein mutant in *Chlamydomonas, FLA10,* would stop the introflagellar transport at restrictive temperature (Kozminski, Beech, & Rosenbaum, 1995). To explore the difference between the normal algea and the *FLA10* mutant at restrictive temperatures, several other IFT components were discovered (Cole et al., 1998). Defects in one of these IFT proteins lead to polycystic kidney disease (PKD) (Pazour et al., 2000). Increasingly, more diseases were discovered to be caused by defects in primary cilia. The primary cilium, as the newly sensory receptor, received a new round of attentions.

**MPF, CSF and *Xenopus* egg extract** The sperm was first observed by Leweenhoek, the fertilisation process of sperm and egg combining were first described in 1840s in sea urchins. Marine animals were often used to study embryo development for the reason of in vitro fertilization. Oskar Hertwig (1836 to 1922), in 1876, first showed two pronuclei in one egg

and the nuclear fusion (Birkhead & Montgomerie, 2009). Then researchers tried to figure out how sperms penetrated the surface of the egg, until they found that the sperm acrosome contained the lytic enzyme acrosin in 1930s. In 1937, Heilbrunn and Wilbur showed that the initiation of nuclear envelope breakdown in eggs is caused by calcium (Heilbrunn & Wilbur, 1937). The African clawed frog *Xenopus*, first used to test pregnancy, soon caught embryo biologists and biochemistry researchers' attentions for its time-unlimited fertilization and large batch eggs from 1950s on.

In 1970s, Rao and Johnson fused different stages of cultured cells, and found that the M phase cells could induce premature chromosome condensation in G1, S and G2 phase cells, passing the mitotic features to interphase cells (Johnson & Rao, 1970). In the late 20 century, when scientists injected the egg cytoplasm to fully grown immature oocyte, this oocyte did go through GVBD, till Meosis II (Masui, 2001). It was observed that the cytoplasm from early embryos could induce immature oocytes to progress to MII phase. Injection of progesterone, however, did not work, which means there is an extracellular signal switched on some "maturation promoting factor" (MPF) in the cytoplasm to control this maturation process. The whole process was not affected by the loss of the nucleus. When injected with the cytoplasm of MII eggs, the two-stage embryo stopped dividing in metaphase, adding somatic cytoplasm not. This inhibition was released by fertilization or pricking. Therefore, special material existed in MII arrested egg cytoplasm that could stop cell division in metaphase, called "cytostatic factors" (CSF) (Masui, 2001). It was observed that, when sperm entered eggs, its nucleus did swell in 20 minutes. In 1972, Barry found that mixing hen erythrocyte nuclei with *Xenopus* egg cytoplasm could also make the nucleus swelling immediately and get ready to replicate (Barry & Merriam, 1972). He obtained the egg extract by the following four methods: micro-needle sucking, squash, directly centrifuging and pre-packed before centrifugation. Through this centrifugation methods, he gained three layers (up yellow lipid layer, middle transparent cytoplasm layer and bottom black pigment layer). The first functional egg extract was reported in 1983 by Lohka and Masui (M. J. Lohka & Masui, 1983). In his egg extract, he could observe the whole process of sperm decondensation, DNA synthesis, prophase condensation and formation of metaphase chromosomes. But not every time, only seven out of ten experiments could he observed the formation of metaphase chromosomes. Egg extract with the addition of EGTA and purified MPF (M. I. Lohka & Maller, 1985) could change the chromatin into chromosomes and form spindles. Egg extract without EGTA could lead to the formation of nuclear envelope. Taxol

induced aster formation was also observed in metaphase egg extract and these asteres were destroyed when dynein was depleted the with UV light (Verde, Berrez, Antony, & Karsenti, 1991). *Xenopus* CSF arrested egg extract is a cell free system which represents the in vivo situation of mature MII arrested eggs. It's a very good tool to study DNA replication, DNA condensation, nuclear envelop breakdown and formation, spindle formation and microtubule dynamic instability.

## 1.2 Nowadays research of cell division and ciliogenesis

The cells divide to increase their number, which is important for organisms' growth and maturation, life continuity and populations' evolution. The most challenging task for a cell is to evenly segregate the replicated chromosome to two daughter cells. To perform this task, a series of complicated activities happen. With the development of technologies ( antibody, GFP tag, electron microscope, super resolution light microscope, mass spectrometry, genome editing), so much progress has been made.

### 1.2.1 Somatic cell division: Mitosis

Mitosis refers to the replication of somatic cells. During mitosis, genome replicates once, cell divides once. Therefore, they successfully double cell number and keep the same amount of DNA. Through cell division, the organisms increase its size or replace the worn out cells, simultaneously passing though the genetic material to each daughter cell. For the dividing cells, they need go through interphase (first growth phase (G1), Synthesis phase (S), the second growth phase (G2)) and mitotic phase (prophase, prometaphase, metaphase, anaphase and telophase).

**Chromosome is replicated during interphase** G1 phase is a phase that cells prepare for chromosome replication in S phase. Cells double their size, synthesis proteins, RNAs and organelles that needed for genome and centrosome duplication. Not only this preparation, G1 cells also perform the daily functions. When organisms need to grow, they need increase their cell number to increase their size. When organisms reach their mature size, the differentiated cell will get out of cell cycle and stay in G0 phase. Senescence (irreversible) and nutrient limitation (reversible) can force cells stay in G0 phase. Cells in G0 phase is their main appearance in their whole life in a organism. G0 phase cells still perform their functions and most cells will form primary cilia. The onset of DNA replication marks the irreversible progress of cell division. How cells decide to stay in G0 phase or re-entry to G1 phase? Restriction point (R-point, G1 checkpoint ) are responsible for the quality control here. Extracellular mitogen activates R point through mitogen receptors. Through a series cascade signal transductions, the recipients (transcription factors) increase cyclin D expression level and Cyclin-Cdk4/6 phosphorylate Retinoblastoma protein (Rb). Hyper phosphorylated Rb protein loose its interaction with elongation factor E2F, which controls lots of DNA

replication related genes (Matson & Cook, 2017). Cells in culture need external mitogens (serum) for proliferation. The most important thing in S phase for a cell is DNA replication. The duplicated sister chromatids are tied by cohesion. Centrosome is also replicated at the onset of S phase. G2 phase is for cell growth and protein synthesis. G2/M checkpoint ensures the chromatin is completely replicated and no DNA damages exist before cell division. High activity of Cyclin B/CDK1 is a pre-requirement to mitotic phase. DNA damage performs a negative regulation upon cyclin B/CDK1, leading to a prolonged G2 phase. P53, the famous oncogene, is also a very important regulator for cell division.

**Open and closed mitosis** For different organisms and species, during mitosis, nuclear envelop either stays intact or dissolves in cytoplasm, we call them open and closed mitosis respectively. For that still have partial nuclear envelop left, we call it semi-open mitosis, such as in *Shizosaccharomyces Japonicus*. Animals and plants are mostly performing open mitosis. In budding yeast, the closed mitosis will form two different shaped cells because of asymmetric segregation of cellular components, resulting in the formation of mother and daughter cells who has different cell proliferation ability (Boettcher & Barral, 2013). The mitosis process I described later is all referred to eukaryotic open mitosis.

**RanGTP controls the transportation between nucleaus and cytoplasma** GTPase is a molecular switch for many fundamental processes. Their functions rely on the ability of binding and hydrolysis of nucleotide guanine triphosphate (GTP) and guanine diphosphate (GDP). There are two big families of GTPase - heterotrimeric G protein and small GTPase. Big G protein complex composes of three subunits, alpha (α), beta (β) and gamma (γ). When G protein-coupled receptor (GPCR) binds to its ligand, α will disassociated with β/γ complex. Than α and β/γ can separately activate the downstream signal proteins. When Gα dydrolyzes GTP to GDP, α can associates with β/γ again to restart the next round of signal transduction. Small G protein, equivalent to the α subunit of heterotrimeric G protein. The best characterized small GTPase is Ras superfamily (Ras, Rho, Ran, Rab and Arf GTPases). Ran is functioning in transporting proteins and RNA in and out of nucleaus. Cargos with NLS (nuclear localization signal) can bind to importin, through nuclear pore complex， transfering into nucleus. RCC1 is a RanGEF (nucleotide exchange factor) that binds to chromatin, so RanGTP is highly riched in nucleus. In nucleus, the RanGTP will bind to importin to release cargos. However, the binding of RanGTP with exportin and cargo will stable their interaction and move together to cytoplasm. Outside the nucleus, RanGAP will

dydrolysis RanGTP to RanGDP and exportin releases its cargo. During mitosis, the RanGTP cargos, such as TPX2 (Gruss et al., 2001) and HURP play an important role in spindle assembly.

**Prophase starts with chromosome condensation** As chromosome compaction occurs, transcriptions shut down and nucleolus disperse. Nuclear pore complexes and lamin fibers are highly phosphorylated to become soluble. But lamin-B is still associated with nuclear envelop membranes. The disperse of lamin fiber weakens nuclear envelop and the influx of $Ca^{2+}$ increases protein kinase C activity, leading to the disperse of nuclear envelop, forming vesicles and cisternae associated with endoplasmic reticulum (ER). Cyclin B and CDK1 has a high activity during the whole mitotic phase (Nasa & Kettenbach, 2018). Microtubule and microfilaments is less stable compared to interphase one because of hyperphosphorylation. In the transition from interphase to mitotic phase, stress fibers disappear but some F-actins still exist at the cell cortex for later cytokinesis. Transcription and translation are repressed. During prophase, more than ¾ protein are phosphorylated at one or more sites in human cells, reaching the highest level in metaphse. Intermediate filaments surrounding the nucleus inhibits the dispersion of chromosomes after GVBD. The centrosome, which is already duplicated in S phase will separate to define the two poles of bipolar spindle in prophase. When the nuclear envelope completely dispersed, the prophase reaches its end.

**Microtubules search for chromosome in prometaphase** During prometaphase, Spindle forms. But the chromosome is not align up at the equator. The kinetochores assembly on chromosome allow centrosome drived microtubule to capture it. This search and capture model is supported by mathematical formulations to prove its efficiency. Spindle Assembly Checkpoint (SAC) ensures the proper attachment of all kinetochores by microtubules. Unattached or improperly attached kinetochore inhibits E3 activity - anaphase promoting complex/cyclosome (APC/C). Otherwise, APC/C can activate separase to degrade the cohesion connections between sister kinetochores. Spindles also help to segregate some non-chromosomal cellular parts.

**Chromosome Segregation** When all chromosomes align up at the equator of spindle, we call this stage metaphase. In different species or even in different cell types from the same species, the durations of metaphase are greatly variable. However, they all maintain a distinct metaphase period. Stabilizing the interaction between MT and kinetochore and waiting for cyclin B and cohesion degradation is the two tasks cells need to complete in metaphse.

Although metaphase spindle looks rigid, actually, the microtubule is highly dynamic, showing 'flux' mode toward spindle pole (Pereira & Maiato, 2012)**.** GTP is consumed for every MT dynamic instability. After the degradation of cohesion, chromatids move to two poles in anaphase by poleward force generated by kinetochore MT. For anaphase A, spindle does not enlong its length, but shorten kinetochore MT to pull chromosome segregation. The motor proteins generate mechanical force through crosslinking and sliding MTs. In Anaphase B, the spindle will become longer by the non-KT fibers elongation. In telophase, nucleus envelop with functional nuclear pores is re-formed; chromosome begins decondensate, and nucleoli reform. Exiting from mitosis needs low protein phosphorylation level. Mere degradation of mitotic phosphoproteins is not enough, the activity of phosphatase need to be increased to dephophorylate the proteins (Richard Mcintosh, 2016). Then, cytokinesis helps to separate cytoplasm.

### 1.2.2 The formation of gametes: Meiosis

**Germ cell and sex determination** Compared to asexual reproduction, meiosis deducts half of its genetic material, fusing two different gametes together, promoting the variety of genome pool as well as the adaptability to the environment. Germ cells are the special cells that can go though meiosis. Most germ cells specialize from early embryo cleavage or gastrulation stage. There are two ways to determine the germ cells : induction ( mammalians) and germ plasma determination (other vertebrates). In mammalians, during early development, few cells with remaining pluro potency will migrate to gonad or testis to perform meiosis. Other pluropotency cells can also go through meiosis under the stimulus of gonad or testis (induction). For *Xenopus*, *Drosophila*, zerafish, only the one has germ granule can be stimulated to process to meiosis. For sex determination, lots of species do not have sex chromosome. Their sex can be determined by chromosome monoploid and bioploid, birth temperature or nutrient. Sometimes, they also go through parthenogenesis and asexual reproduction. Some species can live both with meiotic monoploid chromosome and diploid chromosome. Lots of species evolute sex chromosome with specific genes on it. These genes can control many downstream targets to control the growth of reproductive organs. The surrounding environment of the germ cell produced by gonad or testis is very important to determant whether the germ cell became an egg or sperm.

**Oogenesis** After the promodial germ cell arrived at the gonad, it firstly performs mitosis to increase its cell number (6-8 week embryo) before meiosis happens. The premeiotic interphase is normally 20 times long than premitotic interphase in the same species. Sex chromosome are replicated at the beginning of S phase other than the end of S phase like in mitosis. After a long premeiotic S-phase, mitotic cells are ready for their first meiotic cell division (11-12 week embryo). Then the cells enter the prophase of meiosis I, which is the most complicated stage in all cell division processes. What happens in this prophase is the main difference between meiosis and mitosis. The long prophase I is divided into five substages: leptotene, zygotene, pachytene, diplotene and diakinesis. In leptotene, the duplicated chromosome begins to condense to a string-like structure, the homologous chromosome begins to pair up. In zygotene, the homologous chromosome finishes their pairing, forming synaptonemal complexes. In pachytene, chromosome condenses to clear structure, and cross-over happens. In diplotene stage, the paired homologous chromosomes begin to separate, only attaching to each other at chiasma. Most animals would arrest at this stage, until sex maturation. In fish, amphibian, reptiles and birds, they form the special big lampbrush chromosome. This is because of the decondension of chromosome for transcribing mRNA to accumulate protein, mRNA, nutrienants which are needed in remaining meiosis, fertilisation and early embryo development. At this stage the size of oocyte will enlarge from 50um to 1.2mm. The materials needed, partially is synthesized by itself, partially received through blood stream from surrounding cells. The fully grown oocytes will wait for the organism to achieve its sex maturation, and then process to meiosis (Bolcun-Filas & Handel, 2018). After sex maturation, with hormonal stimulation, oocytes undergo meiotic maturation (from meiosis I prophase to meiosis II metaphase). Meiosis maturation is regulated by post translational modifications of proteins and the translational control of mRNA.

**Spermatogenesis** When promodial germ cell arrived at testis, it will be arrested until puberty, then primordial germ cells undergo mitosis to produce spermatogonium. The spermatogonia double its size to differentiate to primary spermatocytes. The primary spermatocytes proceed to meiosis and form sperm cells. Sperm cells go through a lot of morphology and structural changes to become the functional sperm storing in testes: loosing most of its cytoplasm, keeping mitochondria for energy consumption and forming motile flagella with special structured centrosome.

## 1.2.3 The main microtubule organizing center: Centrosome

Centrosome as the main microtubule organizing centre (MTOC) plays a very important role in bipolar spindle formation during cell division. The majority of microtubules are nucleated by γ-TuRCs, which aggregate at centrosomes. For G0 cells, centrosomes provide template for ciliogenesis. Centrosomes also affect early embryo polarity initiation and organelles asymmetric distribution in somatic cells. Firstly, we need to know some basics of centrosomes.

**Centrosome structure** Theodor Boveri named centrosome with haematoxylin-stained sections of cleaving sea urchins and Ascaris eggs in 1988. With long time destain process, he could still observed centriole in the center, together with pericentriolar material (PCM), which expands during mitosis. Centriole, under EM, are barrel like structure composed of nine-fold MT triplets (A, B and C), with A in the inner, C at the periphery. The size and the length of a centriole differ in different species. For humans centrioles, it's about 330-600nm in length and 100nm in diameter. The two centrioles either orthogonally tight or loosely connected at centain angle. The connection side calls proximal end, and the other side calls distal end. These two centrioles structurally are not the same. There are distal appendages (DAs) and sub-distal appendages (SDAs) on mother centrioles.

PCM are highly stained condense amorphous structure surrounding centrioles observed in EM (Moritz et al., 1995). The mainly components of PCM are scaffold proteins - CEP192, CEP152, CPAP, PCNT (pericentrin), CDK5RAP2 (CEP215) and AKAP450; kinase/phosphatase proteins - PLK1, Aurora A and PP2A; and effector protein: γ-Tubulin (Woodruff, Wueseke, & Hyman, 2014). In interphase, PCM has a very neat circular organization compared to a less ordered proteinous meshwork in metaphase (Fig.2). Most of PCM proteins contain coiled-coil domain for mediating protein protein interactions. A recently detailed review are recommended (Vasquez-Limeta & Loncarek, 2021).

**Centriole duplication** Each cell only contains one centrosome when the cell is not dividing except for multicilium cells which need several basal bodies. Centriole duplication occurs once during one cell cycle, simultaneously with DNA replication. In early S phase, procentriole will form next to the proximal base of each pre-existing centriole. PLK4 plays an important role in this process. In early G1 phase, PLK4 forms a ring around each parental

centriole. The high level of APC leaves no SAS6 and STIL for centrosome binding. With the silence of APC at G1/s transition, then STIL is recruited to bind PLK4 at one spot, which releases PLK4 autoinhibitory status, marking the site for new centriole formation. PLK4 then degrades except the one under STIL's protection. Then, SAS6 and CEP135 is recruited to form the spokes and pinheads of the cartwheel structure (Arquint & Nigg, 2016). CPAP helps to promote incorporation of singlet microtubules in a γ-Tubulin facilitated way (Dammermann, Maddox, Desai, & Oegema, 2008). Centrin is loaded to the centriolar lumen. Capping proteins CP110 and CEP290 contribute to centriolar length control. This replication described here uses existing centriole as the template. When there are no templates, cells can start a de novo centriole formation. But cells have the preference to this templated duplication. The number of new centrioles is controlled by procentrioles and centriole assembly factors. Procentrioles can block centrosome overduplication, but overexpression of centriole assembly factors (PLK4, SAS6 et. al) can overcome procentrioles' block, forming rosette centrioles.

**Centrosome maturation** An interphase centrosome needs to adjust itself to gain high nucleating ability for accurate chromosome segregation in mitotic phase. In G2 phase or early mitotic phase, the centrosome grows in size and MT nucleation capacity - a process coined centrosome maturation - through the recruitment of additional PCM (CEP192, CDK5RAP2 and pericentrin) (Fig.2). Not all PCM components are increased, CEP63, CEP152 and CEP295 remain the same level as in interphase and mitotic phase. Highly ordered PCM (about 1μm Diameter) expands to meshwork ( about 4μm Diameter) during centrosome maturation. PLK1 plays a pivotal role during centrosome maturation by phosphorylating CEP192, CDK5RAP2 and pericentrin to increase their interaction affinity. Inhibition of Plk1 leads to several PCM components disassociate from centrosome (Cabral, Laos, Dumont, & Dammermann, 2019). Phosphorylated CEP192 by PLK1 can dock more γ -TuRCs. The 25-30nm diameter γ-TuRC needs its activator CDK5RAP2, NEED1, and MOZART1 to anchor the minus end of 12-15nm wide MT. γ -Tubulin localizes both in close proximity to centriole walls and PCM region in interphase but only in an extended PCM meshwork in mitotic phase (Sonnen, Schermelleh, Leonhardt, & Nigg, 2012). In metaphase, centrosomes nucleate at least five times more microtubules than in interphase. Although cartwheel is a permanent structure in some species (*Drosophila*, *Chlamydomonas et.al*), in vertebrates, it (STIL and SAS6) will be removed during anaphase by APC-mediated

proteasome degradation (Strnad et al., 2007). CEP135 is still in the centrioles, not only at proximal end, but in the whole centrioles lumen. After the loss of cartwheel in mitosis, new-born centriole will convert to centrosome by recruiting PCM in telophase and G1 phase (W. J. Wang, Soni, Uryu, & Tsou, 2011). CEP295 was shown to mediate centriole to centrosome conversion (Izquierdo, Wang, Uryu, & Tsou, 2014).

DA and SDA assembly is the last step to form a mature mother centriole, which would happens in next cell cycle in G2/M phase. DA helps docking membranes in ciliogenesis and SDA can anchore MTs in interphase.The assembly of SDA is initiated by the recruitment of ODF2 around the centriole's MTs, followed by the recruitment of CCDC68, CCDC120, CEP170, CEP128, and Ninein17-19. Some SDA components are transiently removed from SDAs from late G2 until G1 phase. DA assembly is initiated by the recruitment of C2CD3, followed by CCDC41/CEP83, CCDC123/CEP89, SCLT1, FBF1 and CEP164. Once assembled, DAs are thought to be permanent structures, contrary to SDAs, based on some EM observations that DA densities can be detected throughout whole cell cycle, and SDA's is not in mitosis. Even though, the decreased expression of DA protein CEP164 shows the remodeling of DA in mitosis (Bowler et al., 2019).

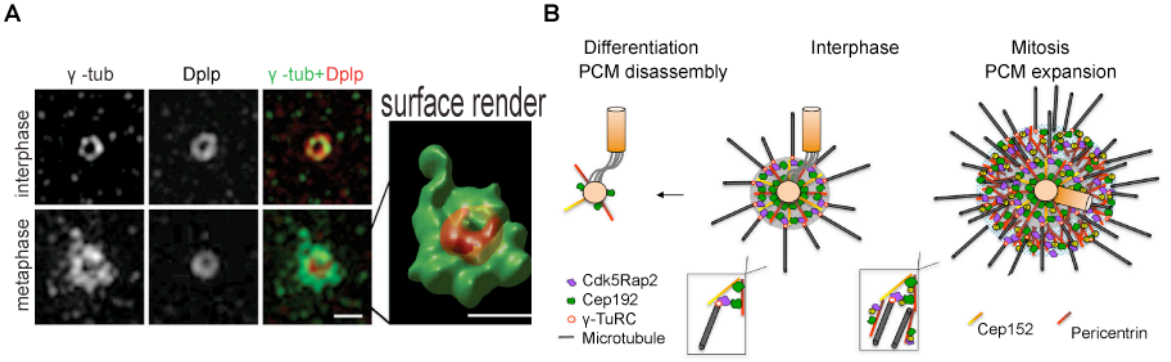


Fig. 2. Centrosome maturation. (A) With *Drosophila* Mel-2 cell line and 3D-SIM microscopy, γ -tubulin (green) and Dplp (red) were stained to show ordered interphase PCM and metaphase meshwork (adapted from Fu & Glover, 2012). Scale bar is 500nm. (B) Schematic figure to describe PCM organisation in differentiated cell stage, interphase and mitotic phase (adapted from Fry, Sampson, Shak, & Shackleton, 2017).

**Centrosome cohesion** There are two types of centriolar connections: S-M linker and G1-G2 tether. The S-M linker (centrioles are tightly orthogonally connected to newly formed procentrioles till the end of mitosis), prevents centriole reduplication, and its removal at late mitosis/G1 transition ("centrosome disengagement") licenses the centrosome for duplication

in next S phase. Ring cohesion complexes were found connecting centriolar pairs, whose dissolve need separase. The second connection, the so-called G1-G2 tether, is a complicated proteinaceous structure composed of C-NAP1, Rootletin and CEP68, which all together keep the two centrioles loosely connected from G1 to late G2 phase. I use centrosome disjunction /splitting /separation to refer G1-G2 linker disassembly. Centriole disengagement liberates the proximal end of the new daughter centriole that is embedded in the PCM of the older centrosome from S phase until mitotic exit. In telophase/G1 phase, centrosome linker proteins (CLPs) are recruited to the proximal end of the two disengaged centrioles (mother/daughter) and form a highly flexible connection that persists from G1 until mitotic entry. Centrosome separation allows bipolar spindle formation and unresolved centrosome linker induces monopolar spindle formation.

**Centriole disengagement** The requirement of protease separase for centrosome disengagement was first discovered in *Xenopus* egg extract. Adding separase inhibitor to egg extract prevented anaphase centriolar disengagement (Tsou & Stearns, 2006). Ring cohesion complex is formed to circle sister chromatids during S phase. Cohesion on chromosome would be removed in a phosphorylation dependent prophase pathway. Centromere and centrosomal cohesions are under the protection of Shugoshin in prophase and would be cleaved in anaphase with a separase dependent pathway. The main splice variance of Shugoshin protects pericentromere cohesion or recruits PP2A to release this protection to satisfy spindle assembly checkpoint. A short splice variance of Shugoshin protects centrosomal cohesion in a Plk1-dependent manner (X. Wang et al., 2008). PLK1 functions in both targeting Shugoshin to centrosome and releasing Shugoshin from centrosome. Perincentrin is also a substrate for separase, and is cleaved at metaphase-anaphase transition and released from centrosome at telophase-G1 transition in a layback way (Matsuo et al., 2012). CDK5RAP2 was shown having two pools, one interacts with PCNT at core PCM region to regulate centriole disengagement, the other interacts with CEP68 at peripheral PCM region to regulate centrosome disjunction (Pagan et al., 2015). Loss of CEP57 causes both centriole disengagement and PCM disorganization (Watanabe, Takao, Ito, Takahashi, & Kitagawa, 2019).

**Centrosome splitting** The research about centrosome separation, in the beginning, focuses on the interactive effects of cytoskeleton. Moreover, centriole distance during G1 phase are highly cell-type-dependent. In L929 cells, mother and daughter centrioles are sufficiently

separated during G1 phase, which is good to check individual centriolar behaviors (Piel, Meyer, Khodjakov, Rieder, & Bornens, 2000). MDCK cells are normally used to address questions related to epithelial cell polarity. Centrioles moved towards to each other when treated with low calcium medium to disperse cell junctions in MDCK cell line and centrosome splitting occurs only after the establishment of cell junctions. The movement of centrioles depend on MTs and F-actins, but after depolymerizaiton of MTs and F-actins, centrioles can still move in a random manner (Buendia, Bré, Griffiths, & Karsenti, 1990). Tumor promoter TPA treatment also causes centrosome splitting (Euteneuer & Schliwa, 1985). EGF and cytochalasin B/D induce centrosome separation in Hela cells (Sherline & Mascardo, 1982). Now we know that EGF induced centrosome splitting is because of the increasement of local Mst2 and NEK2 concentration at centrosome (Mardin et al., 2013).

With the discovery of EM, proteinous structure are found at the proximal end of centrioles. Moreover, purified centrosomes are usually closely paired even though the cytoskeleton has been disrupted during the process of isolation. NEK2, a close relative of mitotic regulator NIMA, localizes at centrosome through out the whole cell cycle and overexpression of NEK2 leads to centrosome splitting (Fry, Meraldi, & Nigg, 1998). Through yeast two-hybrid screening of NEK2 subtracts, C-NAP1 was found locating at centrosome and disappearing during mitosis (Fry, Mayor, et al., 1998). *c-nap1* knockouts in RPE-1 cell line shows abnormal Rootletin localisation in ciliated cell and reduced centriolar duplication after PLK4 overexpression (Flanagan et al., 2017). Rootletin was first found in cilium as the main structure of rootlet. It was then discovered as a substrate of NEK2 that were responsible for centrosome separation (Bahe, Stierhof, Wilkinson, Leiss, & Nigg, 2005). Depletion of CEP68 and CDK5RAP2 also caused centrosome splitting in U2OS, RPE-1 and A549 cell lines (Graser, Stierhof, & Nigg, 2007). C-NAP1, Rootletin and Cep68, as the components of centrosomal linker proteins, are phosphorylated by NEK2 and dissolve in late G2 phase. C-NAP1 is only partially removed from splitting centrioles, remaining a core part throughout the whole cell cycle (Faragher & Fry, 2003). With super resolution light microscope STED, CEP68 and Rootletin were shown forming interwinded aster-like structures surrounding each centriole and C-NAP1 functions as anchoring site for CLPs (Vlijm et al., 2018). Recently, more uncharacterized CLPs were found, CCDC102B is one of them (Xia et al., 2018). To prove the CLP identity of LRRC45 (He et al., 2013), super resolution images are still needed. NEK2 as the key regulator of centrosome splitting can also be regulate by upstream signalings such as: Wnt, beta-Catenin (Bahmanyar et al., 2008), Conductin/axin2

(Hadjihannas, Brückner, & Behrens, 2010), Hippo pathway (Mst2), EGF, regulator protein CEP85 (Chen et al., 2015) and PP1γ.

Dissolvement of the centriolar connection is one thing, centrosome separation also needs force to move them apart. The force was contributes by motor proteins, actins and MTs (regulated by PCM and SDA). Bipolar spindle can still be normally formed after inhibition of NEK2A (a major splice variance of NEK2) and Eg5 generated force can separate centriole pairs, leaving CLPs untouched (Mardin et al., 2010). Actin-dependent Eg5-opposing force slows down separation process in G2 phase (E. Smith et al., 2011). GAS2L1 can bind both F-actin and MT and centrosome splitting caused by overexpression GALS2L1 is aborted by F-actin and MT depolymerization (Au et al., 2017). Centrosome splitting ratio increases greatly when knockout one component of sDAP on top of *c-nap1* knockout (Mazo, Soplop, Wang, Uryu, & Tsou, 2016). SDA proteins increase centrosomal distance without affecting Rootletin and C-NAP1's localization and expression (Pizon et al., 2020). NEK2 was also shown located at DA to displace DA proteins before mitosis (Viol et al., 2020). Except for CDK5RAP2, there were other PCM components' loss were found leading to centrosome splitting. In DT40 cells, *cdk5rap* and *akap450* knockouts show around 50% centrosome splitting phenotype separately and double knockouts only increase a little bit to around 60% (Barr, Kilmartin, & Gergely, 2010). CEP135 siRNA knock down also show premature centrosome splitting (Kim, Lee, Chang, & Rhee, 2008). CEP85 is also a PCM protein that can lead to centrosome splitting which can inhibit NEK2A's activity. PCM can not only regulates forces generated by MT at centrosome and developed a hydrophobic environment to increase protein interactions, it also can regulate NEK2A's activity. Fig. 3 shows the whole centrosome cycle intertwined with cell cycle.

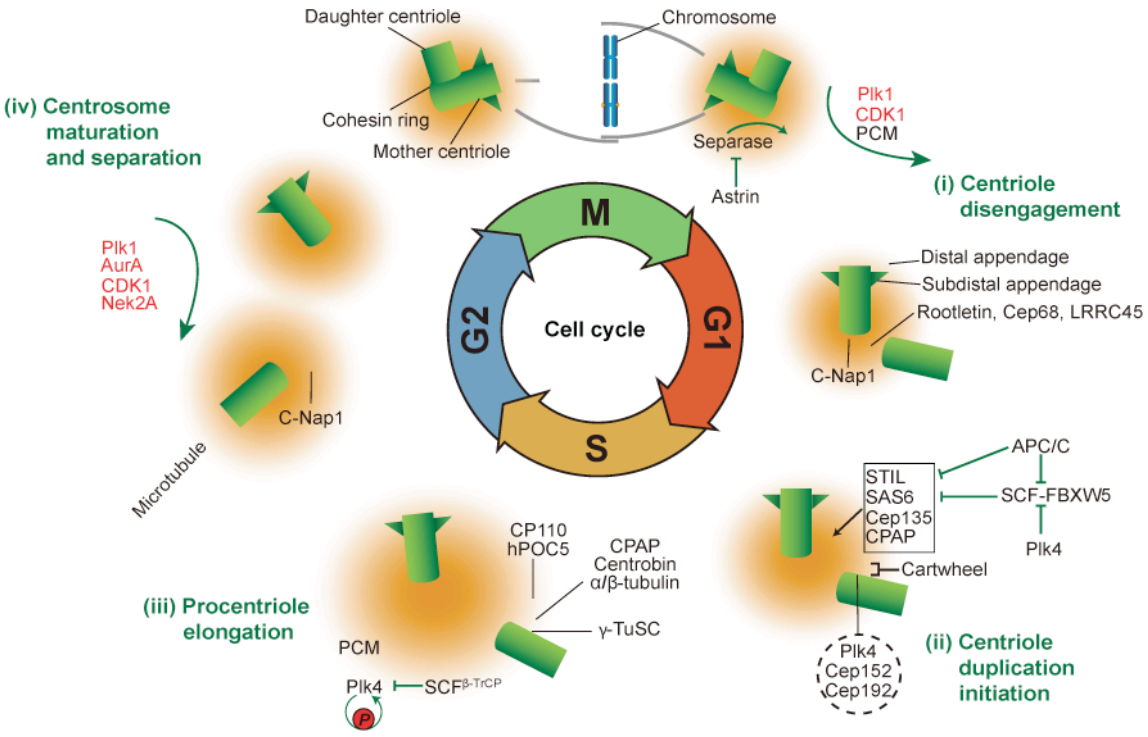


Fig. 3. Coordination between cell cycle and centrosome cycle (adapted from G. Wang, Jiang, & Zhang, 2014).

(i) Centriole disengagement. Centriole disengaged at the end of mitosis by PLK1, separase and PCM regulated cohesion removal. (ii) centriole duplication (S phase) and elongation ( S phase and G2 phase). (iii) Centrosome Maturation and separation. Centrosome separation and maturation happen simultaneously. NEK2 kinase dissolves centrosome linker then the centrosome move apart by MT-dependent force. Newly formed mother centrioles assembly DA and sDA in late G2 and early prophase. PCM is recruited to increase MT nucleation ability. (iv) Bipolar spindle assembly. The inner circle shows the different phases of the cell cycle and centrosome cycle is shown in outer circle. Mitotic kinases are shown in red.

**Centriolar satellites** Centriolar Satellites (CS) were first observed 60 years ago as electron-dense particles of 70-100 nm in diameter in electron microscopy sections surrounding centrosomes and basal bodies. PCM1 was the first CS protein identified (Balczon, Bao, & Zimmer, 1994). PCM1 soon stabilized its status and PCM1 colocalization was used to define whether some proteins are CS proteins. PCM1 integrity is required for many protein's centrosome localisations, but many proteins can affect PCM1 localization. By highthough proteomic methods, 40% of CS proteome were found overlapping with PCM1 interactome (Prosser & Pelletier, 2020). Therefore, PCM1 interaction is not the only yardstick to determine a CS. Except to PCM1, Cep131 and Cep290 are also the main scaffold proteins under normal conditions.

CS localization is not restricted to centrosome surroundings (Kubo & Tsukita, 2003). In different cell types or different tissues, it has different patterns. It localizes at apical region of cytoplasm in intestine. In brain, it scatters to the whole cytoplasma. In vertebrate cells, it typically arounds centrosome and its pattern is cell cycle dependent (dissolve in mitotic phase and reassembly in interphase). CS centrosomal localisation is highly dependent on MT in a dynein-dependent manner. Nocodazole or cold treatment induced MT depolymerisation can disperse majority of CS components, but not PCM1, CEP131, CEP290, OFD1, CCDC14 and CEP72. CS organization is not centrosome dependent. In cells without MTOC, MTs nucleate at nuclear membrane or other organelles instead of a single centrosome point. In this kind of cells, although CS was dissolved in cytoplasm, CS proteome was largely unchanged. That means CS assembly is centrosome and MT independent, but centrosomal localisation is definitely dependent on MT and centrosome (Gheiratmand et al., 2019). The interactomes also show the heterogeneity among different satellite granules. Different subpopulations may exist to perform different functions independently.

Since CS was found around centrosome on MT tracks in cultured cell, its facilitation role for centrosome assembly has been researched for many years. Proteomic data shows lots of centrosomal proteins also exist in CS, except for PLK4, SAS6, CEP152 and STIL. The centrosomal proteins in CS pool didn't provide any real centrosomal functions, may due to the low concentration or the CS inhibited status. The notion that CS functions as a cart transporting centrosomal proteins is based on a insufficient evidences (It is a reasonable proposition based on many results that scientists concluded from different experiments). There are so many pathways and networks are proposed based on reasonable speculations without direct solid evidences. Therefore, cyo-EM and super resolution microscope images are needed. More evidences show CS as a protein pool, can timely exchange with centrosomal proteins and regulate different proteins' functions during centriole duplication, cilium assembly, microtubule nucleation, mitotic progression, autophagy and stress response. The phenotypes between acute and chronic depletions of satellites in cells sometimes are quite different. Except for siRNA off-taget, the compensation mechanism of genetic knockout is the main reason that cause the differences, such as, CEP131 siRNA knockdown show defective ciliogenesis but knockout didn't (Hall et al., 2013).

**Centrosome and phase separation** Phase separation is an old topic in physics and chemistry. The most obvious example is the oil and water mixture. For biologist, they often

observed phase separation in protein crystallization with unawareness. The metastable intermediate phase formed in saturated liquid solution which can give rise to crystal is the separated droplet from liquid solution (Sauter et al., 2015). Until Brangwynne realized the liquid characteristics of P granules (Brangwynne et al., 2009), the campartilization by phase separation in cytoplasm and nuclearplasm is became obvious. Later, Brangwynne also conformed the phase separation of nucleoli, which can dynamically fuse and separate (Brangwynne, Mitchison, & Hyman, 2011). There are so many other granules in different cells such as stress granule and neuronal granules. Most of these granules are composed of RNA and RNA binding proteins. In these granules, RNA is the mRNA that control the polar (P granules) or synaptic protein (neuronal granules). The low complexity sequence in RNA binding protein is a decisive factor for phase separation (Kato et al., 2012). The in vitro formation of phase separation also became a classic method to test whether one protein can form phase separation. Fig.4 shows most recently phase separated condensates in vivo.

For membraneless centrosome, there are still some doubts casting on whether centrosome has phase separation features (Raff, 2019). With in vitro expression, Spd5/CEP192 can form irregular condensates that recruit other PCMs (Woodruff et al., 2015). With PEG treatment, the CEP192 condensates became round particles in vitro (Woodruff et al., 2017). These particles, together with other PCMs, can nucleate MT in 10 minutes. And in vitro, TPX2 condensates can also polymerize MTs (King & Petry, 2020). By checking the dynamic fusion process of PCNT, CEP152 and CEP63 during mitosis(Ahn et al., 2020; X. Jiang et al., 2021), the conclusion that centrosome is a phase separated droplet is unconvincing. In vivo, PCM show different patterns during interphase and metaphase, with a great enlargement in metaphase. PCM and CS are granules, but do not form a smooth surface sphere, which should be for phase separated droplets from physical perspective. It is not a good argument that protein can form phase separation in vitro with particular concentration - most proteins can form phase separation in vitro (crystallization based on that). Also the in vitro situation cannot represents in vivo centrosome structure. Therefore, large is unknown about the phase separation of centrosome.

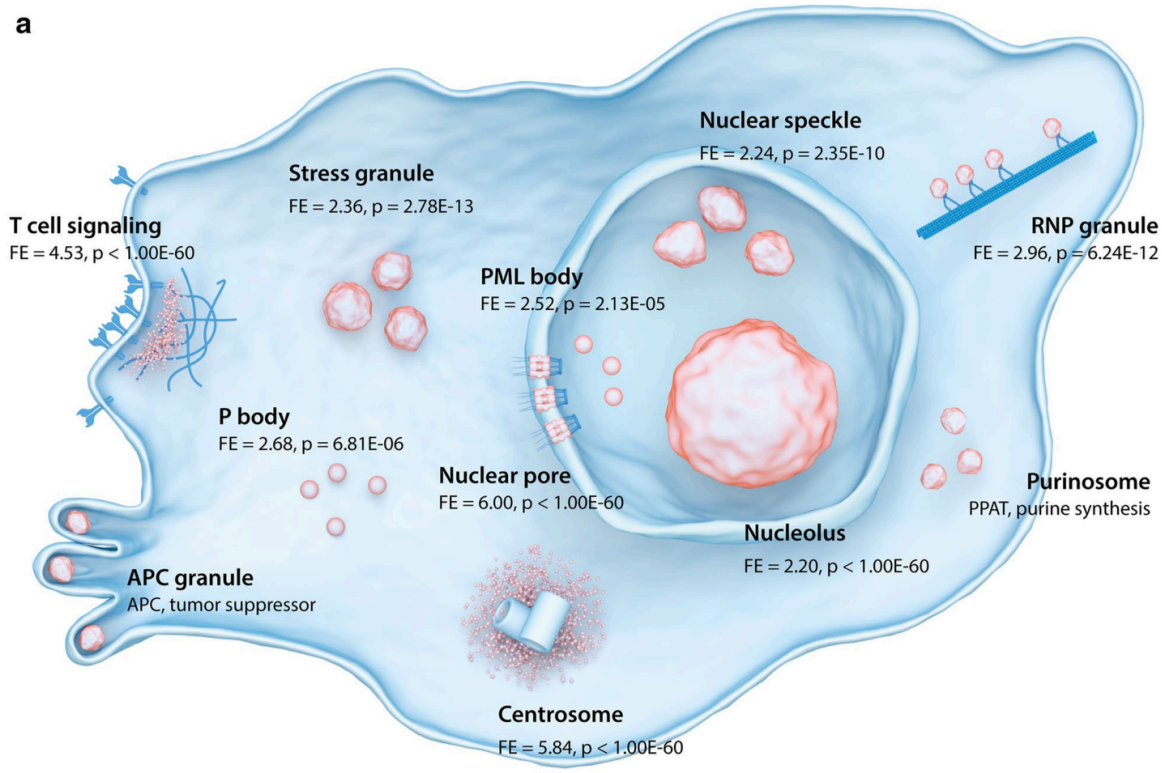


Fig.4. Overview of different membraneless organelles (Pink). The fold enrichment of proteins is shown when there is (adapted from Boeynaems, Tompa, & Van Dan Bosch, 2018).

## 1.3 Research about CEP135, SSX2IP and WDR8

### 1.3.1 CEP135

CEP135 was first discovered 20 years ago in CHO cell (Ryu, Essner, Ohta, & Kuriyama, 2000). Later, CEP135's analogs - bld10 - was found located at cartwheel in *Chlamydomonas* flagella, whose cartwheel exists throughout the whole cell cycle (Matsuura, Lefebvre, Kamiya, & Hirono, 2004). Expressing different parts of bld10 in null mutant shows abnormal cartwheel structure - a transformant with 35% C terminal loss shows 8 triplets arranged flagella and the spoke is short than wildtype. They also found bld10 is a cartwheel tip component (Hiraki, Nakazawa, Kamiya, & Hirono, 2007). *Drosophila bld10* mutants had wider and unstable cartwheels but without obvious defects in centriole duplication (Roque et al., 2012). Male *bld10* mutants in *Drosophila* were sterile and had immotile sperms, short centrioles and short spermatid basal bodies (Mottier-Pavie & Megraw, 2009). In human patients, *cep135* 1 bp frameshift lead to primary Microcephaly and disturbed centrosomal functions (Hussain et al., 2012). In vertebrate DT40 cells, *cep135* knockouts had normally functioned centrosomes (Inanc et al., 2013). PLK4 overexpression induced the formation of rosette centrioles in S phase with the recruitment of SAS6, CPAP, CEP135 and γ-Tubulin (Kleylein-Sohn et al., 2007). CEP135 as the tip of cartwheel can interact with SAS6, CPAP and MT triplet wall. In vertebrate, cartwheel is just a transient structure in procentrioles. SAS6 and STIL will be removed from centriole in late mitosis, but CEP135 and CPAP still occupy the lumen of both mother and daughter centrioles and PCM region. In the centrosome proximal end, CEP135 can interact with C-NAP1, which play a very important role in centrosome cohesion. C-NAP1 phosphorylation is very important to release itself from CEP135' capping (T. Hardy et al., 2014). As we have discussed in centrosome cohesion chapter, CEP135 knock down showed centrosome premature splitting (Kim et al., 2008). Centrosome junction is such a complicated mechanism that so many pathways are working together to regulate centrosome cohesion. Whether CEP135 knockdown induced centrosome splitting is only because of C-NAP1 anchorage defects or CEP135 has other functions? So many questions needs to be answered.

## 1.3.2 SSX2IP

SSX2IP as a centrosome satellite protein that was first discovered by Oliver Gruss (Bärenz et al., 2013). Before that, SSX2IP in a different name ADIP (afadin DIL do- main-interacting protein) was found locating at cell adjunctions (Asada et al., 2003). SSX2IP got the name because of the interaction with Synovial Sarcoma X breakpoint 2 (SSX2) (De Bruijn et al., 2002). SSX2 is a conserved family, highly enriched in testis as well as several tumors including melanomas and synovial sarcomas. In chicken, SSX2IP analog, LCG (light-inducible and Clock-controlled Gene) was a circadian protein and colocalized with γ-Tubulin (Hatori, Okano, Nakajima, Doi, & Fukada, 2006). In *Xenopus* egg extract, ssx2ip depletion induced monopolar spindle formation. SSX2IP knockdown in RPE-1 cells caused γ-Tubulin fragementation in mitosis. In U2OS cell, SSX2IP is required for MT anchoring in interphase by affecting ninien (Hori, Ikebe, Tada, & Toda, 2014). During ciliogenesis, SSX2IP targets CEP290 to ciliary transition zone (Klinger et al., 2014). Highthrough proteome screening shows OFD1, CEP131 and SSX2IP are the top three proteins that correlated with PCM1 (Gheiratmand et al., 2019).

### 1.3.3 WDR8

WD (Trp-Asp) domain is protein protein interaction motif that was found in a wide variety of eukaryotic proteins (T. F. Smith, Gaitatzes, Saxena, & Neer, 1999). Although many proteins have 4-16 WD repeats, their functions are quite different: RNA processing, transcriptional regulators and cell division regulators. Several WD repeats form a propeller-like structure with particular numbered blades where each blade is composed of a four-stranded anti-parallel -sheet. Please note that each WD repeat does not form a complete blade - it normally contains two partial blades to stabilize the structure. The propeller structure provides a platform for reversibly protein binding. The most famous propeller example is Gβ subunit of heterotrimeric G proteins. Not only Gβ can form tight complex with Gα and Gγ, it can also forms complex with several other proteins.

Wdr8 protein was first found in the ear cartilage of the *ttw* mouse. It is ubiquitously expressed among different tissues in mouse (Koshizuka, Ikegawa, Sano, Nakamura, & Nakamura, 2001). The cell division related functions of WDR8 homolog was found in *Aspergillus nidulans* and fission yeast (Shen & Osmani, 2013; Yukawa, Ikebe, & Toda, 2015). Then WDR8 was found, as a centrosome satellites, is a SSX2IP and CEP135 interacting protein in mamailian cells (Gupta et al., 2015; Hori et al., 2015; Kurtulmus et al., 2016). Maternal Wdr8 is required for embryonic mitoses in medaka fish (*Oryzias latipes*) (Inoue et al., 2017). As a novel centrosome satellites protein, WDR8's function is far from clear.

# 2 Aim of my thesis

Centrosome is such an important structure that regulates the most important process - cell division. Each year, the number of newly identified centrosomal proteins increases. Our lab previously discovered two centriolar satellite proteins WDR8 and SSX2IP, that can interact with each other as well as with the centrosomal protein CEP135. The dependency and inter-regulations of these three proteins and how much they can affect cell division and ciliogenesis are not fully understood. Therefore, my aim is to tackle the functions of WDR8, SSX2IP and CEP135 played in cell division and ciliogenesis, as well as their inter-regulations and inter-dependencies. WDR8 functions both as centriole satellite and centrosomal protein. It is the bridge of centrosomal protein CEP135 and centriolar satellite protein SSX2IP. Since WDR8 is a less well understood protein compared to SSX2IP and CEP135, I began my project with the immunoprecipitation of WDR8 in *Xenopus* egg extract. With mass spectrometry analysis, I found SSX2IP and CEP135 are the most abundance proteins in WDR8 immunoprecipitation. CEP135 was found has so many interactors (C-NAP1, SAS6, CPAP, CEP152 and CEP63) and SSX2IP was also found can interact with PCM1and γ-TuRC. Therefore, I made the CRISPR knockouts of these three proteins to see whether they have same defects. Comparing the different phenotypes caused by the loss of centrosomal protein CEP135 or centriolar satellite proteins SSX2IP and WDR8 can show the different roles played by centrosomal proteins and satellite proteins.

# 3 Results

## 3.1 cep135, wdr8 and ssx2ip are functionally and physically closely interacting with each other in *Xenopus* egg extract

### 3.1.1 wdr8 Mass Spectrometry results show high enrichment of ssx2ip and cep135

Compared to CEP135 and SSX2IP, WDR8 is a less well understood protein. Although our lab has published papers to show their interactions in mammalians cell lines, we still want to use the *Xenopus* egg extract system to find new WDR8 interactors and to verify CEP135-WDR8-SSX2IP interaction in the meiotic cytoplasm. CSF-arrested *Xenopus* egg extract represents the cytoplasm of meiosis, which has a different spindle formation mechanisms compared to mitosis. Because Amphibia accumulate high amounts of proteins during oocyte growth and egg maturation, the egg extract is a very good system to do biochemical protein analysis. To do this for wdr8, we generated a WDR8 antibody with synthetic peptides representing different parts of WDR8 primary structure of both human and frog. In the end, we succeed to yield a WDR8 antibody that works in immunofluorescence in human cell lines with both C and N terminal peptides. For *Xenopus* wdr8, we initially generated an antibody that efficiently recognized a Western blot signal at the expected 50kDa, but silver staining and MS identified this as a subunit of the proteasome complex (No wdr8 could be detected in this fraction). In contrast, with another antibody, which I finally used and show here, we observed a very high enrichment of WDR8 peptides after IP in Mass Spectrometry (Fig.5A), although the antibody did not yield a signal in Western blot.

Fig.5A shows the result analysed by tandem mass spectrometry of the wdr8 IP from *Xenopus* egg extract with wdr8, ssx2ip and cep135 as the top3 proteins. This result is consistent with the GFP pull down result in an NIH3T3 WDR8-LAP cell line (Kurtulmus et al., 2016). Mass spectrometry analysis also revealed a novel centrosomal protein, Microtubule-Associated Scaffold Protein 1 (mtus1, Fig.5A, C). MTUS1 was previously reported as a microtubule binding protein that localised on microtubule cytoskeleton and MTUS1 overexpression delays mitotic progression (Rodrigues-Ferreira et al., 2009). However, a

centrosomal locolisation has not been described up to now. I report for the first time that MTUS1 is an interaction partner of a centrosomal protein and verified this interaction by immunoblotting as well as detection of MTUS1 at centrosomes in RPE-1 cell line (Fig.5D, E). The detailed relationships between WDR8 and MTUS1 merits further investigation, while my thesis will focus on WDR8, SSX2IP and CEP135.

From previous and new results we could verify stable interactions of these three proteins both in interphase, mitosis and meiosis, in different species: human, mouse and *Xenopus*. Moreover, in *Xenopus* egg extract, wdr8 depletion could exhaust the majority of cep135 and ssx2ip (Fig.5B). Likewise, with a home-made cep135 N terminal antibody, a cep135 IP from *Xenopus* egg extract identified wdr8 and ssx2ip (Fig.13A). However, in previous ssx2ip IP from *Xenopus* egg extract, we could only observe wdr8 but not cep135 (Bärenz, 2011). From the analysis of subcellular localisation, we know that SSX2IP is a centriolar satellite protein while CEP135 is a centrosomal protein. Therefore, WDR8 could be a bridge connecting centrosomal proteins and satellite proteins. How these three proteins are inter-regulated is worth further exploration.

Fig.5. wdr8 Mass Spectrometry results show high enrichment of ssx2ip and cep135 (Page 34).

(A) Representive proteins found in wdr8 IP MS list. The whole list is shown in Table 1. Homemade wdr8 antibody binding beads to fish in metaphase CSF-arrested *Xenopus* egg extract to explore wdr8 interaction proteins.

(B) Immunoblotting to confirm the interaction between cep135 and ssx2ip. Depleted egg extract twice and each with 50µg wdr8 antibody and IgG was used as control. After twice depletion, there is only little part of cep135 and ssx2ip left. The second round elution has less protein compared to the first round, which proves the completely depletion of wdr8.

(C) Centrosomal locolisation of MTUS1 in RPE-1 cell line was conformed by siRNA knockdown. Scale bar is 10µm and 2µm for the enlarged area.

(D) Quantification of immunofluorescent signal in MTUS1 knockdown cells.

(E) Immunobloting to show MTUS1 expression level after siRNA knockdown.

A

| Description | Entrez Gene | MW(kDa) | Unique Spec | Coverage (%) |
|---|---|---|---|---|
| wrap73 (WD Repeat Containing, Antisense To TP73) | 735062 | 52 | 36 | 46 |
| ssx2ip (SSX Family Member 2 Interacting Protein) | 431921 | 70 | 35 | 36 |
| cep135 (Centrosomal Protein 135) | 100381167 | 133 | 20 | 15 |
| mtus1 (Microtubule Associated Scaffold Protein 1) | 398697 | 147 | 9 | 8.2 |

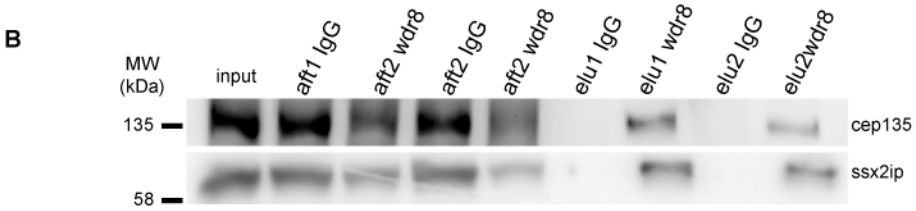


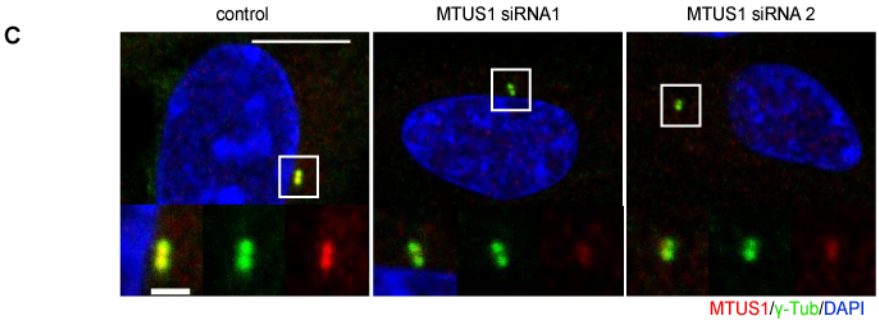


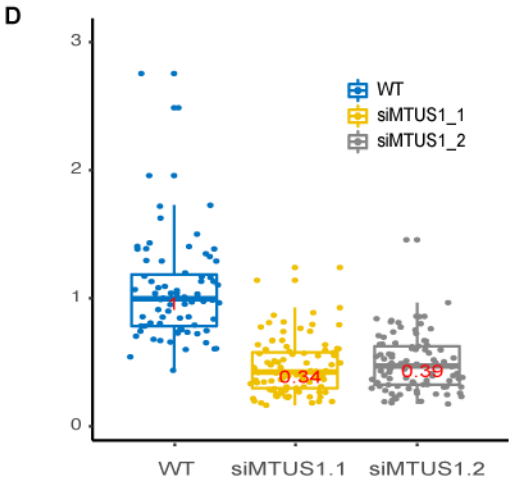


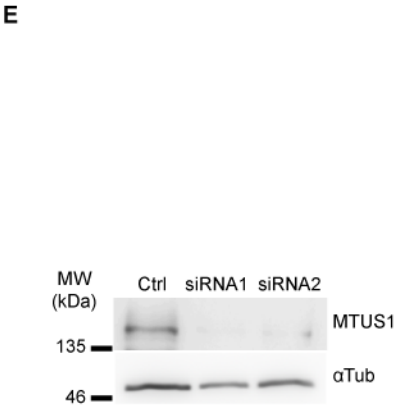

### 3.1.2 ssx2ip and cep135 is increased during oocyte growth and maturation

As we decided to focus on these three proteins (wdr8, ssx2ip and cep135) and we knew that these three proteins are expressed in meiotic egg cytoplasm, we wanted to know how much they contributed to oocyte growth and maturation process. We collected oocytes from the ovary of *Xenopus* and divided them into different stages according to their sizes. The oocytes in different sizes are arrested at the prophase diplotene stage of meiosis I. During this stage, they begin to accumulate proteins and mRNA for late maturation and early embryo cell division. Fig.6A, B, D shows that ssx2ip's signal slowly accumulated during oocyte growth and then sharply increase after maturation, which consists with Bärenz's result of SSX2IP's dynamic expression level in progesterone induced egg maturation progression (Bärenz et al., 2013). Also, cep135 is barely seen in oocyte stages, only visible in egg stage. This means that frog probably needs ssx2ip both for meiosis and early embryonic mitosis and cep135 only functions in mitosis.

Most protein regulations are controlled by transcription and translation only gives a fine tune. However, in oocyte maturation and early embryo development, the translation of dormant mRNA accumulated before is under strict control to initiate some key processes. The initiation of translation needs cap structure ($m^7$GppN) at 5' end of the mRNA to recruit ribosome. Poly(A) tail can facilitate cap structure recruitment through poly(A)-binding protein (PABP), which form a bridge between 5' and 3' mRNA. The masking of dormant mRNA and its activation by cytoplasmic polyadenylation are governed by cytoplasmic polyadenylation element binding protein (CPEB) mediated mechanisms (Mendez & Richter, 2001). Cytoplasmic polyadenylation needs the cytoplasmic polyadenylation element (CPE: for recruting CPEB) and hexanucleotide AAUAAA (Hex, for recruiting CPSF: cleavage and polyadenylation specificity factor) in 3' UTR. CPEB regulated mRNA masking also needs a Pumilio binding element (PBE). Upon oocyte activation, CPEB can be phosphorylated at different stages by different kinases to release this repression state (Villalba, Coll, & Gebauer, 2011). Accordding to a "CPE code" proposed by Roderic Guigo's Lab (Piqué, López, Foissac, Guigó, & Méndez, 2008), I predicted cis-elements that exist at the 3'UTRs of cep135, ss2ip and wdr8 (Fig. 6C). We can see that cep135 and ssx2ip have all the elements involved in CPEB regulation. At the beginning of their 3'UTRs, there are tandem CPE clusters which indicate CPEB repression before hormone activation. PBE,

together with three CPEs, can increase the repression greatly. Translational activation requires a single CPE and Hex with an optimal distance of 25nts. ssx2ip showed a consistent activation pattern after hormone injection. In contrast, the distance of single CPE and Hex of cep135 3'UTR is not the optimal value. This data strongly suggests that both cep135 and ssx2ip are regulated by CPEB controlled protein translation. In contrast, due to a short 3'UTR, there was no full set cis-element detected on wdr8. Either wdr8 is not controlled by a CPEB mechanism or what we know is an incorrect 3'UTR sequence.

We next compared the protein expression levels in *Xenopus* egg extract and *Xenopus* xl177 somatic cell lysates with coomassie staining as loading control (Fig. 6E,F). While abundant marker proteins are enriched in the egg cytoplasm (α-tubulin, gapdh, nedd1), cep135 has a higher expression in the somatic cell lysates. This is consistent with the fact that oocytes do not bear centrioles while somatic cells do. The satellite protein ssx2ip seemed to have a strong Metaphase-dependent modification.

Fig. 6. ssx2ip and cep135 protein expression level is increased during oocyte growth and maturation (page 38).
(A) Immunoblotting of ssx2ip, cep135 and α-tubulin. The total amount protein was controlled by gapdh, as well as commassie staining (D).
(B) Measurement of immunoblotting bands with the strongest band as 1 to show relative intensity.
(C) CPEB regulated cis-element prediction (web sever: https://genome.crg.es/CPE/server.html). Different colors represent different cis-element as indicated.
(D) Commassie loading control of different sized oocytes.
(E) Protein expression level beween egg extact and somatic xl177 cell lysate.
(F) Commassie loading control of egg extract and somatic xl177 cell lysate.

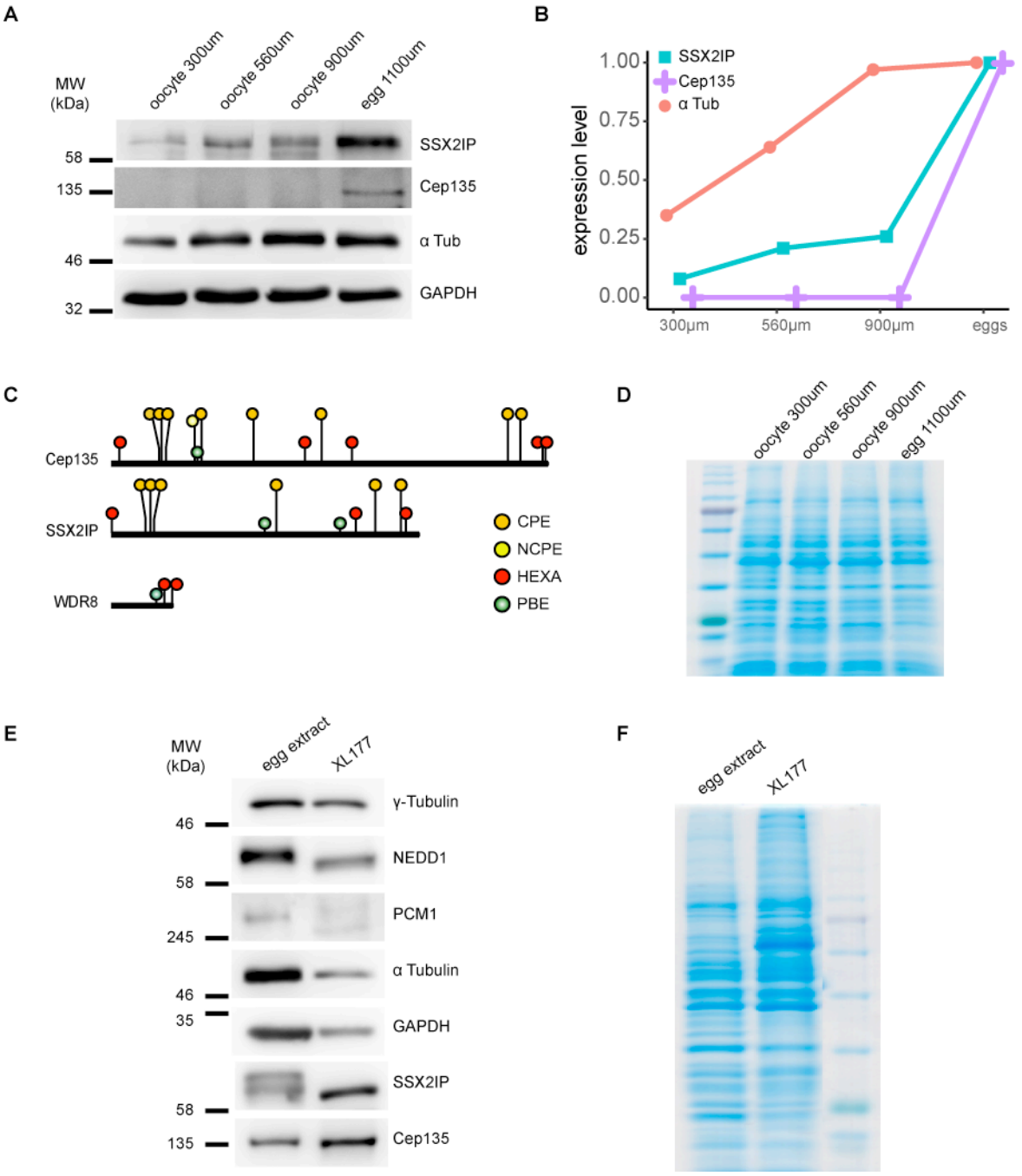
A
MW (kDa)
oocyte 300um
oocyte 560um
oocyte 900um
egg 1100um
58
135
46
32
SSX2IP
Cep135
α Tub
GAPDH
B
SSX2IP
Cep135
α Tub
expression level
1.00
0.75
0.50
0.25
0.00
300μm
560μm
900μm
eggs
C
Cep135
SSX2IP
WDR8
CPE
NCPE
HEXA
PBE
D
oocyte 300um
oocyte 560um
oocyte 900um
egg 1100um
E
MW (kDa)
egg extract
XL177
46
58
245
46
35
58
135
γ-Tubulin
NEDD1
PCM1
α Tubulin
GAPDH
SSX2IP
Cep135
F
egg extract
XL177

### 3.1.3 cep135 depletion effects bipolar spindle formation in *Xenopus* egg extract

*Xenopus* egg extract is a very good system to study spindle formation. *Xenopus* oocytes get rid of centrioles during meiosis and the low nucleus/cytoplasm ratio makes it quite different from somatic cells. Since the large amount of proteins accumulated by oocytes are required for cell division during early embryogenesis, which happens very quickly without interphase, egg extract with centrosomes also recapitulate early embryonic mitosis. In order to check cep135's function, we tested aster formation after cep135 depletion in RanQ69L added egg extract, which mimics chromosome addition (Bärenz et al., 2013). Asters readily were formed despite cep135 depletion. Then we tested bipolar spindle formation with sperm addition in cycled egg extract. We added sperm (comprising chromosomes and centrioles) into metaphase arrested egg extract and sent it to interphase to replicate chromosome and centrioles (Sawin, LeGuellec, Philippe, & Mitchison, 1992). In the cycled egg extract, cep135 depleted samples formed monopolar spindles instead of bipolar spindle in controls. cep135 expression by addition of a respective mRNA to depleted egg extract could rescue the formation of bipolar spindles (Fig.7). This means that Cep135 maybe not required for meiosis but for early embryo mitosis. It make sense that cep135 as cartwheel tip component and component of the pericentriolar material is required in mitosis. This results is also consistent with Fig.6A in which cep135 was only detectable in eggs not in oocytes. cep135 expression may prepare the formation of new centrosomes after sperm fusion and these new centrosomes will facilitate early embryonic mitosis.

Our lab has previously published that ssx2ip depletion in sperm added egg extract caused the assembly of monopolar spindles (Bärenz et al., 2013). Our immunoprecipitation results showed that wdr8 depletion co-depleted the majority of cep135 and ssx2ip proteins. The outcome of wdr8 depletion is quite obvious and self-explained. It is impossible to check depletion efficiency with our homemade wdr8 antibody which do not give an band on Western blot. Therefore, we moved to somatic cell line to explore the functions of these three tightly related proteins.

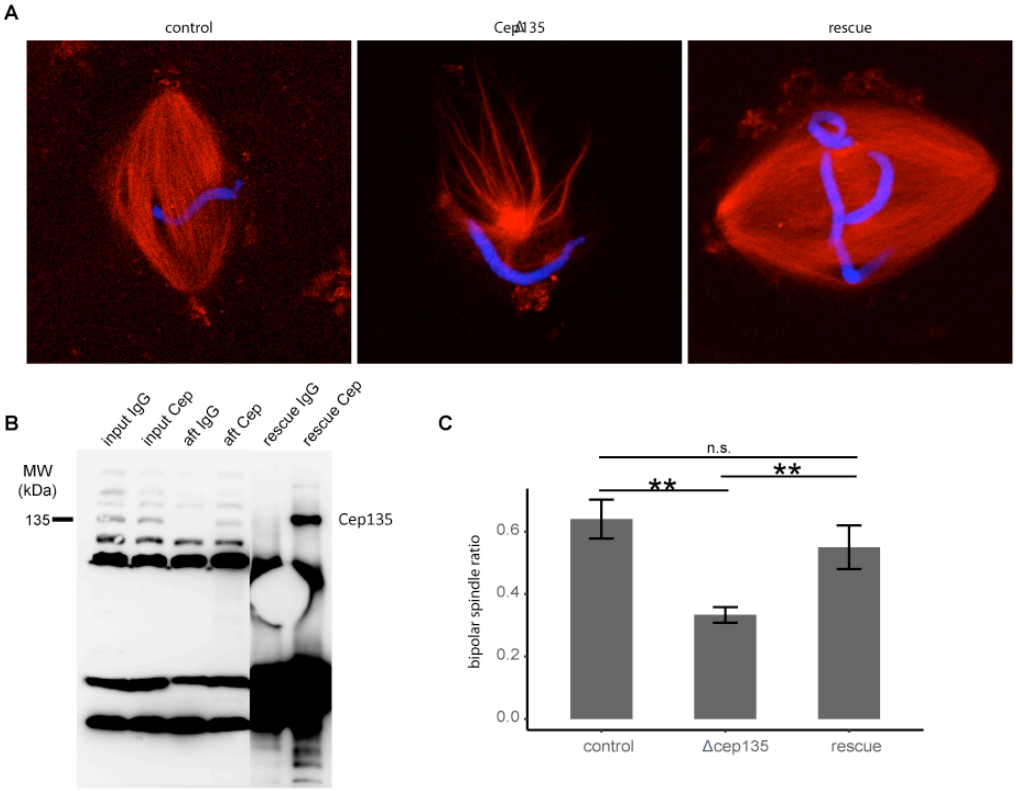


Fig.7 cep135 depletion effects bipolar spindle formation in *Xenopus* egg extract.

(A) Representive images of bipolar spindles formed in IgG control or monopolar spindle formed in cep135 depletion and bipolar spindle formed in cep135 rescue samples after depletion.

(B) Immunoblotting shows the efficiency of depletion and rescue experiments.

(C) Quantitative analysis of bipolar formation in control, depletion and rescue samples. Three indenpent experiments are done. P value are calculated with t-test, two tail.

## 3.2 *cep135*, *wdr8* and *ssx2ip* knockouts generated by CRISPR-cas9 show proliferational abnormality

The hTERT-RPE-1 cell line is a telomerase reverse transcriptase immortalized human Retinal Pigment Epithelial cell line. Its diploid and non-transformed characteristics make it very suitable for genome editing. This polarized epithelial cell line is fit to study cell migration, cell division and ciliogenesis (Bodnar et al., 1998). Although in recent years, many papers used siRNA to monitor the consequences of loss-of-funtion of gene products in somatic cell lines, knockdowns could not erase all the proteins that are expressed. In addition, one needs to consider transfection efficiency, harm caused by tranfection chemical and time-limited analysis. With the availability of the CRISPR-cas9 system, we can monitor

cells after a complete knock-out of individual gene products. Moreover, knockout clones generated by CRISPR-cas9 yield homogeneous cells that can be confirmed by DNA sequencing. Therefore, I generated crispr knockouts of *cep135*, *wdr8* and *ssx2ip* to check their functions in somatic RPE-1 cell lines. All knockouts were confirmed by DNA sequencing, immunofluorescence and immunoblotting.

For Cep135, I used a gRNA that located in exon 1 to generate several knockout (ko) clones (named *6*, *8* ,*9*) which showed different ko alleles (Fig.8A, B). Cep135's signal disappeared in these three knockouts while γ-Tubulin remained as in control cells (Fig.8C). In Western blot, we could not detect CEP135 in ko lysates (Fig.8D). To exclude the possibility of a second in-frame start codon on exon2 for the wdr8 genes, I generated gRNAs on exon 1, 3 and 5 of wdr8 (Fig.9A). *ko9*, whose gRNA is located on exon 1 showed a big fragment deletion (including the start codon). *ko308* and *ko510* showed 1bp plus and minus frameshifts separately (Fig.9B). Since we could not detect WDR8 by western blotting, we conformed the knockouts through immunofluorescence with antibodies against both C and N terminal peptides of WDR8. WDR8's signal disappeared in the knockouts with both C and N terminal antibodies as seen by immunofluorescence (Fig.9C). This also showed that, in the RPE-1 cell line, the second predicted ATG in exon 2 did not exist. If it were, *ko9* would not have lost its signal with both C and N terminal antibodies. For SSX2IP, gRNAs that located on exon2 and 3 were generated (Fig.10A). Five clones were isolated. The separate sequencing results of the two alleles of *ko2-5* with T-A cloning as shown in Fig.10B. *ko2-13* and *ko3-7* had the same two alleles. Although we didn't separate the two alleles of *ko3-9* and *ko3-15*, we could still observed the frameshifts for both alleles (Fig.9B). WDR8's signal around gamma Tubulin disappears in all knockouts when using both the C and N terminal antibody (Fig.9C).

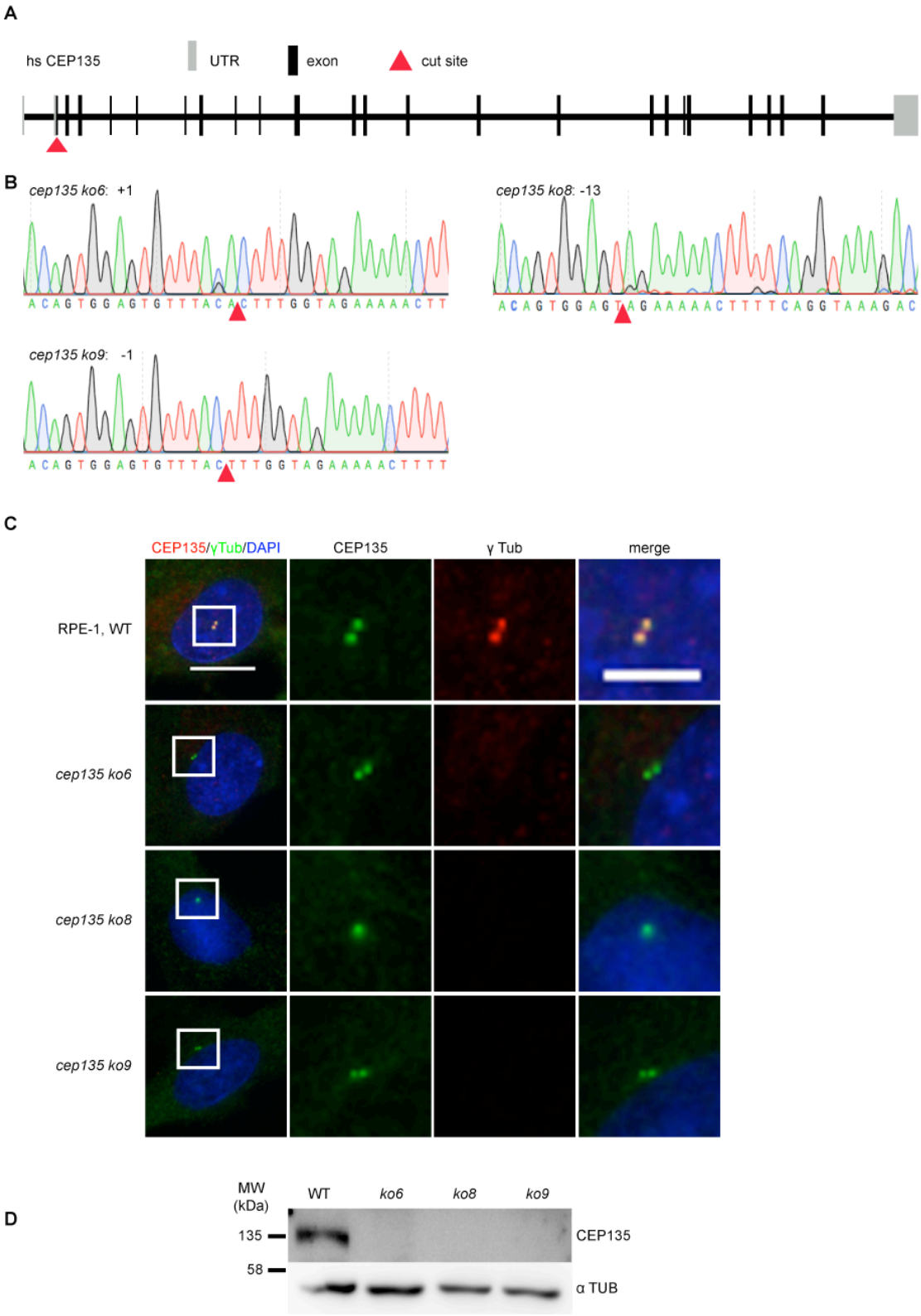
A
hs CEP135
UTR
exon
cut site
B
cep135 ko6: +1
cep135 ko8: -13
cep135 ko9: -1
C
CEP135/γTub/DAPI
CEP135
γ Tub
merge
RPE-1, WT
cep135 ko6
cep135 ko8
cep135 ko9
D
MW (kDa)
WT
ko6
ko8
ko9
135
58
CEP135
α TUB

Fig.8 Confirmation of *cep135* knockouts in RPE-1 cell line (page 42).

(A) Schematic image to show the location of CEP135 crispr guide RNA.

(B) Sequencing results of separated *cep135* knockout cell lines. A-T-C-G are as indicated in green-red-blue-black colors.

(C) Immnuofluorescence shows the disappearance of CEP135 signal in knockout cell lines. Scale bar is 10μm and 5μm for the enlarged area.

(D) Immunoblotting shows that the CEP135 band is lost in knockout cell lysates.

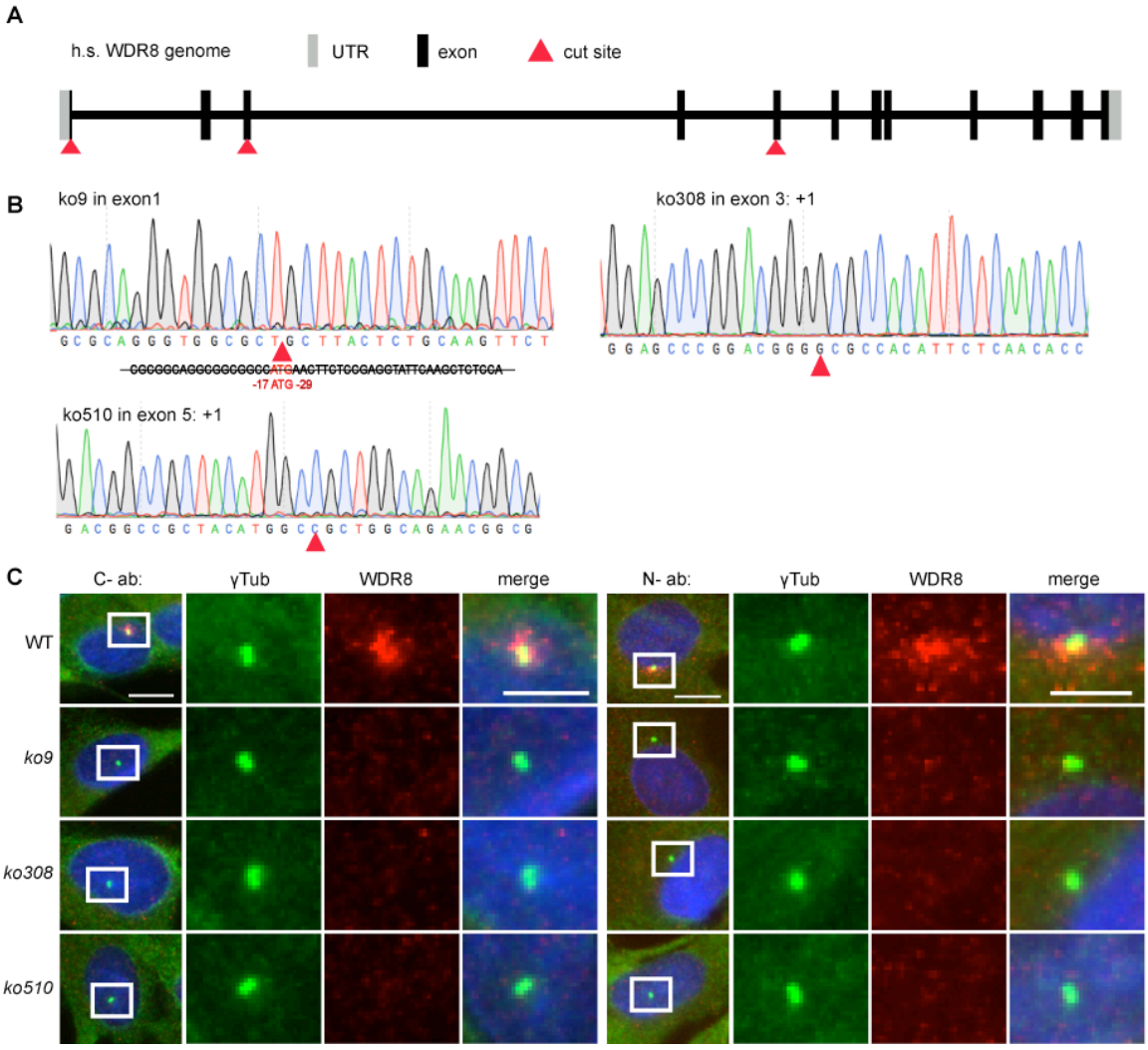


Fig.9 Confirmation of *wdr8* knockouts in RPE-1 cell line

(A) Schematic image to show the WDR8 crispr guide RNA location in exons 1, 3 and 5.

(B) Sequencing results of separated *wdr8* knockout cell lines. A-T-C-G are as indicated in green-red-blue-black colors.

(C) Immnuofluorescence shows the disappearance of WDR8 signal in knockout cell lines with WDR8 both C and N terminal generated antibodies. Scale bar is 10μm and 5μm for the enlarged area.

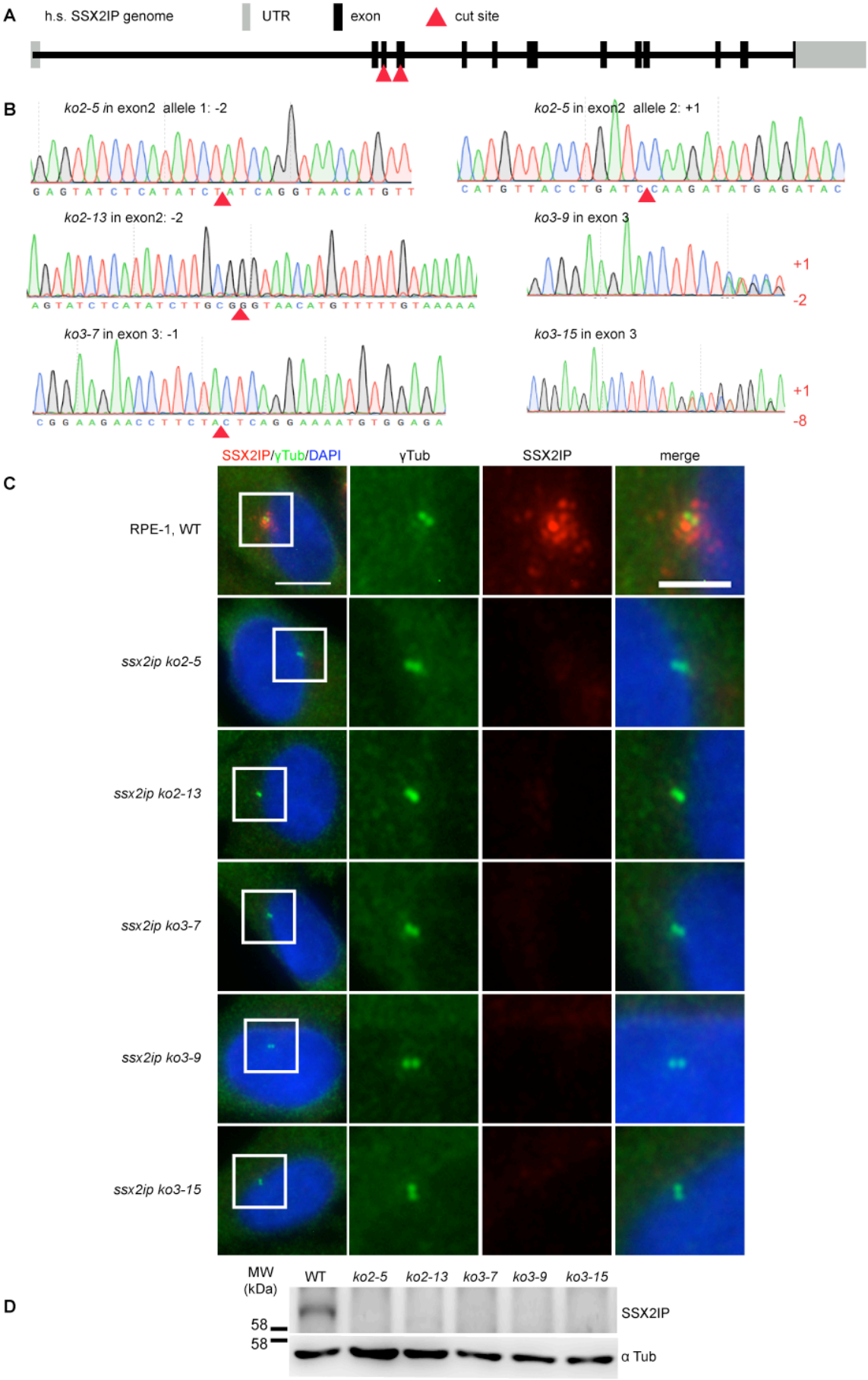
A
h.s. SSX2IP genome
UTR
exon
cut site
B
ko2-5 in exon2 allele 1: -2
ko2-5 in exon2 allele 2: +1
ko2-13 in exon2: -2
ko3-9 in exon 3
+1
-2
ko3-7 in exon 3: -1
ko3-15 in exon 3
+1
-8
C
SSX2IP/γTub/DAPI
γTub
SSX2IP
merge
RPE-1, WT
ssx2ip ko2-5
ssx2ip ko2-13
ssx2ip ko3-7
ssx2ip ko3-9
ssx2ip ko3-15
D
MW (kDa)
WT
ko2-5
ko2-13
ko3-7
ko3-9
ko3-15
58
58
SSX2IP
α Tub

Fig.10 Confirmation of *ssx2ip* knockouts in RPE-1 cell line (page 44).

(A) Schematic image to show the SSX2IP crispr guide RNA location in exon 2 and exon 3.

(B) Sequencing results of separated *ssx2ip* knockout cell lines. A-T-C-G are as indicated in green-red-blue-black colors.

(C) Immnuofluorescence show the disappearance of SSX2IP singal in knockout cell lines. Scale bar is 10μm and 5μm for the enlarged area.

(D) Immunoblotting shows SSX2IP band is lost in knockout cell lysates.

After we got CRISPR knockout cells, we first checked whether there were consequences to the cell cycle using a proliferation assay and DNA content an with Propidium Iodide. During daily cell handlings, I observed that *ssx2ip* knockout grew slowly, which was consistent with our proliferation assay (Fig.11A). *wdr8* knockout cells, in turn, show slightly faster growth speed, while *cep135* knockout cells do not show any growth abnormalities. MTUS1, as a novel WDR8 interactor, represses cell proliferation and delays metaphase process (Rodrigues-Ferreira et al., 2009). The impacts of WDR8, MTUS1 and SSX2IP on cell cycle need to be further checked. To further analyse their cell cycle, we quantified the Propidium Iodide stained samples. Even though there was no very obvious change between control and knockout cells, we could see that, *wdr8* knockout had more G2/M cells and *ssx2ip* knockout less G2/M cells (Fig.11B, C, D). *cep135* knockout cells did not show any defects both in the proliferation assay and flow cytometry assay.

Fig.11 Centrosome satellite proteins *wdr8* and *ssx2ip* knockouts show some growth abnormalities while cell growth is unaffected in *cep135* knockout (page 46).

(A) Cell proliferation assay of *wdr8*, *ssx2ip* and *cep135* knockouts. 1x10^5 cells were seeded on 3.5cm plate and cells were collected by trypsinization at indicated times (20h, 32h, 44h, 56h).

(B) Gating method of flow cytometry to check cell cycle of these knockouts. Propidium Iodide staining gives the signal for detection. P2 gating is to screen cell debris out (left); P6 gating is to screen doublets out (middle); representative images of Propidum Iodide signal (right).

(C) Overlapping plot of PI measurement of three knockouts to show the cell cycle differences between control and knockouts.

(D) Statistical value of tetraploid DNA content. Three independent samples were collected. The P value was calculated with a t-test, two tailed.

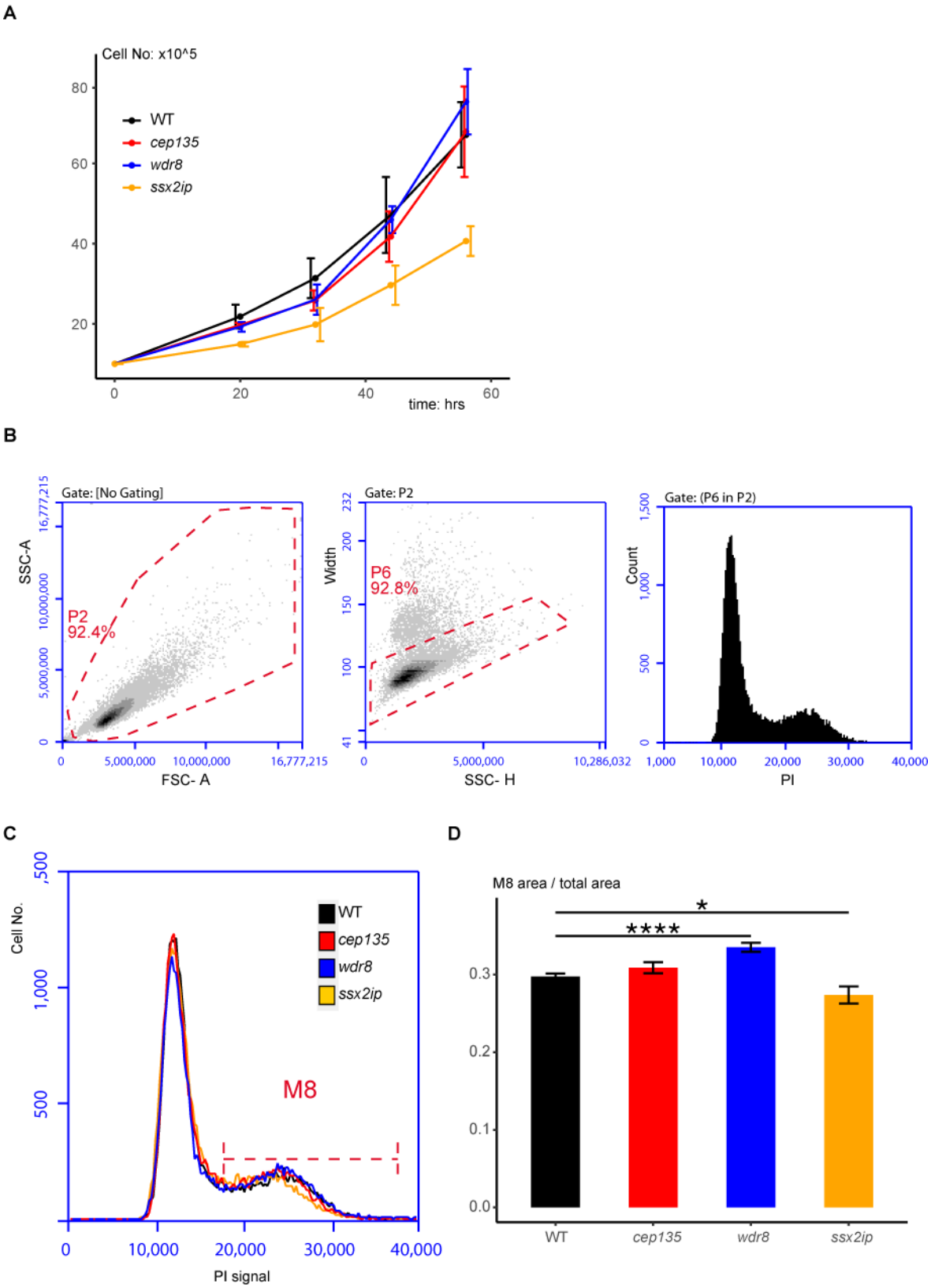
A
Cell No: x10^5
WT
cep135
wdr8
ssx2ip
time: hrs
B
Gate: [No Gating]
P2
92.4%
SSC-A
FSC- A
Gate: P2
P6
92.8%
Width
SSC- H
Gate: (P6 in P2)
Count
PI
C
Cell No.
M8
PI signal
D
M8 area / total area
WT
cep135
wdr8
ssx2ip

## 3.3 Protein expression level of CEP135, WDR8 and SSX2IP is dependent on each other in RPE-1 cell line

The Mass Spectrometry results in Fig.5 and the already published data confirmed the interaction of the three proteins and suggested complex formation, so we speculated that their functions are interdependent. To explore whether loss of one protein affects the other two proteins' expression level, I used both immunoblotting and immunofluorescence. Fig.12A shows that CEP135 total expression level was decreased both in *wdr8* and *ssx2ip* knockouts. While, the centrosomally localized CEP135 signal remained unchanged (Fig.12F, G). Although PCM1 expression level was decreased in *ssx2ip* knockout (Fig.12A), the centriolar satellite signal intensity was not significantly changed. In contrast, the centrosomal PCM1 was more dispersed (Fig.12B, C). The SSX2IP total protein level was slightly decreased in *cep135* knockout and obviously decreased in *wdr8 knockout* (Fig.12A). The SSX2IP centriolar satellite signal is obviously reduced and dispersed in both *wdr8* and *cep135* knockouts (Fig.12D, E). In contrast, the total expression level of γ-Tubulin was unchanged in the three knockouts as seen by immunoblotting.

In summary, loss of the satellite proteins WDR8 and SSX2IP affected expression levels of the centrosomal protein CEP135 while its targeting to the centrosome seemed to be conmpensated, so that the CEP135 signal at the centrosome remained unchanged. As an evolutionary conserved interaction partner, loss of WDR8 affected SSX2IP expression levels as well as localization as show by both immunoblotting and immunofluorescence. As a centrosomal protein, CEP135 may be regulated and targeted by additional interaction partners. As centriolar satellite protein, SSX2IP and WDR8 could have downstream targets, which may effect cell growth while the specific functions of CEP135 can be compensated.

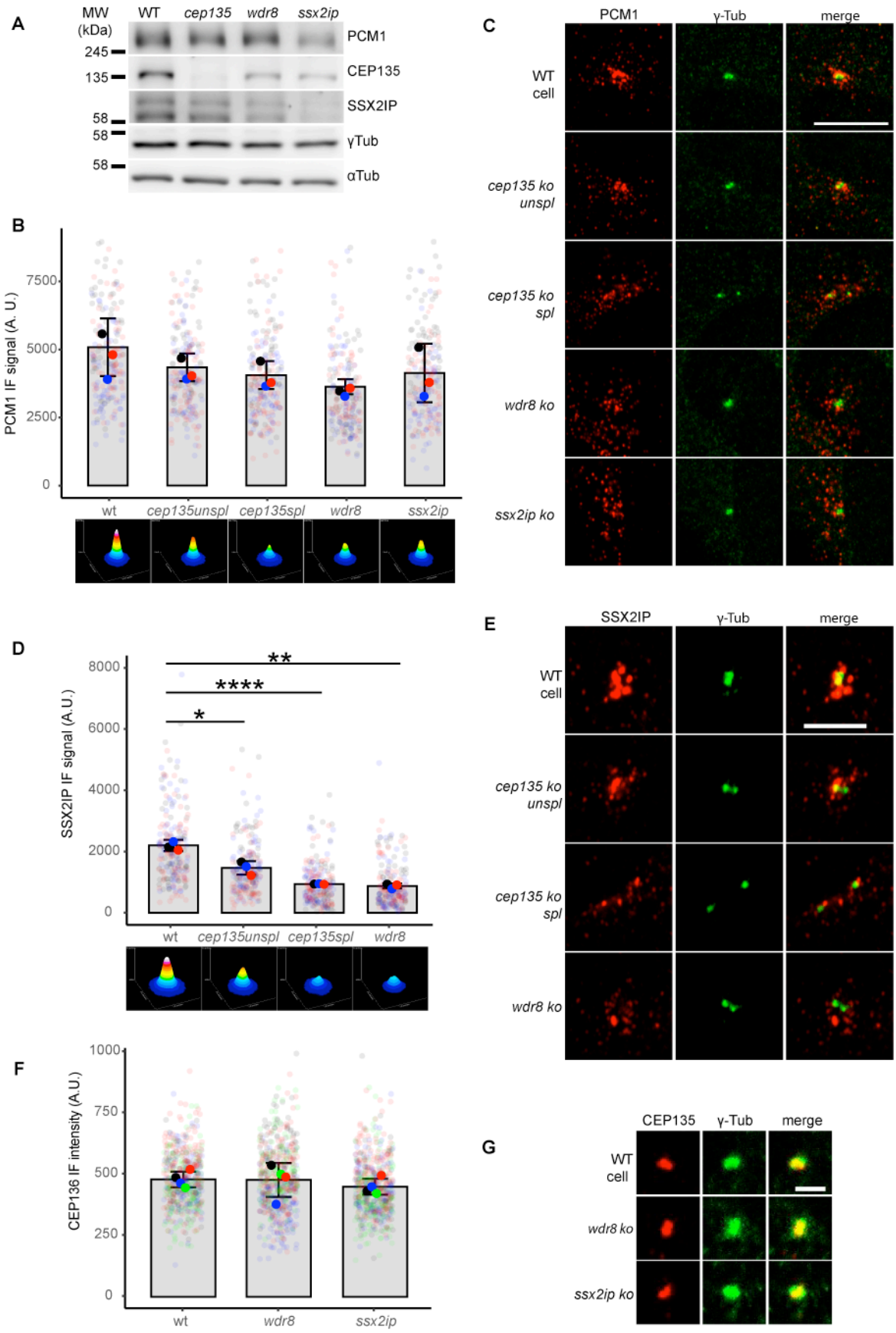
A
MW (kDa)
WT
cep135
wdr8
ssx2ip
245
135
58
58
58
PCM1
CEP135
SSX2IP
γTub
αTub
B
PCM1 IF signal (A. U.)
7500
5000
2500
0
wt
cep135unspl
cep135spl
wdr8
ssx2ip
C
PCM1
γ-Tub
merge
WT cell
cep135 ko unspl
cep135 ko spl
wdr8 ko
ssx2ip ko
D
SSX2IP IF signal (A.U.)
8000
6000
4000
2000
0
**
****
*
wt
cep135unspl
cep135spl
wdr8
E
SSX2IP
γ-Tub
merge
WT cell
cep135 ko unspl
cep135 ko spl
wdr8 ko
F
CEP136 IF intensity (A.U.)
1000
750
500
250
0
wt
wdr8
ssx2ip
G
CEP135
γ-Tub
merge
WT cell
wdr8 ko
ssx2ip ko

Fig.12 Protein expression levels of CEP135, WDR8 and SSX2IP are dependent on each other (page 48).

(A) Immunoblotting to show total protein expression levels of PCM1, CEP135, SSX2IP and γ-Tubulin. α-Tubulin was used as the control of total protein loaded.

(B) Statistics of PCM1 signal around the centrosome. A square with 14.5μm side length was drawned with γ-Tubulin in the center.

(C) Representative images of the PCM1 signal together with γ-Tubulin. Scale bar is 10 μm.

(D) Statistics of SSX2IP signal around γ-Tubulin. A square with 8.6 μm side length is drawned with γ-Tubulin in the center.

(E) Representative images of the PCM1 signal together with γ-Tubulin. Scale bar is 5 μm.

(F) Statistics of the CEP135 signal in immunofluorescence. ImageJ threshold was used to choose the region of CEP135' signal.

(G) Representative images of the CEP135 signal. Scale bar is 2 μm.

(B, D, F) Bar graphs show the total intensity of each indicated-sized area in each cell. The detailed data points are shown in transparent spots with a big nontransparent spot showing the mean value. The surface plot is the sum of all the images to show its signal dispersion. Three or four replicates were done. Error bar is the stdv with the mean of all replicates, P value was calculated with a t-test, two tailed.

## 3.4 *cep135*, *wdr8* and *ssx2ip* knockouts have no defects on ciliogenesis and spindle formation in somatic cell line

Next, we checked whether the knockouts affected ciliogenesis and spindle formation. In *wdr8* and *ssx2ip* knockdown cells, we had previously observed ciliogenesis defects (Kurtulmus et al., 2016). In contrast, the knockouts did not show any defects in ciliogenesis or cilium length (Fig.13A, B). This may seem surprising, however, many proteins have been reported to bear different phenotypes in cell upon knockout compared to knockdown conditions. *Drosophila* undergoes normal development even without centrosomes (Basto et al., 2006) and mammalian cells form bipolar spindles after laser centrosome ablation (Khodjakov, Cole, Oakley, & Rieder, 2000). In *cep135* knockouts, cilia could still form normally but showed premature split centrioles. This is consistent with a *c-nap1* knockout which also didn't show any ciliogenesis defects but premature centrosome splitting in interphase (Mazo et al., 2016). Of note, spindle length was also not affected in these knockouts (Fig.13C), which shows a different phenotype compared to knockdown in Hela cell that producing shorter spindles (Hori et al., 2015).

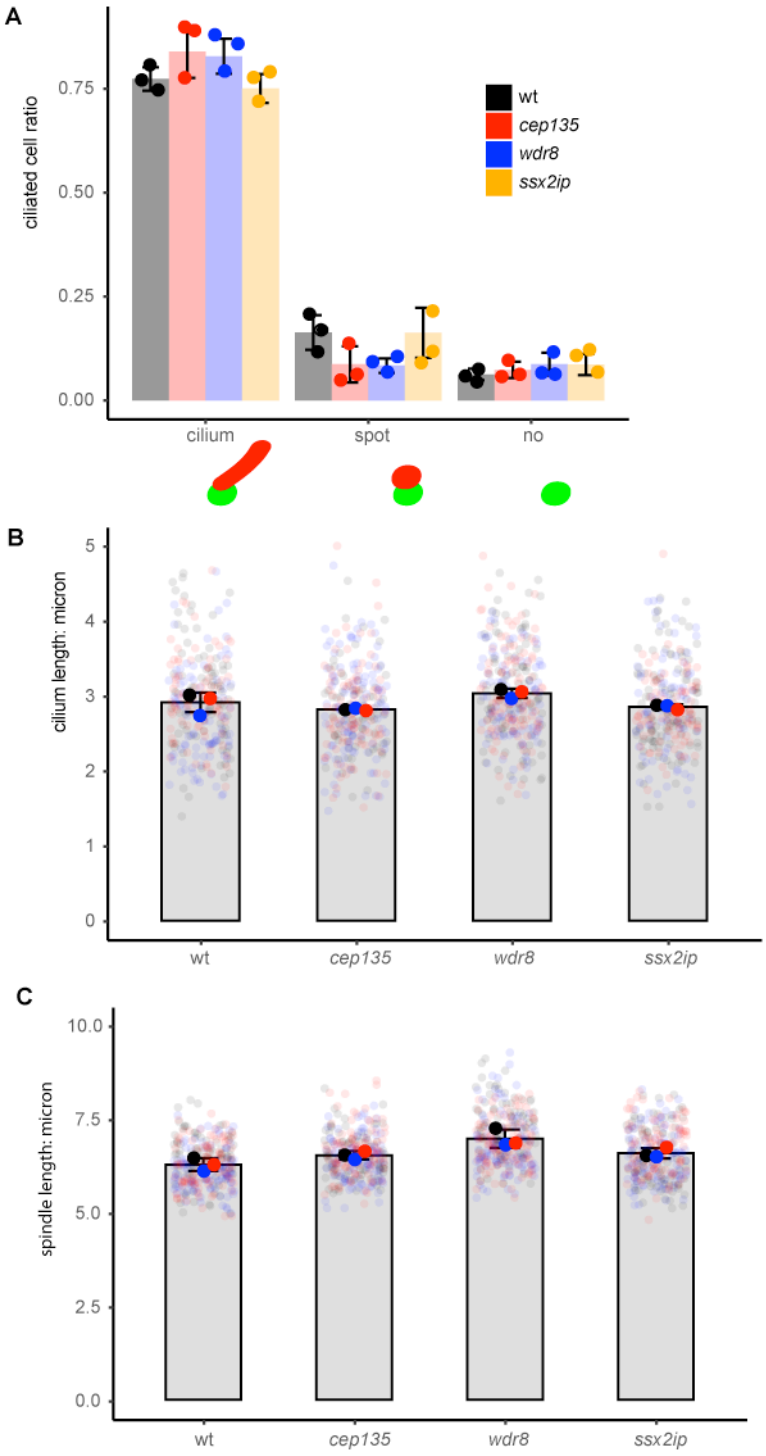


Fig.13 *cep135*, *wdr8* and *ssx2ip* knockouts have no defects on ciliogenesis and spindle formation in RPE-1 cells.

(A) ARL13b staining to show ciliogenesis of *cep135*, *wdr8* and *ssx2ip* knockouts. The ciliogenesis was shown as complete cilia, spot signal and no signal. Green represents γ-Tubulin signal and red represents ARL13b signal.

(B) Cilia length of *cep135*, *wdr8* and *ssx2ip* knockout cells.

(C) Spindle length of *cep135*, *wdr8* and *ssx2ip* knockouts. For (A)(B)(C), three replicates were done and the P value were calculated with a t-test, two tailed.

## 3.5 *cep135* knockouts show premature centrosome splitting

### 3.5.1 *cep135* knockouts show premature centrosome splitting and diminished pericentrosomal material

As reported previously, a CEP135 knockdown showed premature centrosome splitting (Kim et al., 2008), and our *cep135* CRISPR knockout showed a consistent phenotype (Fig.14A). As shown in Fig.14B, around 30% of centrosomes in an unsychronized, population with cells most cells being in G1 or S phase cells were split. That suggests that splitting may happen even early during the cell cycle. The intercentrosomal distance was greatly increased after Nocodazole treatment for 1 hour and with the split centrosome ratio (intercentrosomal distance is more than 1μm) increased to 67% (Fig.14D). This may seem counterintuitive as the movement of centrosomes for splitting needs microtubules as tracks. With Nocodazole depolymerisation, the increment of centrosome distance could have been due to random movement (Buendia, Bré, Griffiths, & Karsenti, 1990). Importantly, the γ-Tubulin intensity was greatly decreased in split centrosome in *cep135 knockout* cells (Fig.14C). Likewise, a main PCM component, CDK5RAP2, was decreased as well (Fig.14E). CDK5RAP2 siRNA knockdown has been previously shown to undergo premature centrosome splitting in interphase in a somatic cell line (Graser, Stierhof, & Nigg, 2007). CDK5RAP2 is involved in centrosome maturation and strongly increases in G2 and mitotic phases. Proper degradation of CDK5RAP2 in telophase ensures normal centrosome disengagement and separation (Pagan et al., 2015). We also compared the γ-Tubulin and CDK5RAP2 signal intensities between two split centrioles in individual cells. In Fig.14G we can see that most centrosome pairs had comparable γ-Tubulin signals in individual cells. In contrast, CDK5RAP2 showed different amounts in a centrosome pair in the same cell (the density plot peak for CDK5RAP2 is around 0.2 and for γ-Tubulin is 0.5-0.9). One should keep in mind that the γ-Tubulin and CDK5RAP2 signal of both centrsomes was still decreased. γ-Tub localizes both in the centriolar wall and in the PCM in interphase. It might be speculated that some γ-Tubulin in the core part was unaffected in cells showing premature centrosomes splitting and mother and daughter centrosomes had almost the same amount. For CDK5RAP2, as a main PCM component, only the mother centrosomes retained large amounts of PCM, while the daughter centrosome had only little PCM assembled. Normally, daughter centrosomes will recruit their own PCM in G1 phase to complete centriole to centrosome transition before centriolar duplication. However, in *cep135* knockout cell, we

don't know whether the split daughter centrosome will recruit its PCM in G1, S phase, or G2 phase (centrosome maturation). This also underlines that CDK5RAP2 is a main component for PCM assembly.

In *cep135* knockout cells, the interphase PCM was diminished without affecting centrosome maturation in G2 and Prophase, which covers the imperfection of interphase PCM. In telophase, mitotic PCM needs to change back to interphase PCM, then the imperfection of interphase PCM in *cep135* knockout is shown which leads to premature centrosome splitting. With diminished PCM, a variety of forces (actin driven cohesion force, motor protein driven splitting force, centrosome linker proteins and PCM driven cohesion force) lost the balance to keep centrosome together, so they split. This splitting concurrently caused PCM scattering (Fig.14F). In a regular cell cycle, the daughter centrosome recruits new PCM components after disengagement and before splitting. Therefore, two perfect centrosomes build before centrosome separation in G2 phase. Premature split centrosomes seem not to not affect later centrosome maturation and centrosome separation as a prerequisite for bipolar spindle formation. Apparently, there is no checkpoint to monitor that each centriole recruits a minimal amount of PCM before separation.

Fig.14 *cep135* knockout cells show premature centrosome splitting and diminished PCM (page 53).

(A) *cep135* knockout cells that show premature centrosome splitting. γ-Tubulin was stained to indicate centrosomes. Scale bar, 20μm.

(B) Centrosome splitting ratio at different stages in *cep135*, *wdr8* and *sx2ip* knockouts cell lines.

(C) The distance between centrosomes is greatly increased after 33mM Nocodazole one hour treatment in *cep135* knockouts.

(D) The intensity of γ-Tubulin is decreased in splitting centrosomes in *cep135 knockout* cells.

(E) CDK5RAP2 intensity in wildtpe and *cep135* knockout cells.

(F) Density plot to show the ratio of two centrosomes in one cell (the ratio is calculated by low signal intensity/high signal intensity). The figure shows the total result of three replicates, 300 γ-Tubulin signals and 300 CDK5RAP2 signals were measured in total.

(G) Representative images to show γ-Tubulin and CDK5RAP2 signal in split and unsplit centrosomes in wildtype and *cep135* knockout cells. Scale bar 10μm and 2μm for enlarged area.

(D)(E)The signal intensity of split centrosome in *cep135* knockout cells was measured singlely (each data point refers to one centrosome) or in pairs (each data point refers to the value of two centrioles in one cell). Three independent experiments were done, the error bar was the stdv of the mean value of three experiments. The P value was calculate with a t.test, two tailed.

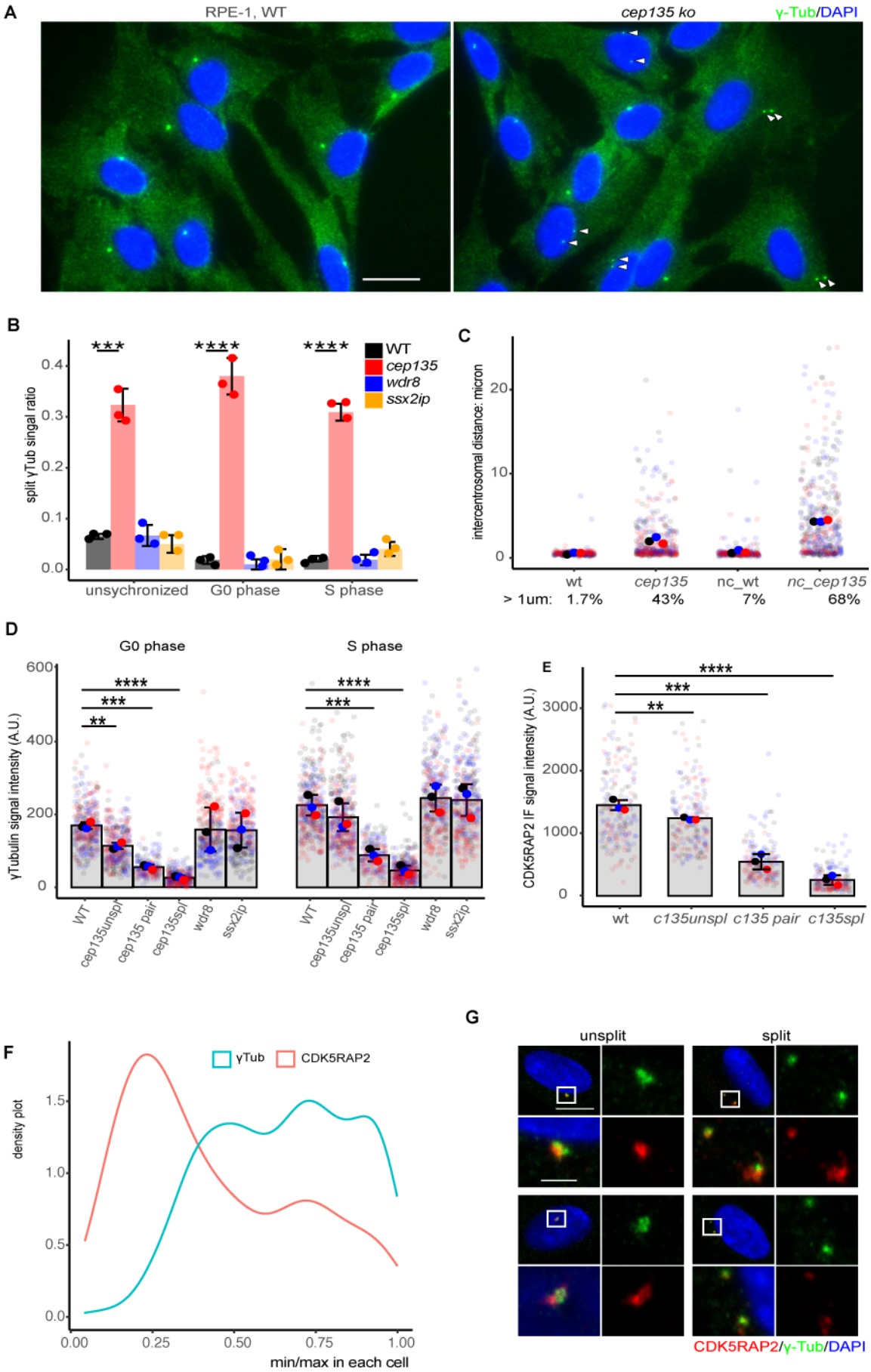
A
RPE-1, WT
cep135 ko
γ-Tub/DAPI
B
split γTub singal ratio
WT
cep135
wdr8
ssx2ip
unsychronized
G0 phase
S phase
C
intercentrosomal distance: micron
wt
cep135
nc_wt
nc_cep135
> 1um: 1.7%
43%
7%
68%
D
G0 phase
S phase
γTubulin signal intensity (A.U.)
WT
cep135unspl
cep135 pair
cep135spl
wdr8
ssx2ip
E
CDK5RAP2 IF signal intensity (A.U.)
wt
c135unspl
c135 pair
c135spl
F
γTub
CDK5RAP2
density plot
min/max in each cell
G
unsplit
split
CDK5RAP2/γ-Tub/DAPI

### 3.5.2 Abnormal microtubule polymerization in *cep135* knockout cells

As *cep135* knockout lead to diminished PCM in interphase, we performed a microtubule regrowth assay after depolymerization of MT in the cold to check whether this diminished and split centrosome will change the microtubule cytoskeleton arrangement. Fig.15 shows all the different aster types formed 15 seconds after regrowth in *cep135* knockout cells. For this experiment, we only counted structures formed by split centrosomes and abnormal structures formed by unsplit centrosomes in *cep135* knockout cells. From Fig.15A we can see that most split centrosomes can form an aster with centrosomes at the center within 15 seconds of regrowth. The two split centrosomes either formed two distinctive asters or two nearby centrosomes so close that the asters were merged. The naturally split centrosomes in L929 cells in interphase reminiscent of the split centrosomes in *cep135* knockout cells (Piel et al., 2000). The PCM was diminished both in split and unsplit centrosomes in *cep135* knockout cells. Consistently, the microtubule regrowth assay revealed scattered microtubules even in unsplit centrosomes (Fig.15D), which suggested an abnormality of the PCM structure in these cells. The scattered MT could also be caused by both split centrosomes, or one centrosome formed aster and the other one formed scattered MTs (Fig.15B, E). After 15 seconds of regrowth, we could observe an aster with centrosome that did not recruit its own MTs (Fig.15C). At 5min of regrowth the MT cytoskeleton rearranged to a single MTOC even in cells with split centroosmes, which have the same situation as in L929 cells (Piel et al., 2000).

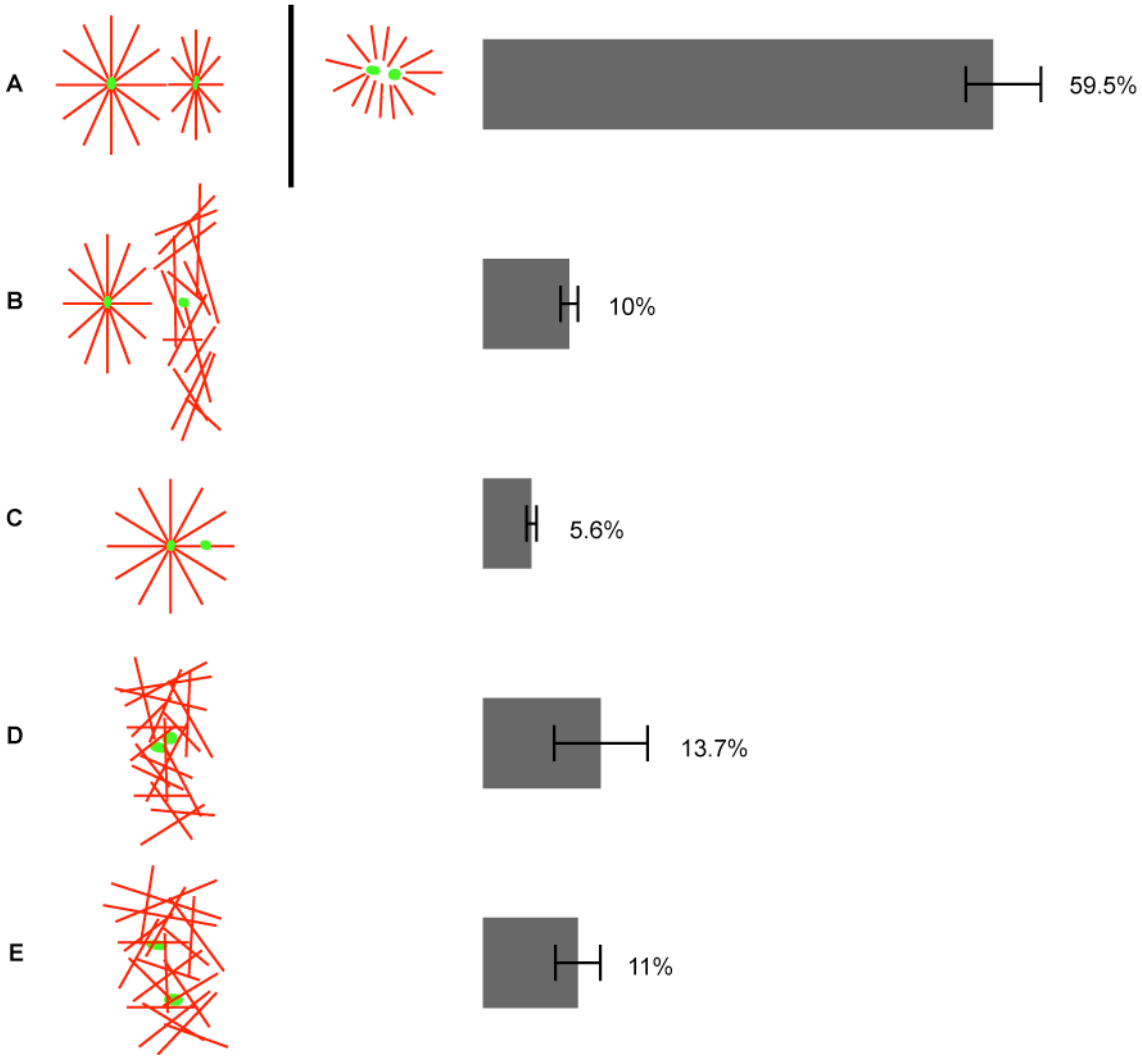


Fig.15 Abnormal microtubule polymerization in *cep135* knockout cells.

The typical patterns of MT regrowth 15 seconds after pre-warmed medium change is shown here. Three replicates were done and around 60 cells were count for each replicate. Error bar is calculated by stdv.

### 3.5.3 Centrosome splitting in *cep135* knockout cells is not dependent on the loss of C-NAP1

The established mechanism of centrosome separation under normal condition involves NEK2A regulated degradation of centrosome linker proteins (CLPs). NEK2A is a kinase that localizes at the centrosome which has a low activity in G1 and mitotic phases, and a high activity in S and G2 phases (Rellos et al., 2007). Centrosome linker proteins that phosphorylated by NEK2A will be disassembled and degraded to allow the separation of

centrosomes (Hossain, Shih, Xiao, White, & Tsang, 2020). Therefore, we stained centrosome linker proteins C-NAP1 and Rootletin and found that these two proteins were lost in split centrosomes in *cep135* knockout cells (Fig.16A). The ones that were not split in *cep135* knockout cells still anchored CLPs. When we calculated the signal intensity in these unplit centrosome in knockout compared with wildtype, the intensity was, however, significantly deduced (Fig.16A,B). To check whether the loss of CLPs is due to NEK2A abnormal upregulation, we checked the NEK2 protein expression level in immunoblotting. These showed that NEK2 had the same expression level as in wildtype and knockout cells. However, C-NAP1's expression was decreased while Rootletin remained at the same expression level (Fig.16C). However, NEK2A's expression level does not necessarily represent its kinase activity , so a kinase assay should be done. C-NAP1's expression may have decreased due to its close relationship with CEP135. Rootletin's expression level was unchanged cannot rule out Rootletin's degradation in 30% split centrosomes with the limited sensitivity of detected proteins. From the results shown in Fig.14, we concluded that split and even unsplit centrosomes in *cep135 knockout* cells have diminished PCM. Diminished PCM and CNAP1 may interfere with proper CLPs recruitment to centrosomes in *cep135* knockout. It remains unclear if the loss of CLPs in split centrosomes was caused by NEK2A-dependent regulated degradation, or if the CLPs could not be recruited to a diminished PCM. Live imaging with Rootletin-GFP cell line or comparing NEK2A activity in wildtype and *cep135* knockout cells would be good methods to answer this question.

C-NAP1 is very important for anchoring centrosome linker proteins. The functions of CEP135 in centrosome cohesion was thought to be mediated by the interaction with C-NAP1 (Kim, Lee, Chang, & Rhee, 2008; T. Hardy et al., 2014). Here we show that, in *cep135* knockout cells, CNAP1 can still recruit to centrosomes before premature splitting indicating that CEP135 is not the only targeting and anchoring factor for CNAP1. Publications and our results both show that the loss of CEP135 will decrease the efficiency of CLPs recruitment to centrosome. Loss of CEP135, as a component of the PCM, may have more severe effects on PCM structure than anchoring C-NAP1. The Centrosome splitting phenotype in *cep135* knockout can not be rescued with PACT-CEP135C (responsible for CNap1 interaction formulate in detail) (Fig.16D). Therefore, CEP135 must have other functions in regulating centrosome separation than just being a CNap1 anchoring protein, while C-NAP1 must have other interacting proteins to anchor itself to the proximal end of the centrosome. Fig.16E

shows the expression of CEP135 in the knockout cells can rescue γ-Tubulin and CDK5RAP2's centrosomal signals.

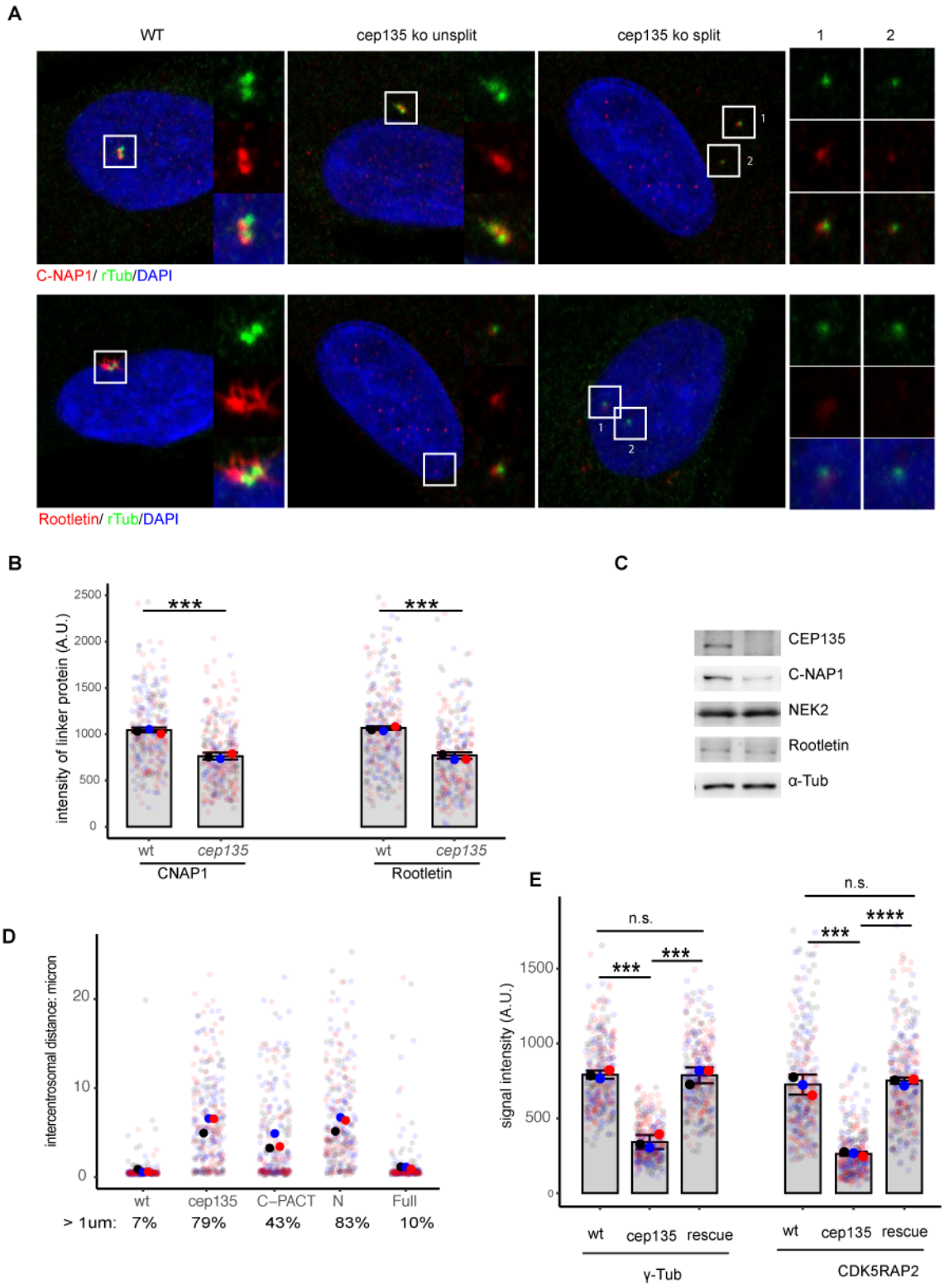

Fig.16 Centrosome splitting in cep135 knockout cells is not dependent on the loss of C-NAP1 (page 57).
(A) Representative images shows the signals of centrosome linker protein CNAP1 and rootletin. In *cep135* knockout cells, unsplit one still anchors CLPs, for the split one, CNAP1 and Rootletin is lost.
(B) Signal intensity of CNAP1 and Rootletin in wildtype and unplit *cep135* knockouts.
(C) Immunoblotting to check protein expression level of NEK2, CNAP1 and Rootletin. Alpha Tubulin was used as the loading control.
(D) Centrosomal distance after nocodazole treatment in wildtype, cep135 knockout and rescue cells (PACT tagged CEP135 C terminal peptides, CEP135 N terminal peptides and CEP135 full length were stably expressed in cep135 knockout cells.)
(E) γ-Tubulin and CDK5RAP2 signals were back to normal level in rescue cells.
(B)(D)(E) The detailed data points are shown in transparent spots with a big nontransparent spot showing the mean value. Three replicates were done. Error bar is the stdv with the mean of all replicates, P value was calculated with a t-test, two tailed.

## 3.6 Mass Spectrometry results of cep135 immunoprecipitation in *Xenopus* egg extract show the subpopulations of cep135 and wdr47 is a novel interactor of cep135

We also generated some cep135 antibodies against cep135 C terminal and N terminal peptides separately (see start of results). Using both cep135 N and C terminal antibodies, we performed immunoprecipitation in Xenopus egg extract. The results we got show two different subpopulations of cep135 and the two subpopulations are functionally related (Fig.17). CEP135 is the tip protein of centriolar cartwheel which templates the formation of the centriolar wall. Fig.17B shows the coimmunoprecipitation of cep135 and centriole duplication proteins cep152 and cep63. Fig.17A showed the coimmunoprecipitation of cep135 with ssx2ip, wdr8 and wdr47. wdr47 is a novel protein that we found to interact with cep135. Just this year, the Zhu lab published a paper about WDR47. They show centrosomal localization of WDR47 and that WDR47 regulates ciliary central microtubules (Liu et al., 2021, Fig.17C). Cep135's loss lead to immotile sperm in Drosophila whose axonemes lack central pair microtubules (Mottier-Pavie & Megraw, 2009). WDR47 and CEP135 must function together to regulate the central MT pair in axonemes. Satellite proteins are the pool that stock or facilitate transporting of PCM proteins. Therefore, SSX2IP, WDR8 and other satellite proteins are responsible for maintaining proper centrosomal localization of CEP135. WDR8 and SSX2IP are paired proteins with the dyfunction of one protein effecting the other. Therefore, we propose that there must be other satellite proteins that can compensate WDR8 and SSX2IP's loss to target enough CEP135 to the centrosome.

A

| Description | Entrez Gene | MW (kDa) | anti-wdr8 | | anti-IgG | |
|---|---|---|---|---|---|---|
| | | | Uniq Spec | Cover (%) | Uniq Spec | Cover (%) |
| cep135 (Centrosomal Protein 135) | 100381167 | 133 | 46 | 40 | 0 | 0 |
| cep152 (Centrosomal Protein 152) | 446951 | 189 | 6 | 4.1 | 0 | 0 |
| cep 63 (Centrosomal Protein 63) | 496369 | 81 | 19 | 37 | 0 | 0 |
| prc1 (Regulator of Cytokinesis 1) | 108711442 | 72 | 17 | 52 | 0 | 0 |

| Description | Entrez Gene | MW (kDa) | anti-cep135 | | anti-IgG | |
|---|---|---|---|---|---|---|
| | | | Uniq Spec | Cover (%) | Uniq Spec | Cover (%) |
| cep135 (Centrosomal Protein 135) | 100381167 | 133 | 23 | 20 | 0 | 0 |
| ssx2ip (SSX Family Member 2 Interacting Protein) | 431921 | 70 | 18 | 23 | 0 | 0 |
| wrap73 (WD Repeat Containing, Antisense To TP73) | 735062 | 52 | 7 | 18 | 0 | 0 |
| wdr47 (WD repeat-containing protein 47) | 108714440 | 102 | 10 | 9.4 | 0 | 0 |

B

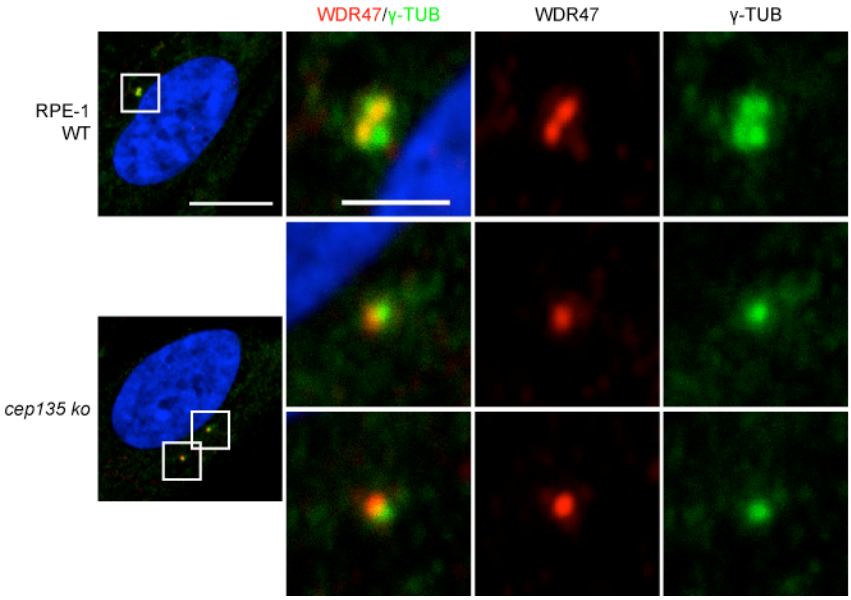


Fig.17 Mass Spectrometry results of cep135 immunoprecipitation in *Xenopus* egg extract

(A) Representative proteins found in cep135 N terminal IP MS list. The whole list is shown in Table 2. Homemade cep135 N terminal antibody binding beads to fish in metaphase CSF-arrested *Xenopus* egg extract to explore cep135 interaction proteins.

(B) Representative proteins found in cep135 C terminal IP MS list. The whole list is shown in Table 2.

(C) WDR47's centriolar localization was show by immunofluorescence. scale bar 10um and 2um.

## 3.7 Phase separation feature of centrosomal proteins

One material can change their phases when the concentration or temperature changed, like water vaporization and protein crystallization. In here, we only talk about the liquid-liquid phase separation (LLPS), which exists in the normal regulation of life activities. The regulation of biological macro-molecular complexes via LLPS is such an idea that once it is discovered, we immediately thought it is reasonable. The Centrosome as membraneless particles undergoing cell cycle dependent changes in composition is often regarded as a phase separation regulated particle (Zwicker, Decker, Jaensch, Hyman, & Jülicher, 2014). The LLPS describes that proteins are highly concentrated in droplets but can also exist in a diluted phase. The droplet are not rigid but dynamically recruit and release different components to compartmentalize different reactions. Concentration is a very important factor to cause phase separation. Lots of researchers used different concentrated proteins in vitro to check protein's phase separation, however, the in vitro expression is not so comparable to in vivo conditions. Recently, PEG, NaCL and sucrose were used as crowding material to achieve the phase separation caused by protein concentration increase. This hyperosmotic stress will give rise to many responses: loss of water, cell volume decreases, production of misfolded proteins and self-protected reactions in cells. Phase separation is driven by many factors caused by hyperosmotic stress.

Centriolar satellite proteins are particles that were firstly observed in the electron microscope. With fluorescence staining, we could observe a more dynamic localization of satellite proteins around centrosomes. Some appeared as tiny particles dispersed in the cytoplasm while some were like merged big particles localizing nearby the centrosome. To explore whether satellite particles are phase separation regulated condensates, we d hypo- and hyperosmotic stress and monitored their behaviour. Satellite proteins SSX2IP and PCM1 dispersed upon hypo-osmotic stress and round particles were formed upon hyperosmotic stress. Centrosomal localization of the PCM component γ-Tubulin remained unchanged upon both stresses, but some fibers were formed under hyperosmotic stress (Fig.18A). There were large amounts of fibrous γ-Tubulin formed under hyperosmotic stress in the cytoplasm. Two hours release from both stresses could restore the signal of satellite proteins SSX2IP and PCM1. There is a feature about the phase separated droplet that it can dynamically merge and separate move up. To test this, we used a stable NIH3T3 cell line expressing SSX2IP-LAP (Kurtulmus et al., 2016). During the release process from sucrose treatment, we

observed a dynamic merge and separation of SSX2IP, consistent with the droplet being phase separated (Fig.18B). When we transfected GFP tagged CEP135 to RPE-1 cells, we could observe aggregates formed in the cytoplsma typical for phase separation after increase of protein concentration (Fig.18C). These aggregates could recruit the centrosomal protein γ-Tubulin and the satellite protein SSX2IP, indicaing their close relationship. Intrinsically disordered regions (IDR) can provide muti-valent binding contributing to LLPS. With the IDR predictor we found all PCM1, SSX2IP and CEP135 having IDR that could drive phase separation under particular conditions (Fig.18D). This further underlines the phase separating feature of centrosomal proteins.

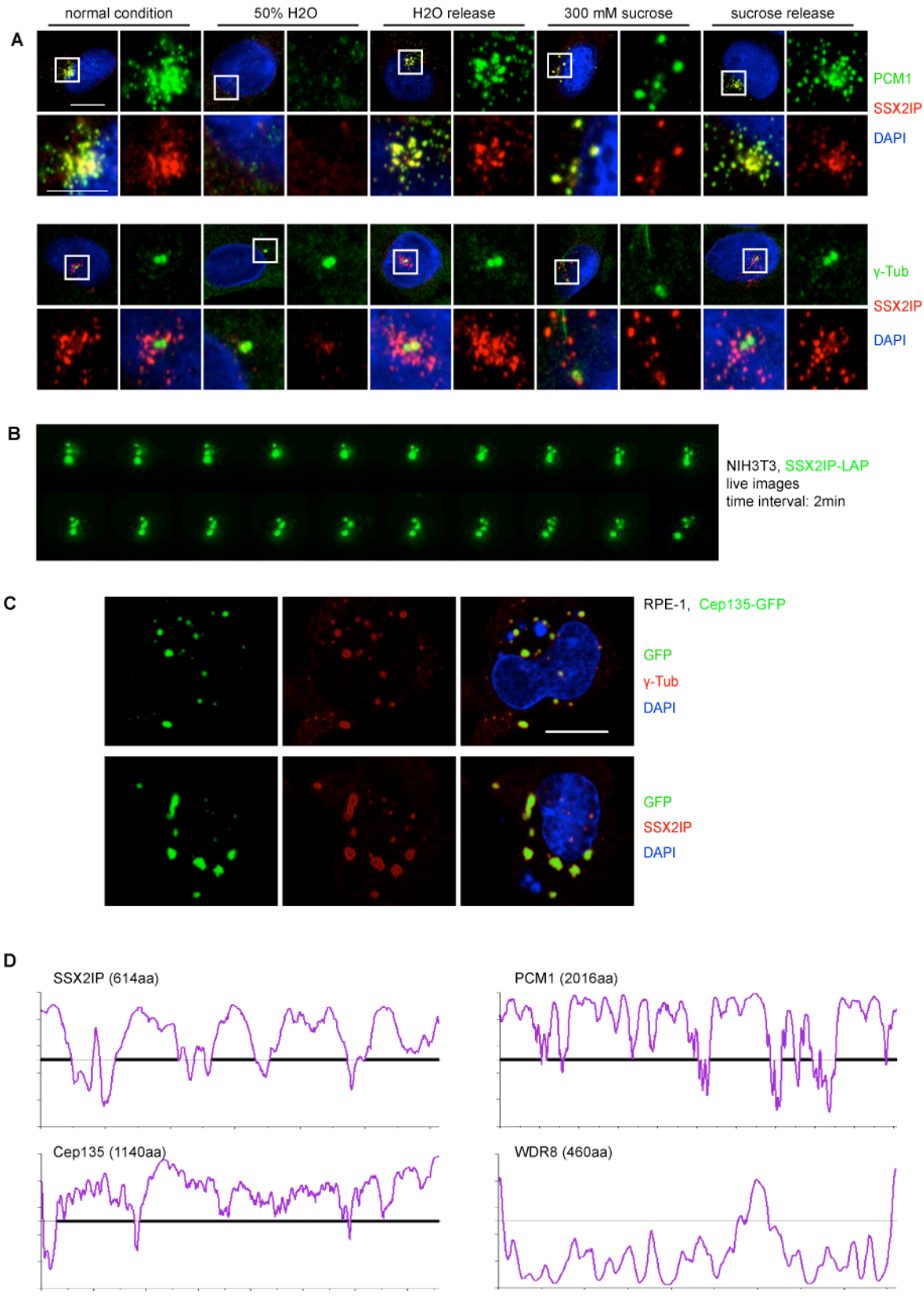
A
normal condition
50% H2O
H2O release
300 mM sucrose
sucrose release
PCM1
SSX2IP
DAPI
γ-Tub
SSX2IP
DAPI
B
NIH3T3, SSX2IP-LAP
live images
time interval: 2min
C
RPE-1, Cep135-GFP
GFP
γ-Tub
DAPI
GFP
SSX2IP
DAPI
D
SSX2IP (614aa)
PCM1 (2016aa)
Cep135 (1140aa)
WDR8 (460aa)

Fig.18 Phase separation feature of centrosomal proteins (page 62).

(A) The dynamic changes of SSX2IP, PCM1 and γ Tubulin upon hypo (50% water) and hyper (300mM sucrose) osmotic stresses. The cells were treated for 2 hours in osmotic stress conditions. After 2 hours osmotic stress, the cells were release to normal conditions for 2 hours. Scale bar, 10μm and 5μm.

(B) Live images of release process after 2 hours 300mM sucrose treatment show the merge and separation of SSX2IP particles.

(C) CEP135 transient overexpression recruit SSX2IP and γ Tubulin. Scale bar, 10μm .

(D) Prediction of natural Disordered Regions with PONDR VSL2 (http://www.pondr.com/) of protein SSX2IP, CEP135, PCM1 and WDR8.

In summary, we have explored the relationships of CEP135, WDR8 and SSX2IP. Firstly, we confirmed they are closely related in *Xenopus* egg extract physically and functionally. Meiosis eggs do not have centrioles and these proteins still form complexes and possibly assembly particles scattering in egg cytoplasm. ssx2ip and cep135 function in early embryo development and their protein expression repression in eggs could be regulated by CPEB. Moreover, cep135 depletion in *Xenopus* egg extract phenocopied ssx2ip' depletion (Bärenz et al., 2013), forming monopolar spindles in a cycling reaction upon sperm addition.

Knockout RPE-1 cells of *cep135*, *wdr8* and *ssx2ip* showed different phenotypes. The satellite protein knockouts of *ssx2ip* and *wdr8* showed abnormal cell growth. *cep135* knockout cells, although they did not show any growth defects, revealed premature centrosome splitting. Fig.19 summarize our conclusions and hypotheses. Fig.19A explains the different functions played by centrosomal proteins and satellite proteins. WDR8 and SSX2IP could be localized in the cytoplasm with unknown downstream targets affecting cell growth. In the neighbouring centrosome, the CS proteins could transport stock or balance many PCM proteins. CEP135 mainly located at centrosome. As CEP135's function is unique and may not be be replaced by other proteins and it centrosomal protein level is controlled robustly by several mechanisms.

Fig.19B shows premature centrosome splitting caused by the loss of CEP135. In metaphase, *cep135* knockout cells formed normal bipolar spindle. In telophase, the mitotic centrosome needs to degrade CDK5RAP2, PCNT and other PCM proteins to change back to an interphase centrosome. The degradation of CDK5RAP2 and PCNT also ensures timely centrosome disengagement. In normal cells, the disengaged centrioels still stay together as the a consequence of a balanced variety of forces (splitting force by motor protein, cohesion force by the actin network and PCM driven cohesion force). However, in *cep135* knockout cells, the two centriosomes split as the outcome of the imbalance of centrosome cohesion forces. The split centrosomes lost PCM partially.

The Interphase PCM is a very tidy structure unlike the meshowork in the mitotic phases. The scattered PCM in *cep135* knockout must arise as a consequence of the loss of CEP135 that changes the perfect tidy structure of the PCM with a loosely imperfect, unstable PCM. The *cep135* knockout cells still have normal mitotic spindle and γ-Tubulin intensity was unchanged in metaphase which suggests that *cep135* knockout cells undergo normal centriole duplication, normal centrosome maturation and proper bipolar spindle formation. We propose that a properly assembled PCM structure is not needed for mitotic centrosome function in somatic cells but they only need enough PCM to nucleate MTs. The daughter centriole of normal centrosomes, after disengagement in telophase or G1 phase, will go through “centriole to centrosome conversion”. At the same time, centrome linker protein will be recruited to stabilize the two disengaged centrosomes; then the centrosome pairs are ready to duplicate. After centrosome duplication, they dissolve the centrosome linker proteins and the separation of two already duplicated centrosomes as well as centrosome maturation occurr simultaneously. In the end, a bipolar spindle can be formed.

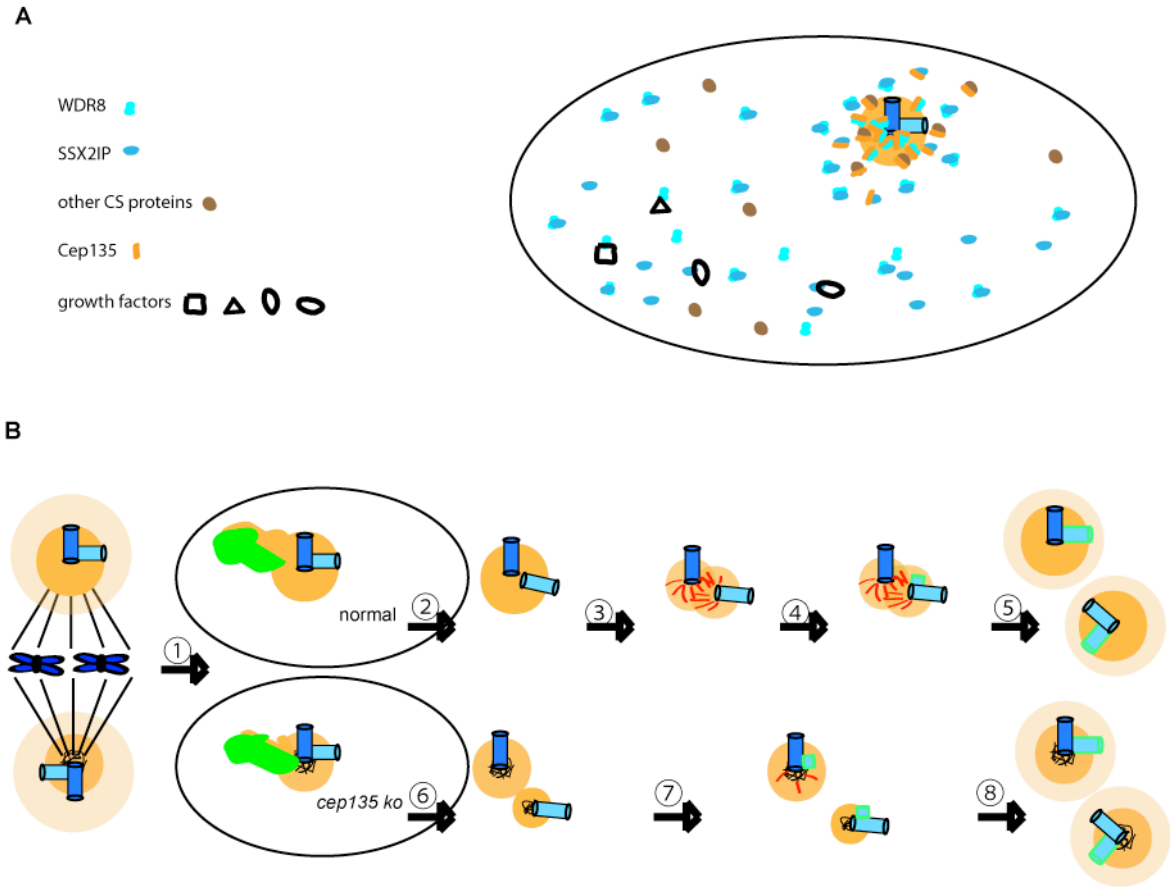


Fig.19 Basic model we proposed to explain our conclusion

A The different functions played by centrosomal protein and satellite proteins.

B Premature centrosome splitting caused by the loss of CEP135.

① the transition of mitotic centrosome to interphase centrosome

② centriole disengagement

③ centrosome linker protein recruitment

④ centriole duplication

⑤ centrosome maturation

⑥ premature centrosome splitting in *cep135* knockout cell

⑦ centriole duplication in split centrosome in *cep135* knockout cell

⑧ centrosome maturation in split centrosome in *cep135* knockout cell

# 4 Discussion

## 4.1 Different functions performed by centrosomal protein CEP135 and satellite proteins SSX2IP and WDR8

The aim of this project is to explore the functions of CEP135, WDR8 and SSX2IP in cell division and ciliogenesis. In a SSX2IP pull down in NIH3T3 SSX2IP-LAP cells, WDR8 was recognized as a novel SSX2IP interacting protein (Kurtulmus et al., 2016). Not only in mouse cell line, our lab also found the interaction between WDR8 and SSX2IP in SSX2IP immunoprecipitation in *Xenopus* egg extract. Considering WDR8 and SSX2IP's interaction in yeast, *nidulans* and other results generated by high through experiments (Gupta et al., 2015; Hori et al., 2015; Kurtulmus et al., 2016; Inoue et al., 2017), WDR8 and SSX2IP must be a very conserved protein pair. Then in WDR8 pull down in NIH3T3 WDR8-LAP cells, except for SSX2IP, CEP135 was found as a novel interacting protein of WDR8. WDR8's interactions with SSX2IP and CEP135 consistent with its subcellular localization both in centrosome and centriolar satellite. Therefore, we are very interested in their interactome of these three proteins and the specific functions executed by each one.

We started with immunoprecipitation of WDR8 in *Xenopus* egg extract. After we got the very short list of WDR8 immunoprecipitation in *Xenous* egg extract (Fig.1), we thought these three proteins must be responsible in one task or function in one pathway. Moreover, depletion of ssx2ip and cep135 can both lead to monopolar spindle formation in sperm added cycled egg extract. Therefore, we generated the knockouts of these three proteins in RPE-1 cells to further explore their functions. Turns out, the phenotypes of these knockouts are quite different. However, from the perspective of subcellular localisation, it is obviously that these three proteins have different functions, as they are occupied different parts in centrosomal structures (PCM and centriolar satellite). Also in cep135 immunoprecipitation in *Xenopus* egg extract, we found both wdr8 and ssx2ip. When we mentioned CEP135, the first impression is always the tip protein of centriolar cartwheel, whose structure has been shown in *Chlamydomonas* by electron microscope images (Hiraki, Nakazawa, Kamiya, & Hirono, 2007). *Chlamydomonas* has a permanent cartwheel structure, but for vertebrate the cartwheel is removed in the end of mitosis with the removal of SAS6 and STIL. But CEP135 is always there in centrolar lumen and pericentrosomal material. *Cep135* knockout cells have

the same centrosome splitting phenotype with the loss of other PCM components CDK5RAP2 and CEP85. Premature centrosome splitting caused by the loss of CEP135 is accompanied with PCM diminishment. Whether PCM diminishment lead to premature centrosome splitting or premature centrosome splitting lead to PCM dissolvement, we still don't have a conclusion about that. Cartwheel as the template to recruit triplet tubulins to form centriolar wall, its function in centriole duplication is crucial. Whether the loss of CEP135 will cause narrowed centriole or imperfect arrangement of triplets is unknown, it is on our to-do list to check centriolar structure with super resolution microscopy.

SSX2IP and WDR8 are a pair of very conserved protein partners even in *Aspergillus nidulans* which localized at spindle pole bodies (Shen & Osmani, 2013). Under most circumstances, the localization of satellite proteins is very dynamic. Even in *nidulans*, An-WDR8 and TINA (SSX2IP homologs) localised in nucleus in G2 and changed to spindle pole bodies during mitosis. In RPE-1 cells, satellite proteins localize at centrosome and basal body in interphase and largely are dispersed in metaphase. This is the case for SSX2IP and WDR8. With more and more papers reported different phenotypes by knockouts and knockdown, we can see the reasons why *ssx2ip* and *wdr8* knockout don't show any ciliogenesis defects. Even though protein expression level is dependent on each other for WDR8 and SSX2IP, the knockouts of these two protein show opposite tendency in affecting cell cycle in flow cytometry results. *ssx2ip* knockout show a clear slow growth rate and low ratio of mitotic cells. With the loss of SSX2IP, cells are less sensitive to extracellular nutrient to go to cell division. SSX2IP can also localised at cell-cell adhesions junctions. Therefore, it's worth checking the adhesion formation in *ssx2ip* knockouts.

Novel protein as WDR8 now has two stable interactors: SSX2IP and CEP135. WDR8 is a special protein that localised both at centrosome and satellites. So, WDR8 has two pools that interacts with SSX2IP and CEP135 separately. As shown in Fig.1A, WDR8 devotes most of itself to SSX2IP and CEP135. Fig1B also show IP of WDR8 can deplete most of CEP135 and SSX2IP. Loss of WDR8 show fast growth speed and increased ratio of G2/M cells. The novel WDR8 interactor protein we discovered here MTUS1was shown can also repress cell growth. Whether WDR8 and MTUS1 can work together, against SSX2IP to control cell cycle need further to be checked. For WDR8, generating a good antibody that work both in immunoblotting and immunofluorescence is a pre-requirement for further exploring the functions of WDR8.

## 4.2 Different subpopulations in PCM and CS

Centrosomes compose of nine triplets microtubule centrioles embed in PCM and satellite proteins at the surroundings. All of these proteins are not disorganised – they are in a fine regulated system. There are so many examples that reported the centrosomal proteins occupy different parts of PCM area or centriolar llumen area. γ-Tubulin localize to centriolar wall and inner PCM in interphase but only in PCM in metaphase (Sonnen et al., 2012). CEP192 can localize both in centriolar wall and PCM which functions in centriole duplication and PCM organization separately (Fry, Sampson, Shak, & Shackleton, 2017). CDK5RAP2 also has two pools that one interact with PCNT at proximal PCM to regulate centriole disengagement and the other localized at peripheral PCM to regulate centrosome disjunction (Pagan et al., 2015). The review paper (Vasquez-Limeta & Loncarek, 2021) summarize the detail localization of some centrosomal proteins, many of them show both centriolar wall and PCM localisation, such as CPAP and CEP135.

Our immunoprecipitation results of cep135 with antibody against both C and N terminal peptides show the different functions play by cep135: one contributes to centriole duplication and the others interact with some satellite protein to make sure the efficient assembly of PCM of embryo centrosomes. Cartwheel templates the assembly of centriolar wall and CEP135 as the tip component of cartwheel could interact with CEP63 and CEP152 which was required for centriole duplication. For CEP135's interaction with CS proteins, we cannot say there is a complex of CEP135-WDR8-SSX2IP. But CEP135 use the same several regions to regulate the interactions with satellite proteins to ensure its efficient localisation to PCM or ensure there is enough backup in surroundings when needed. The interaction site with centriole duplication factors also share same regions, so with different antibodies, we can fish different pools. Each CEP135 pool has the same available C or N terminal epitopes for antibody binding.

The cartwheel pool of CEP135 do not effect centrosome duplication. Whether the detailed structure of centriole will be affect, we need a further check. The splitting phenotype was caused by PCM pool of CEP135. CEP135 as the cartwheel tip protein does not affect so

much of the cartwheel formation- *cep135* knockout in DT40 cells still can form normal centriole with ninefold symmetry (Inanc et al., 2013). The loss of cartwheel spoke protein STIL cause the loss of centrioles and loss of CEP152 cause disrupted centrioles. One explanation is that CPAP rely on Cep152 and STIL more to recruit triplet microtubules to centriolar wall (Sir et al., 2013).

Compared to the subpopulations of centrosomal proteins which localize at different parts of centrosome (inner centriolar wall, inner PCM, middle PCM and outer PCM) to interact with different interactors, centrosome satellite proteins do not have a specific region to separate different interactors to decide different subpopulations. When we check the subcellular colocalisation of satellite protein with PCM1, from immunofluorescence, we could see different enrichment of PCM1 signal on top of other satellite proteins and sometimes PCM1 is not completely overlapping with some satellite proteins. Highthrough Mass Spectromey method give us some ideas about the subpopulations of satellite proteins (Gheiratmand et al., 2019). PCM1 interactome is 40% of total satellite protein interactome, which may suggest a subpopulation of CS proteins. With Mass Spetromety analysis in acentrosomal cell, the satellite proteome is largely unchanged compared to centrosomal cells. For the some proteins that could stably stick together even when they dispersed in cytoplasm, normally from the same subpopulation. In that perspective, *Xenopus* egg extract is a good system since it's a natural system without centrosome and the satellite proteins will disperse in cytoplasm with its interacting proteins which main belong to a same subpopulation.

## 4.3 Interactions between CEP135, WDR8 and SSX2IP

Checking protein protein interaction is a very powerful way to explore their functions. For a new unknown protein, how do we explore its functions? We can generate a tagged protein and check its localisation in cell line. It has some disadvantages: first, when the protein's signal is unspecifically scattered in cytoplasm, one probably cannot get a decisive conclusion about its localization since it could be the problem of antibody or staining skills; second, the localization of transient transfection normally relies on overexpressed proteins that may have different patterns compared to the endogenous protein. In that case, a stable cell line is preferred, but generating an antibody against a novel protein may often be the best choice. However, we also know that generating an antibody is both time and money consuming. Even though we already successfully generated an antibody, how to confirm that the signal

we got is the right one? Knockdown or knockout control helps to estimate about the specificity. In turn, the confirmation of knockdown or knockout needs antibody or sequencing results. Normally, protein localization based on both antibodies against tagged or endogenous protein with the facilitation of knockdown and knockout generates a very solid evidence. To check the protein expression in different tissues, we could use western blot to check the SDS samples from different tissues or check the mRNA level which do not need antibodies. However, the mRNA level is only an indication of protein level, and not equivalent to protein level. Southern blotting can also be used to check protein level. In plant, β-glucuronidase reporter system (GUS ) is also a good method to check protein expression in different stage seedlings.

If we knew the exact localization of one protein, we may have some hints of its functions. Such as centrosomal proteins, satellite proteins and proteins localized to mitotic microtubules are probably involved in cell division regulation; proteins localized to cell membrane may be a component of a cell adherent complex. However, finding a protein interactor that with a known function is a very good way to relate the protein's function with already known ones. There are many methods to check protein protein interaction. Co-immunoprecipitation and pull down is often used way to check protein interactions and mass spectrometry analysis of the elution sample can find unknown interactors. With crosslinking chemicals, you can fish more or transient or weak interactions. Proximity-dependent biotin identification (BioID) take advantage biotin and streptavidin tight affinity to distinct transient and weak interactions. Förster resonance energy transfer (FRET) and Bimolecular fluorescence complementation can detect protein interactions by the change of fluorophore. All of these are checking the indirect protein interactions. Yeast two-hybrid is a method can check direct protein interaction. However, the interaction is depedent on conserved protein domains and is not so presentative of an in vivo situation. Moreover, how do you know that several proteins can form a complex? Sucrose gradient sedimentation and native gel electrophoresis can show the same migration behavior of proteins of the same complex. Sucrose sedimentation still does not give very detailed information, it is also depends on a large ratio is incorporated in the complex. Native gel electrophoresis requires a specific antibody and a good gel running system. The ultimate method is to collect large amounts of highly purified complex and check it with Cryo-EM.

For our proteins CEP135, WDR8 and SSX2IP, we have detected their subcellular localization in RPE-1 cells and pull down/immunoprecipitation results of *Xenopus* egg extract and mouse cell lysate. We can get the following conclusions: First, WDR8 interacts with SSX2IP (evidences: colocalization, pull down/IP in *Xenopus* egg extract and mouse cell lysate). Second, WDR8 interacts with CEP135 (evidences: colocalization, pull down/IP in *Xenopus* egg extract and mouse cell lysate). Third, the interaction between CEP135 and SSX2IP may exist even though under normal condition we cannot see their colocalization. In cep135 IP in *Xenopus* egg extract we could find ssx2ip and these interactions could be due to a cep135-wdr8-ssx2ip complex or a direct interaction between cep135 and ssx2ip. We favor the second hypothesis. SSX2IP as the satellite protein can transport many PCM proteins such as γ-Tubulin. Under normal conditions, you couldn't see their colocalization, but sometimes I could observed some weak SSX2IP signal colocalized with γ-tubulin. Therefore, I think, there is some portion of SSX2IP that is responsible for PCM recruitment. In ssx2ip IP in *Xenopus* egg extract, we couldn't find cep135. Maybe SSX2IP has many interactors, CEP135 is not ranged on top. Fourth, the CEP135-WDR8-SSX2IP complex may not exist. From subcellular localization we know that Cep135 is a centrosomal protein, SSX2IP is a satellite protein and WDR8 is both centrosomal and satellite protein. So majority is not form Cep135-WDR8-SSX2IP complex. We also ran sucrose gradient sedimentation of *Xenopus* egg extract and SSX2IP and Cep135 did not show a clear complex distribution. Therefore, we concluded that Cep135-WDR8-SSX2IP may not exists.

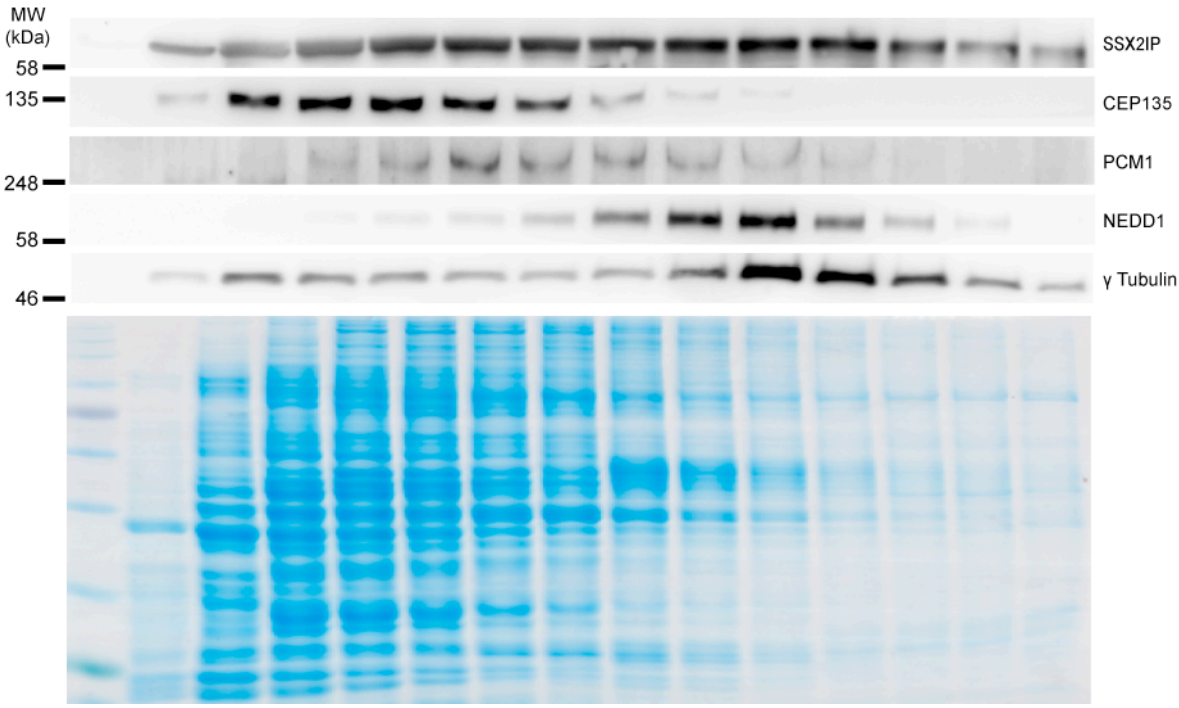


Fig.20. Sucrose gradient sedimentation of *Xenopus* egg extract.

## 4.4 Phase separation of centrosomal proteins

Phase separation exists in natural daily life activities, like P-granules, which can concentrate mRNAs related to polar determination. These granules exhibit different behavior to their surrounding liquid and form a new boundary. And at the same time, these granules are also liquid like that as they can merge and separate. When cells encounter stresses (e.g. heat, toxic substances, UV, osmotic stress), stress granules will formed to survive these stresses. Loss of stress granule was shown under phase separation regulation. In here, we show that centrosome satellite proteins undergo a big change under osmotic stress. With hypo-osmotic stress, we could observe the disappearance of the satellite protein PCM1 and SSX2IP and the appearance of the signal after release. With hyperosmotic stress, we could see PCM1 and SSX2IP to form round particles, which were colocalized with each other. γ-Tubulin as a PCM protein is embedded in a very stable structure that is not affected by osmotic stress. Some fiberous γ-Tubulin could be seen together with the centrosomal γ-Tubulin signal. We then checked the dynamic behaviour of satellite granules under hyperosmotic stress with SSX2IP tagged GFP in live imaging under sucrose release process. The merge and separation of SSX2IP can be seen in 10 minutes. This dynamic and reversible formation of satellite protein droplets shows phase separation under osmotic stress leads to protein concentration increase under physiological conditions.

In vivo, under normal condition, in interphase, the PCM is a tidy circular structure around the centriole. The structure is tightly packed and does not show any dispersion under hypo osmotic treatment. However, most of the PCM proteins are scaffold proteins with high molecular weight. Quite a lot of PCM proteins have intrinsically disordered regions (CDK5RAP2, PCNT, CEP135 and MTUS1). CEP135 overexpression leads to the formation of aggregates in the cytoplasm in Hela cells (Kim et al., 2008), like C-NAP1. When we transiently transfected CEP135 in RPE-1 cells, the same kind of aggregates were seen. Some of these aggregates were very small particles while some were merged into big ones and changing the round shape to smooth irregular shape. Thus, I think, under some extreme conditions (overexpression), PCM proteins can form phase separated particles that can merge. Whether this liquid particles in the end can grow into solid gel like aggregates is still unknown. CEP135 overexpression can also form filamentous polymers in some cell lines (Ryu et al., 2000).

In short we propose that interphase PCM is a very tightly organized structure that is unaffected in both hypo and hyper osmotic stress. Satellite proteins may use phase separation features to efficiently trafficking or store some proteins. Although PCM proteins do not show phase separation, most PCM proteins have intrinsically disordered regions to facilitate protein protein interactions and PCM proteins can undergo phase separation when ecotopically overexpressed.

## 4.5 The different phenotypes caused by knockdown and knockout cells

siRNAs are double stranded RNAs that can lead to the degradation of specific mRNA while miRNAs are initially single strand non-coding RNAs that regulate gene expression and post-transcriptional gene silencing. In vivo, the generation of siRNA needs Dicer to cut the long pre-dsRNA. The siRNA generated in vivo or transfected artificially recruits a RISC (RNA-induced silencing complex) complex with other proteins (Argonaute, Dicer, TRBP et.al.) to form single strand RNA to search for its complementary target mRNA. siRNA functions in transposon activation, protection from virus infection and some developmental regulations. TALEN (transcription activator-like effector nuclease), ZFN (Zinc-finger nuclease) and CRISPR (clustered regulatory interspaced short palindromic repeat) are the methods that are used to generate knockouts. TALEN, a method used by bacteria to infect plants, is composed of an NLS (Nuclear localization signal) part, a specific DNA sequence recognization part and a Fokl nuclease part. ZFN is composed of a zinc finger DNA-binding domain that can recognize specific DNA sequences and a DNA cleavage domain. Both methods rely on the protein that can specifically bind a particular region of a gene and the protein that can cut the DNA. After the cut, scientists take advantage of self repair of the genome which may generate mistakes. Generating a protein that can recognize a specific gene sequence is challenging and time consuming. CRISPR provides a much easier way to target specific genes with a guide RNA. CRISPR, a mechanism existing in the bacterial immune system for cutting a forgein DNA fragement, is composed of a guide RNA (for gene searching) and the Cas9 enzyme (for cutting genome).

Although both the siRNA and CRISPR can disturb a protein functions, the mechanism is quite different. With knockdown, after 2 days of transfection, normally one can observe the decreased expression of a specific protein. For the CRISPR knockout, in theory, the cut and

repair could be done in 12 hours and the disturbed gene cannot produce any new proteins. We have to wait for the degradation of the endogenous protein like in a knockdown. To generate a knockout cell line, we normally isolate a single cell colony to establish a new homogenous cell line which takes almost two months and cells already divide more than fifty times. During this time, the cell will develop some mechanisms to compensate defects caused by protein loss. Also mutations may be accumulated during each chromatin replication. Therefore, every knockout colony isolated from one gene maybe different with respect to some phenotypes. In this thesis, for every gene knockout, I isolated at least three different patterned cell colonies, and pre-checked their phenotypes to pick the one that was most representive. Therefore, the siRNA knockdown and CRISPR knockout represent acute and chronic disturbances of proteins' functions differently.

With around twenty years' application of siRNA knockdown and genome knockout, many proteins were assigned to much clearer functions. With more and more publications, we can see that some proteins show different phenotypes under acute knockdown and chronic knockouts. The centriolar satellite protein Cep131 siRNA knockdown shows defective ciliogenesis while knockout cells did not (Hall et al., 2013). *cep131* knockout mouse show normal ciliogenesis in most tissues except sperm. Many satellite proteins mutants mouse show tissue specific ciliary defects (Chang et al., 2006; S. T. Jiang et al., 2008; Kulaga et al., 2004; Mykytyn et al., 2004). However, knockdown of some proteins are more likely to have a sever defects compared to knockouts. The different phenotypes caused by siRNA knockdown and CRISPR knockout were reported in different research topic of different model systems (De Souza et al., 2006; El-Brolosy & Stainier, 2017; Evers et al., 2016; Karakas et al., 2007; Kok et al., 2015; Morgens, Deans, Li, & Bassik, 2016; Peretz et al., 2018). For the papers that our lab published on the knockdown of WDR8 and SSX2IP, they ruled out off-target activity with rescue experiments. Therefore, the different phenotypes between knockdown and knockout cells of WDR8 and SSX2IP were likely caused by the compensation mechanisms.

## 4.6 Centriole to centrosome conversion

Centriole to centrosome conversion was first proposed to involve PLK1 dependent modifications of the centrosome in early mitosis that assist full-length daughter centrioles to

convert to MTOC in late mitosis/G1 phase. PLK1- modified centrioles can recruite PCM in telophase/G1 and two same-size disengaged centrosomes can duplicate and be segregated in G2/prophase (W. J. Wang et al., 2011). Centriole disengagement and centriole to centrosome conversion (CCC) happen simmutaneously at the end of mitosis. Cohesion maintains the orthogonally connected mother and daughter centrioles from G2 to late mitosis. Chromosome cohesion is removed in a phosphorylation (PLK1) dependent Prophase pathway. Cohesion protected by shugoshin at the entromere and cthe entrosome is cleavaged by separase at ´anaphase onset. Shugoshin's targeting or release from the centrosome are both regulated by PLK1(X. Wang et al., 2008). PLK1 is also a main regulator for centrosome maturation during G2/prophase. For CCC, we know quite little. How to uncouple centriole disengagement and CCC? Sas-6 negative and C-Nap1 positive centrosomes are used to decide whether it's been modified. This standard may only represents cartwheel removal and centrosome linker protein anchoring while CCC happens in between or simultaneously. PLK1 is an important protein that it affects many functions. In here, I propose that we should only refer to the daughter centriole recruitment of PCM in late mitosis and G1 phase as centriole to centrosome conversion. Recently, more and more paper include centriole duplication and assembly as a part of CCC (Atorino, Hata, Funaya, Neuner, & Schiebel, 2020; Fu et al., 2016). Centriole disengagement, CCC, centrosomal linker protein recruitment happen simultaneously to ensure that two equal centrosomes are formed, a bipolar spindle arises and, finally, two equal daughter cells. I think CCC is also a mechanism to mask the asymmetry of centrioles. The asymmetric cell divisions in early embryos need to take advantage of the asymmetry of centrioles to form two daughter cells with different fates.

*cep135* knockout cells have prematurely split centrosomes. Normally, centrosome maturation and centrosome separation are coupled. Apparently, the split centrosome in interphase in *cep135* knockout cells did not undergo a CCC process in its previous cell cycle. To check whether the centrioles have undergone CCC, we compared the signals of the two split centrosomes in each cell. The γ-Tubulin and CDK5RAP2's signals were decreased for both centrosomes and the difference between two centrioles in each cell is much bigger for the CDK5RAP2 signal. So they haven't undergone CCC. In here, I would like to suggest a new cellular standard to check the completion of CCC to the equal amounts of CDK5RAP2 anchoring to the proximal end of centrioles before centriole duplication.

# 5. Materials and Methods

## 5.1 Materials

### 5.1.1 Reagents

All standard chemicals were bought form New England Biolab (Frankfurt, Germany), Serva (Heidelberg, Germany), Gibco BRL (Eggenstein, Germany), Sigma-Aldrich (Steinheim, Germany) or Carl Roth (Karlsruhe, Germany) unless otherwise indicated.

### 5.1.2 Buffers

- PBS: 10 mM Na2HPO$_4$, 2 mM KH$_2$PO$_4$, 137 mM NaCl, 2.7 mM KCl, adjust pH to 7.6
- PBST: PBS plus 0.05% Tween X-100
- 10x TBS (1L): 24 g Tris, 88 g NaCl, adjust pH to 7.6
- TBST: TBS plus 0.05% Triton X-100
- 10x MMR: 1M NaCL, 20mM KCL, 10mM MgCL$_2$, 20mM CaCL$_2$, 1mM EDTA, 50mM HEPES. Adjust pH with NaOH to 7.8, autoclave, store at room temperature
- 20x XB salts (1L): 149.12g KCL, 20ml 1M MgCL$_2$, 2ml 1M CaCL$_2$ filter sterilze and keep at 4 degree.
- 1x XB (1L): 1xXB buffer, 17.12g sucrose, 2.38 HEPES, adjust pH to 7.7 with KOH/HCL
- 1x XB-CSF (1L): 1xXB buffer, 17.12g sucrose, 2.38 HEPES, 1ml 1M MgCL$_2$, 10ml 0.5M EGTA, adjust pH to 7.7 with KOH/HCL
- CSF basic: 10mM HEPES pH7.7, 2mM MgCL$_2$, 100mM KCL
- Dejelly solution: 10g L-cysteine in 0.5L of 0.24x MMR. Add Cystein before use. Adjust pH to 7.8
- Cytochalasin B: Dissolve in DMSO, 10mg/ml (21mM), store at minus 20 degree
- 4x Laemmli buffer: 250 mM Tris, 8 % SDS, 20% (v/v) glycerol, 0.01% Bromophenol Blue, 400 mM DTT, pH6.8
- GEL Lower Buffer: 1.5M Tris, 0.4% SDS, pH8.8
- GEL Upper Buffer: 0.5M Tris, 0.4% SDS, pH6.8

- 6% SDS PAGE gel (2x): $H_2O$ 8.3ml, lower buffer 3.8ml, ROTIPHORESE®Gel 30 (37.5:1, ROTH) 3ml, 25% APS 30µl, TEMED 10µl
- 8.5% SDS PAGE gel: H2O 7ml, lower buffer 3.8ml, ROTIPHORESE®Gel 30 (37.5:1, ROTH) 4.2ml, 25% APS 30µl, TEMED 10µl
- 10% SDS PAGE gel: H2O 6.3ml, lower buffer 3.8ml, ROTIPHORESE®Gel 30 (37.5:1, ROTH) 5ml, 25% APS 30µl, TEMED 10µl
- 6.3% SDS PAGE gel: H2O 8.15ml, lower buffer 3.8ml, ROTIPHORESE®Gel 30 (37.5:1, ROTH) 3.15ml, 25% APS 30µl, TEMED 10µl
- Stacking gel: $H_2O$ 2.5 ml, upper buffer 1ml, ROTIPHORESE®Gel 30 (37.5:1, ROTH) 0.8ml, 25% APS 15µl, TEMED 4µl
- WB 10x running buffer (1L): 30g Tris, 144g Glycine, 10g SDS palette
- WB 10x blotting buffer (1L): 30g Tris, 144g Glysine
- WB blocking buffer: 5% milk in TBST
- Ponceau S: Ponceau S stain (product No: K793-500ML, VWR international)
- InstantBlue: Biozol (Leipziger, Germany)
- Mini-prep solution I: 50 mM glucose, 25 mM Tris-HCl pH 8.0, 10 mM EDTA, 10 µg/mL RNAse I
- Mini-prep solution II: 0.2 M NaOH, 1% weight per volume (w/v) SDS
- Mini-prep solution III: 3 M potassium acetate, 11.5% volume per volume (v/v) acetic acid

### 5.1.3 Antibiotics

| name | Stock Concentration | Working Concentration |
|---|---|---|
| Kanamycin | 25mg/ml | 25µg/ml |
| Ampicillin | 100mg/ml | 100µg/ml |
| Spectinomycin | 25mg/ml | 100µg/ml |
| Puromycin | 1mg/ml | 5µg/ml |
| G418 | 50mg/ml | 800µg/ml |
| Nocodazole | 1mM, 10mM | 5µg/ml (17µM), 100nM |
| Doxycycline | 1mg/ml | 1µg/ml |
| Thymidine | 100mM | 2mM |

## 5.1.4 Antibodies

**Primary antibodies**

- xlwdr8 antibody for *Xenopus* depletion and Mass Spectrometry: synthesis *Xenopus* peptide CYLDTEEEKK, serum produced by Seramun Diagnostica GmbH (Heidesee, Germany).
- hsWDR8 antibody used in IF generated by injecting rabbit with synthesis peptide N terminal (MNFSEVFKLSSLLCK) and C terminal (ETEAVVGTACRQLGGHT).
- CEP135 antibody: proteintech Cat No. 24428-1-AP (using CEP135 N terminal as antigen). Abcam, ab75005 (using CEP135 C terminal as antigen). Both worked in IF, 1:1000 (after methanol fixation, permeabilization with 0.5% Triton in PBS for 30min). Western blot with dilution 1:2000.
- Cep135 antibody for MS: home-made antibody with N terminal peptide (AERKFINLRKRLDQLGYKQ) and C terminal peptide (PERSILRTADRDGDRS AEKSVSFKE)
- Guinea pig SSX2IP antibody: IF 1:200 (Bärenz et al., 2013)
- Rabbit SSX2IP: WB 1:400 (blocking with milk overnight) (Bärenz et al., 2013)
- Rabbit PCM1: IF 1:500. WB 1:300 (Bärenz et al., 2013)
- Mouse α-Tubulin: IF 1:4000, WB 1:4000
- Mouse γ-Tubulin: IF 1:1000, WB 1:2000
- Rabbit γ-Tubulin: IF 1:1000
- ARL13b: 1:1000
- Rootletin (CROCC): (NBP1-80820, Novus Biologicals) 1:200. First antibody incubate overnight
- CNAP1 for IF: proteintech, Cat no: 14498-1-AP. 1:300
- CNAP1 for WB: Santa Cruz, sc-390540. 1:750
- NEK2 for WB: Santa Cruz, sc-55601, 1:750
- MTUS1: BOSTER Biological Technology, Cat no A04047-1. For IF, Rote blocking buffer incubate overnight.
- CDK5RAP2 for IF: Sigma-Aldrich, Cat no: 06-1398
- WDR47 antibody: a gift from Xuelang Zhu lab. IF: 1:500, WB:1:2000.

**Second antibodies**

| Second antibody | dilution |
|---|---|
| Mouse-IgG-HRP | 1:10000 |
| Rabbit-IgG-HRP | 1:10000 |
| Rabbit Alexa 488 | 1:500 |
| Rabbit Alexa 594 | 1:500 |
| Mouse Alexa 488 | 1:500 |
| Mouse Alexa 594 | 1:500 |
| DAPI | 1:2000 |

## 5.1.5 Plasmids

- eSpCas9(1.1): (Addgene, #71814)
- pSpCas9 (BB)-2A-Puro (Addgene, #48139) (gift from Prof. Dagmar Wachten)
- pSpCas9 (BB)-2A-Puro-WDR8gRNA1.2
- pSpCas9 (BB)-2A-Puro-WDR8gRNA3
- pSpCas9 (BB)-2A-Puro-WDR8gRNA5
- pSpCas9 (BB)-2A-Puro-SSX2IPgRNA1
- pSpCas9 (BB)-2A-Puro- SSX2IPgRNA2
- pSpCas9 (BB)-2A-Puro- SSX2IPgRNA3
- pSpCas9 (BB)-2A-Puro-CEP135gRNA1
- pSpCas9 (BB)-2A-Puro- CEP135gRNA2
- pSpCas9 (BB)-2A-Puro- CEP135gRNA3
- pEGFP C1- Cep135 1-1141 (KpnI and BamHI ligation)
- pEGFP C1- Cep135 1-658 (KpnI and BamHI ligation)
- pEGFP C1- Cep135 648-1140-PACT (SacI, HindIII and BamHI ligation)

## 5.1.6 Stable cell lines used in this study

- hTERT-RPE-1, wildtype: Human retinal pigment epithelial-1
- IMR90 wildtype
- NIH3T3 wildtype
- RPE-1, WDR8en GFP (Gupta et al., 2015). GFP is inserted in WDR8 C terminal

with puromycin resistance, heterozygous.

- NIH3T3, WDR8-LAP (Kurtulmus et al., 2016)
- NIH3T3, SSX2IP-LAP (Kurtulmus et al., 2016)
- RPE-1, WDR8 ko308
- RPE-1, SSX2IP ko213
- RPE-1, Cep135 ko8
- RPE-1, pEGFP C1- CEP135 1-1141 in ko8 (clone 2,3)
- RPE-1, pEGFP C1- CEP135 1-658 in ko8 (clone 4, 5)
- RPE-1, pEGFP C1- CEP135 648-1140-PACT in ko8 (mixture)

## 5.2 Methods

## 5.2.1 Molecular biology

#### 5.2.1.1 PCR

| GoTaq protocol (20ul) | |
|---|---|
| H2O | 10.5µl |
| GoTaq Buffer | 4µl |
| $MgCl_2$(25mM) | 1.2µl |
| dNTP (2mM) | 2µl |
| Primer (10mM) | 0.5µl |
| GoTaq DNA Polymerase | 0.2µl |
| template | 1µl |

GoTaq PCR Thermal Cycling Conditions

| Step | Temperature | Time | Cycle No. |
|---|---|---|---|
| initial Denaturation | 95°C | 2min | 1 |
| Denaturation | 95°C | 45s | |
| Annealing | 60°C | 45s | |
| Extension | 72°C | 1min/kb | 35 |
| Final Extension | 72°C | 5min | 1 |
| hold | 4°C | indefinite | 1 |

| Q5 protocol (25ul) | |
|---|---|
| $H_2O$ | 13.75µl |
| Q5 buffer | 5µl |
| dNTP (2mM) | 2.5µl |

| | |
|---|---|
| Primer (10mM) | 1.25µl |
| Q5 DNA Polymerase | 0.25µl |
| template | 1µl |

Q5 PCR Thermal Cycling Conditions

| Step | Temperature | Time | Cycle No. |
|---|---|---|---|
| initial Denaturation | 98°C | 30s | 1 |
| Denaturation | 98°C | 10s | |
| Annealing | 65°C | 30s | |
| Extension | 72°C | 30/kb | 35 |
| Final Extension | 72°C | 2min | 1 |
| hold | 4°C | indefinite | 1 |

For regular genotype, GoTaq was used. For plasmid cloning, Q5 was used. The components were added according to the system protocols shown here, as well as Thermal Cycling conditions. The primer designed with primer3: https://bioinfo.ut.ee/primer3-0.4.0/. Tm value was calculated as Tm = 81.5 + 16.6(log10([Na+])) + .41*(%GC) - 600/length. Normally, I set the Tm value around 60°C. For overlapping PCR, around 32bp overlapping primers were designed. For each fragment, around 16bp nucleotides were complementary to the primers.

#### 5.2.1.2 Genome precipitation of mammalian cells

Seeded cells on 3.5cm plate one day before use. Washed the plate two times with PBS and harvested cells by scratching with 500ml Laird buffer (Laird buffer: 100mMTris pH8.0, 5mM EDTA pH8, 200mM NaCl, 0.2% SDS, 100ug/ml Proteinase K). Incubated the collecting solution at 55°C for two hours and after that, added same volume of isopropanol to precipitate the genomic DNA.

#### 5.2.1.3 Normal cloning procedure

The PCR products were purified either with gel purification or PCR product purification with QIAquick PCR Purification Kit. Around 3µg purified PCR products and 1µg midi-prep plasmid were cut with NEB restriction enzyme at 37°C for two and half hours. T4 DNA Polymerase was used to ligate PCR product and plasmid at 4°C overnight. Ligation products were transformed into DH5α with 1 minute heat shock. After picked the transformed

colonies, plasmids were extracted with Mini-Prep solution I/II/III. The right colonies were confirmed by sequencing.

### 5.2.2 Cell culture

RPE-1 cells were grown in DMEM/F12 (Life Technologies) supplemented with 10% FBS and 2mM L-glutamine. G418 (800μg/μl) were added to medium if needed. NIH3T3 cells were grown in DMEM supplemented with 10% FBS. All cell lines were grown at 37℃ with 5% CO2. To get G0 phase ciliated cell, RPE-1 cell line was cultured with serum free medium for two days. For metaphase cell synchronization, cells were treated with 2mM Thymidine for 16-20 hours, then release for 8.5-9 hours. For NIH3T3 SSX2IP-LAP cell line, 1μg/ml Doxycycline was used for 24 hours to induce protein expression.

### 5.2.3 cDNA and siRNA

Gene sequences were from NCBI or ensembl.org, or Xenbase for frog sequences. WDR8's splice variants were from ensembl genome browser website. WDR8's sequence graph was drawn with website tool (IBS: Illustrator for Biological Sequences): http://ibs.biocuckoo.org/online.php#. Cep135 cDNA was bought from Biocat, Accn.No. BC136535.

All siRNAs were synthesized at Ambion Silencer Select Pre-designed oligos (life technologies) with 20mM stock solution. Lipofectamine RNAiMAX (Thermo Fisher) was used for transfection. MTUS1 siRNA1: F- UCAUGUAUCUAGAACAGGAtt R-UCCUGUUCU-AGAUACAUGAtc. MTUS1 siRNA2: F-GAAUUGACGCAAUAU AAAAtt R-UUUUAUA-UUGCGUCAAUUCaa

### 5.2.4 *Xenopus* Egg extract preparation and bipolar spindle formation

*Xenopus* egg extract method was as in paper (M. J. Lohka & Masui, 1983). Primed frogs 4-10 days before injection with 1000U/frog chorion-gonadotropin (hCG). Frogs were injected 17-18 hours before collection eggs. On that day, collected each tank eggs separately and selected apoptotic eggs with cut plastic Pasteur pipettes. After selection, prepared fresh

dejellyed buffer and adjusted pH to 8.8 with KOH. When dejellyed eggs, pour the buffer gently and shake torridly during dejelly. Kept the dejelly time less than 5min. After dejelly, immediately washed the eggs two times with XB buffer, two times with XB-CSF buffer. Prepared fresh Beckman tube (50 Ultra-Clear Tubes, 13x51mm, Lot No. Z91016SCA) with 1ml XB-CSF and 1µl 10mg/ml Cytochalasin B (destroying actin network). Carefully transfered the dejelly eggs into Beckman tubes with cut plastic pipette. Packed egg with swing out bucket centrifuge for 30sec 500rpm, then 1.5min 2000rpm without interval break. Sucked off top buffer to avoid the dilution of *Xenopus* egg cytoplasm. Then centrifuged the packed eggs with JS13 rotor at 11000rppm for 25min, three layers are got: top yellow lipid layer, middle transparent cytoplasm layer and bottom pigment layer. Collected middle egg extract layer with yellow tip syringe punctuation. Then added 0.1µl 10mg/ml Cytochalastin B to one epp extract to further disrupt cytoskeleton. Tested the egg extract with RanQ69L and cy3 labelled tubulin in 20°C water bath for 30min to check the asters formation.

For cep135 immunodepletion, cep135 antibody was bind to Dynabeads overnight. Normal IgG was used as control. Re-suspended beads in 50µl egg extract with cut tips and incubated on ice for half an hour. Repeat depletion twice to deplete as much as possible protein. cep135 depleted egg extract was send to interphase by add $CaCl_2$ to a final concentration at 0.4mM. Added same volume of metaphase egg extract to interphase one to induce bipolar spindle formation with sperm. The cep135 depletion that shown on Fig.3 was done by Oliver Gruss.

## 5.2.5 Mass spectrometry

wdr8 Mass Spectrometry: used 150µl Invitrogen Dynabeads with 200µl (50µg) purified wdr8 antibody from serum wdr8-91 to deplete 100µl egg extract. Same amount of IgG coupled beads was used as control. Washed 3 times with CSF-XB, 3 times with CSF-XB plus 250mM KCL plus 0.3% triton, 2 times with PBST, eluted in 25µl 0.5% SDS and took 10µl to verify protein expression level by immunoblotting, took 15µl to run commercial gradient SDS-PAGE gel to MS analysis. cep135 MS had the same procedures except with different antibody. The sample of cep135 IP were prepared by Oliver Gruss.

## 5.2.6 Preparation of SDS sample from different sizes of oocytes

Ovaries were dissected from female *Xenupos Laevis* frogs. Used scissors to separate oocyte clumps into small pieces. Put half volume oocytes and half volume 2.5mg/ml Liberase in MBS to defolliculate oocytes by rotating 2-3 hours at room temperature. Washed the separated oocytes with MBS buffer. Then separated different sizes oocyte by different sieves. In the end, we got oocytes whose diameter are: smaller than 120µm, 120-300µm, 300-560µm, 560-900µm. loaded 50µl oocyte to 1.5ml eppi tube with cut tips, washed it with MBS until the transparent supernant become clear. Added 450µl CSF buffer and crashed eggs by passing through with blue tips. Centrifuged for 5min at 3500rpm, 4°C. Took 400µl supernant and leave 300µl for further use and the remaining 100µl to precipitate proteins with 900ul isopropanol. Add 50ul four times Laemmli buffer to desolve protein palettes. Modified Barth's saline (MBS)(1X, pH7.8) (88mM NaCL, 1mM KCL, $MgSO_4$ 1mM, HEPES 5mM, $NaHCO_3$ 2.5mM, $CaCl_2$ 0.7mM)

## 5.2.7 Knockout cell lines generated by CRISPR-Cas9

All CRISPR knockouts were done by cloning guide RNA to eSpCas9(1.1) addgene: plasmid#71814 or eSpCas9(1.1)-Puro addgene: Plasmid #117686. Guide RNAs were selected according to zhang Lab: http://crispor.tefor.net/. The cloning methods are as followings:

(1) sgRNA oligos phosphorylation and annealing

| component | Amount (µl) |
|---|---|
| sgRNA forward(100µM) | 1 |
| sgRNA reverse(100µM) | 1 |
| ATP(10mM) | 1 |
| T4 PNK | 1 |
| PNK Buffer | 1 |
| $H_2O$ | 5 |
| total | 10 |

Phosphorylated and annealed the oligos in a thermocycler by using the following parameters: 37°C for 30min; 95°C for 5 min; ramp down to 25°C with speed 5°C per min.

(2) Digesting eSpCas9 plasmid with BbsI and purifying with gel extraction.

| component | amount(μl) |
|---|---|
| eSpCas9(1μg/μl) | 2 |
| NEB buffer 2.1 | 2 |
| BbsI | 1 |
| $H_2O$ | 15 |
| total | 20 |

reaction condition: 37°C in the water bath for 2.5 hours.

recycled the digested product with gel extraction: 0.8% agarose gel, dilute with 30ul EB.

(3) Ligation with T4 Ligase.

For selecting efficient guide RNA, T7 Endonuclease I was used. Extracted genomic DNA two days after neo transfection. Then performed the following procedure:

(1) Designed primers at the two sides of cutting site to get around 500bp fragment. PCR with gRNA transfected genome for 30 cycles (Important!) with colorless GoTaq reaction buffer.

(2) Combined the followings in a PCR tube: PCR product (from last step) 10μl, 10xNEBuffer2 1.5μl, Nuclease-Free Water 1.5μl. Then performed the annealing process:

| Step | Temperature (°C) | Time |
|---|---|---|
| Denature | 95 | 10min |
| Ramp1 | 95-85 | Ramp rate -2°C/sec |
| Ramp2 | 85-25 | Ramp rate -0.3°C/sec |

(3) Diluted T7EI 10 times to a final concentration of 1U/μl in 1X NEBuffer 2. Then add 2μl diluted T7EI to step2 PCR mixture. Then performed the digestion at 37°C for one hour. Run agarose gel to check cut efficiency.

Used the most efficient one to generate stable knockout cell line. The selected gRNAs are listed here. WDR8 gRNA1.2 (GGCGGCCATGAACTTCTCCG), WDR8 gRNA3 (TTGAGAATGT-GGCGCCCGTC), WDR8 gRNA5 (GGACGGCCGCTACATGGC-GC). CEP135 gRNA2 (G-ACAGTGGAGTGTTTACCTT), SSX2IP gRNA2

(GAGTATCTCATATCTTGATC), SSX2IP gRNA3 (GCGGAAGAACCTTCTAGCTC). Once I had checked the gRNA efficiency, re-transfected plasmid with neo kit. One day after transfection, diluted transfected cells to 96 well plate, or treated cells with puromycin two days after transfection for 3-5 days then diluted to 96 well plate. It normally took two weeks for the cells on 96 well plate to form a good colony. Transferred the cells to 3.5cm plate for further analysis. Immunofluorescence, immunoblotting and gene sequencing were used to confirm knockout cell lines.

## 5.2.8 Flow cytometry

Cell cycle analysis by flow cytometry was stained with Propidium Iodide. 1x $10^5$ RPE-1 cells were seeded in 6cm plate. 56 hours later (the cells were still less than 50% confluent), fixed cells with cold 70% methanol overnight (cold methanol was added drop by drop to weakly vortexed cells). Propidium Iodide (working concentration: PI 2.5µg/ml, RNAase A, 50µg/ml) stained the cells for more than six hours. Filtered samples before loaded to BD Accuri C6 Plus Flow Cytometer. Unstained cells were used to define background signal. For each sample, more than 30,000 cells were counted. Data were analyzed with CFlow Plus software.

## 5.2.9 Microtubule regrowth assay

Seeded 1.5x10^5 cells on 3.5cm plate for more than 24 hours. Mixed the ice with water to make sure the plate was immerged on a homogenous temperature. Put this plate on ice-water mixture for one hour to depolymerize microtubule. To regrowth microtubule, put the ice-cold converslips to new pre-warmed plates. Changed the medium in the old plate may causes uneven MT regrowth because of the iced liquid under coverslip which will creat a cold environment. Fixed plate with 4%PFA plus 1% TritonX-100 by shaking for 20min at room temperature. ( method was adapted from: Warren, Rutkowski, & Cassimeris, 2006).

## 5.2.10 Sucrose gradient sedimentation

10%, 20%, 30%, 40% sucrose gradient fractions are prepared in CSF buffer for frog egg and embryo extract, or HEPES buffer for xl177 cell lysate. One day before, sequentially loaded around 550ul sucrose fractions into 2.2ml Beckmann tube. Vertically place tubes in refrigerator overnight to get linear gradient (around 16-18 hours). Dilute the egg extract with

same volume of CSF basic buffer. Load 100-180ul mixture on top of the tube with cut tips. Centrifuge the tubes in a swing out rotor TLS-55 (Beckman, Fullerton, CA) for 2.5 h at 55,000 rpm at 4°C.

## 5.2.11 CEP135 rescue stable cell line and transient transfection

CEP135 full length cDNA sequence from amino acid 1 to 1141 was cloned to pEGFP-C1 plasmid with a CMV promotor with KpnI and BamHI. CEP135 N terminal cDNA from amino acid 1 to 658 was cloned to same pEGFP-C1 with KpnI and BamHI. CEP135 C terminal cDNA from amino acid 648 to 1140 with SacI and HindIII, together with AKAP450 PACT sequence with HindIII and BamHI was cloned to same pEGFP-C1. The midi prep plasmids were cut with MluI for linearization. The plasmids were transfected with lipofectamine2000 or PeiMAX (3µg plasmid and 12µg Pei). Two days after transfection, transfered cells to 10cm plate and treated with 800µg/ml G418 for 4 days, then diluted to 96-well plate. Mixture (C terminal) or signal colony (full length 2 and 3; N terminal 4 and 5) were collected. Rabbit polyclone GFP antibody (1:200) was used to check protein expression. For mixture Cep135 C terminal rescue cell line, more than ninety percent cells were positive. colonies full length 2, N terminal 5 and C terminal mixture were used to further check the centrosome splitting phenotype.

To check the localization pattern of CEP135 ovexpression, GFP-CEP135 plasmids with full length, C or N part (which were also used for CEP135 rescue experiment) were transfected with PeiMAX (3ug plasmid and 12ug Pei in 3.5cm plate). Changed medium after 6 hours and fix the cells with methanol after 20 hours. Rb GFP antibody, ms γ-tubulin antibody and gp SSX2IP anitibody were used to check colocalization.

## 5.2.12 Indirect immunofluorescence

Coverslips were seeding on the plate for more than 24 hours before fixation. Normally coverslips were fixed with 100% cold methanol for 5 minutes unless otherwise indicated. The incubation time of blocking buffer, first antibody and second antibody differs according to different antibodies. First antibody incubation time was either 4 degree overnight or room temperature 2 hours. Second antibody always incubates at room temperature for one hour. Immunofluorescence blocking buffer: 10% Goat serum, 0.2% TritonX-100 in PBS.

Blocking time were either overnight or room temperature for 1-2 hours. Coverslips were mounted in Fluoromount-G medium (SouthernBiotech).

## 5.2.13 Microscopy and fluorescence intensity measurement

RPE-1, SSX2IP-LAP live image were taken from Keyence microscope. Cells were seeding on ibidi plate (15ul-Slide 8 well, 80826 and 60u-Dish, 35mm high, 81156). Time laps images were taken with Keyence software. Images for quantification were taken with Axiphot epi-microscopy and ZEISS LSM confocal microscopy. Quantification of fluorescence intensity was performed with Fiji Image J. For punctuated signal, threshold was set to choose proper area and measure intDen value. For satellite protein signal intensity, a square was set around γ Tubulin signal. Analysis processes were: rolling ball 50 pixels background subtract – math subtract - stack Z project - look up table "16 colors" - Surface Plot. Error bar were calculated from the mean value of three replicates. P value was calculated with t-test, two tailed. The significant levels *: 0.01-0.05, **: 0.001-0.01, ***: 0.0001-0.001, ****: < 0.0001. R software (https://www.r-project.org/) and illustrator were used for image generation and typography.

# 6 Reference

A. Huges, M. S. (1948). Anaphase Movements in the Living Cell. *Journal of Experimental Biology*, *25*(1), 45–72. https://doi.org/10.1242/jeb.25.1.45

Ahn, J. Il, Park, J. E., Meng, L., Zhang, L., Kim, T. S., Kruhlak, M. J., … Lee, K. S. (2020). Phase separation of the Cep63•Cep152 complex underlies the formation of dynamic supramolecular self-assemblies at human centrosomes. *Cell Cycle*, *19*(24), 3437–3457. https://doi.org/10.1080/15384101.2020.1843777

ARCE, C. A., RODRIGUEZ, J. A., BARRA, H. S., & CAPUTTO, R. (1975). Incorporation of l-Tyrosine, l-Phenylalanine and l-3,4-Dihydroxyphenylalanine as Single Units into Rat Brain Tubulin. *European Journal of Biochemistry*, *59*(1), 145–149. https://doi.org/10.1111/j.1432-1033.1975.tb02435.x

Arquint, C., & Nigg, E. A. (2016). The PLK4-STIL-SAS-6 module at the core of centriole duplication. *Biochemical Society Transactions*, *44*(5), 1253–1263. https://doi.org/10.1042/BST20160116

Asada, M., Irie, K., Morimoto, K., Yamada, A., Ikeda, W., Takeuchi, M., & Takai, Y. (2003). ADIP, a novel afadin- and α-actinin-binding protein localized at cell-cell adherens junctions. *Journal of Biological Chemistry*, *278*(6), 4103–4111. https://doi.org/10.1074/jbc.M209832200

Atorino, E. S., Hata, S., Funaya, C., Neuner, A., & Schiebel, E. (2020). CEP44 ensures the formation of bona fide centriole wall, a requirement for the centriole-to-centrosome conversion. *Nature Communications*, *11*(1). https://doi.org/10.1038/s41467-020-14767-2

Au, F. K. C., Jia, Y., Jiang, K., Grigoriev, I., Hau, B. K. T., Shen, Y., … Qi, R. Z. (2017). GAS2L1 Is a Centriole-Associated Protein Required for Centrosome Dynamics and Disjunction. *Developmental Cell*, *40*(1), 81–94. https://doi.org/10.1016/j.devcel.2016.11.019

Bahe, S., Stierhof, Y. D., Wilkinson, C. J., Leiss, F., & Nigg, E. A. (2005). Rootletin forms centriole-associated filaments and functions in centrosome cohesion. *Journal of Cell Biology*, *171*(1), 27–33. https://doi.org/10.1083/jcb.200504107

Bahmanyar, S., Kaplan, D. D., DeLuca, J. G., Giddings, T. H., O'Toole, E. T., Winey, M., … Barth, A. I. M. (2008). β-catenin is a Nek2 substrate involved in centrosome

separation. *Genes and Development*, *22*(1), 91–105. https://doi.org/10.1101/gad.1596308

Balczon, R., Bao, L., & Zimmer, W. E. (1994). PCM-1, a 228-kD centrosome autoantigen with a distinct cell cycle distribution. *Journal of Cell Biology*, *124*(5), 783–793. https://doi.org/10.1083/jcb.124.5.783

Baltzer, F. (1964). Theodor Boveri. *American Association for the Advancement of Science*, *144*(3620), 809–815. https://doi.org/10.1126/science.144.3620.809

Bärenz, F. (2011). *Differential proteomics identifies SSX2IP as a novel regulator of centrosome function*. University of Heidelberg.

Bärenz, F., Inoue, D., Yokoyama, H., Tegha-Dunghu, J., Freiss, S., Draeger, S., … Gruss, O. J. (2013). The centriolar satellite protein SSX2IP promotes centrosome maturation. *Journal of Cell Biology*, *202*(1), 81–95. https://doi.org/10.1083/jcb.201302122

Barr, A. R., Kilmartin, J. V., & Gergely, F. (2010). CDK5RAP2 functions in centrosome to spindle pole attachment and DNA damage response. *Journal of Cell Biology*, *189*(1), 23–39. https://doi.org/10.1083/jcb.200912163

Barry, J. M., & Merriam, R. W. (1972). Swelling of hen erythrocyte nuclei in cytoplasm from Xenopus eggs. *Experimental Cell Research*, *71*(1), 90–96. https://doi.org/10.1016/0014-4827(72)90267-4

Basto, R., Lau, J., Vinogradova, T., Gardiol, A., Woods, C. G., Khodjakov, A., & Raff, J. W. (2006). Flies without Centrioles. *Cell*, *125*(7), 1375–1386. https://doi.org/10.1016/j.cell.2006.05.025

Birkhead, T. R., & Montgomerie, R. (2009). *Three centuries of sperm research*. *Sperm Biology* (First Edit). Elsevier Ltd. https://doi.org/10.1016/B978-0-12-372568-4.00001-X

Bodnar, A. G., Ouellette, M., Frolkis, M., Holt, S. E., Chiu, C. P., Morin, G. B., … Wright, W. E. (1998). Extension of life-span by introduction of telomerase into normal human cells. *Science*, *279*(5349), 349–352. https://doi.org/10.1126/science.279.5349.349

Boettcher, B., & Barral, Y. (2013). The cell biology of open and closed mitosis. *Nucleus (United States)*, *4*(3), 160–165. https://doi.org/10.4161/nucl.24676

Boeynaems, S., Tompa, P., & Van Dan Bosch, L. (2018). Phasing in on the cell cycle. *Cell Division*, *13*(1), 1–8. https://doi.org/10.1186/s13008-018-0034-4

Bolcun-Filas, E., & Handel, M. A. (2018). Meiosis: The chromosomal foundation of

reproduction. *Biology of Reproduction*, *99*(1), 112–126. https://doi.org/10.1093/biolre/ioy021

Borisy, G. G., & Taylor, E. W. (1967a). The mechanism of action of colchicine. Binding of colchincine-3H to cellular protein. *The Journal of Cell Biology*, *34*(2), 525–533. https://doi.org/10.1083/jcb.34.2.525

Borisy, G. G., & Taylor, E. W. (1967b). The mechanism of action of colchicine. Colchicine binding to sea urchin eggs and the mitotic apparatus. *The Journal of Cell Biology*, *34*(2), 535–548. https://doi.org/10.1083/jcb.34.2.535

Bowler, M., Kong, D., Sun, S., Nanjundappa, R., Evans, L., Farmer, V., … Loncarek, J. (2019). High-resolution characterization of centriole distal appendage morphology and dynamics by correlative STORM and electron microscopy. *Nature Communications*, *10*(1). https://doi.org/10.1038/s41467-018-08216-4

Bowne-Anderson, H., Zanic, M., Kauer, M., & Howard, J. (2013). Microtubule dynamic instability: A new model with coupled GTP hydrolysis and multistep catastrophe. *BioEssays*, *35*(5), 452–461. https://doi.org/10.1002/bies.201200131

Bracegirdle, B. (1989). The development of biological preparative techniques for light microscopy, 1839–1989. *Journal of Microscopy*, *155*(3), 307–318. https://doi.org/10.1111/j.1365-2818.1989.tb02892.x

Brady T, S. (1985). A novel brain ATPase with properties expected for the fast axonal transport motor. *Nature*, *317:73-75*, 73–75.

Brangwynne, C. P., Eckmann, C. R., Courson, D. S., Rybarska, A., Hoege, C., Gharakhani, J., … Hyman, A. A. (2009). Germline P Granules Are Liquid Droplets That Localize by Controlled Dissolution/Condensation. *Science*, *324*(5935), 1729–1732. https://doi.org/10.1126/science.1172046

Brangwynne, C. P., Mitchison, T. J., & Hyman, A. A. (2011). Active liquid-like behavior of nucleoli determines their size and shape in Xenopus laevis oocytes. *Proceedings of the National Academy of Sciences of the United States of America*, *108*(11), 4334–4339. https://doi.org/10.1073/pnas.1017150108

Buendia, B., Bré, M. H., Griffiths, G., & Karsenti, E. (1990). Cytoskeletal control of centrioles movement during the establishment of polarity in Madin-Darby Canine kidney cells. *Journal of Cell Biology*, *110*(4), 1123–1135. https://doi.org/10.1083/jcb.110.4.1123

C. Elizabeth Oakley, B. R. O. (1989). Identification of γ-tubulin, a new member of the

tubulin superfamily encoded by mipA gene of Aspergillus nidulans. *Nature*, 662–664. https://doi.org/https://doi.org/10.1038/338662a0

Cabral, G., Laos, T., Dumont, J., & Dammermann, A. (2019). Differential Requirements for Centrioles in Mitotic Centrosome Growth and Maintenance. *Developmental Cell*, *50*(3), 355–366.e6. https://doi.org/10.1016/j.devcel.2019.06.004

Chang, B., Khanna, H., Hawes, N., Jimeno, D., He, S., Lillo, C., … Swaroop, A. (2006). In-frame deletion in a novel centrosomal/ciliary protein CEP290/NPHP6 perturbs its interaction with RPGR and results in early-onset retinal degeneration in the rd16 mouse. *Human Molecular Genetics*, *15*(11), 1847–1857. https://doi.org/10.1093/hmg/ddl107

Chen, C., Tian, F., Lu, L., Wang, Y., Xiao, Z., Yu, C., & Yu, X. (2015). Characterization of Cep85 - A new antagonist of Nek2A that is involved in the regulation of centrosome disjunction. *Journal of Cell Science*, *128*(17), 3290–3303. https://doi.org/10.1242/jcs.171637

Cole, D. G., Diener, D. R., Himelblau, A. L., Beech, P. L., Fuster, J. C., & Rosenbaum, J. L. (1998). Chlamydomonas kinesin-II-dependent intraflagellar transport (IFT): IFT particles contain proteins required for ciliary assembly in Caenorhabditis elegans sensory neurons. *Journal of Cell Biology*, *141*(4), 993–1008. https://doi.org/10.1083/jcb.141.4.993

Cremer, T., & Cremer, M. (2010). Chromosome territories. *Cold Spring Harbor Perspectives in Biology*, *2*(3), 1–22. https://doi.org/10.1101/cshperspect.a003889

Dahm, R. (2008). Discovering DNA: Friedrich Miescher and the early years of nucleic acid research. *Human Genetics*, *122*(6), 565–81. https://doi.org/10.1007/s00439-007-0433-0

Dammermann, A., Maddox, P. S., Desai, A., & Oegema, K. (2008). SAS-4 is recruited to a dynamic structure in newly forming centrioles that is stabilized by the γ-tubulin-mediated addition of centriolar microtubules. *Journal of Cell Biology*, *180*(4), 771–785. https://doi.org/10.1083/jcb.200709102

De Bruijn, D. R. H., Dos Santos, N. R., Kater-Baats, E., Thijssen, J., Van Den Berk, L., Stap, J., … Van Kessel, A. G. (2002). The cancer-related protein SSX2 interacts with the human homologue of a Ras-like GTPase interactor, RAB3IP, and a novel nuclear protein, SSX2IP. *Genes Chromosomes and Cancer*, *34*(3), 285–298.

https://doi.org/10.1002/gcc.10073

De Souza, A. T., Dai, X., Spencer, A. G., Reppen, T., Menzie, A., Roesch, P. L., … Ulrich, R. G. (2006). Transcriptional and phenotypic comparisons of Ppara knockout and siRNA knockdown mice. *Nucleic Acids Research*, *34*(16), 4486–4494. https://doi.org/10.1093/nar/gkl609

Desai, A., & Mitchison, T. J. (1997). Microtubule polymerization dynamics. *Annual Review of Cell and Developmental Biology*, *13*, 83–117. https://doi.org/10.1146/annurev.cellbio.13.1.83

Earnshaw, W. C., & Rothfield, N. (1985). Identification of a family of human centromere proteins using autoimmune sera from patients with scleroderma. *Chromosoma*, *91*(3–4), 313–321. https://doi.org/10.1007/BF00328227

El-Brolosy, M. A., & Stainier, D. Y. R. (2017). Genetic compensation: A phenomenon in search of mechanisms. *PLoS Genetics*, *13*(7), 1–17. https://doi.org/10.1371/journal.pgen.1006780

Euteneuer, U., & Schliwa, M. (1985). Evidence for an involvement of actin in the positioning and motility of centrosomes. *Journal of Cell Biology*, *101*(1), 96–103. https://doi.org/10.1083/jcb.101.1.96

Evers, B., Jastrzebski, K., Heijmans, J. P. M., Grernrum, W., Beijersbergen, R. L., & Bernards, R. (2016). CRISPR knockout screening outperforms shRNA and CRISPRi in identifying essential genes. *Nature Biotechnology*, *34*(6), 631–633. https://doi.org/10.1038/nbt.3536

Faragher, A. J., & Fry, A. M. (2003). Nek2A kinase stimulates centrosome disjunction and is required for formation of bipolar mitotic spindles. *Molecular Biology of the Cell*, *14*(7), 2876–89. https://doi.org/10.1091/mbc.e03-02-0108

Fine, R. E. (1971). Heterogeneity of tubulin. *Nature New Biology*, *233*(43), 283–284. https://doi.org/10.1038/newbio233283a0

Flanagan, A. M., Stavenschi, E., Basavaraju, S., Gaboriau, D., Hoey, D. A., & Morrison, C. G. (2017). Centriole splitting caused by loss of the centrosomal linker protein C-NAP1 reduces centriolar satellite density and impedes centrosome amplification. *Molecular Biology of the Cell*, *28*(6), 736–745. https://doi.org/10.1091/mbc.E16-05-0325

Foot, K., & Strobell, E. C. (1905). Prophases and metaphase of the first maturation spindle of allolobophora fætida. *American Journal of Anatomy*, *4*(2), 199–243.

https://doi.org/10.1002/aja.1000040206

Fry, A. M., Mayor, T., Meraldi, P., Stierhof, Y. D., Tanaka, K., & Nigg, E. A. (1998). C-Nap1, a novel centrosomal coiled-coil protein and candidate substrate of the cell cycle-regulated protein kinase Nek2. *Journal of Cell Biology*, *141*(7), 1563–1574. https://doi.org/10.1083/jcb.141.7.1563

Fry, A. M., Meraldi, P., & Nigg, E. A. (1998). A centrosomal function for the human Nek2 protein kinase, a member of the NIMA family of cell cycle regulators. *EMBO Journal*, *17*(2), 470–481. https://doi.org/10.1093/emboj/17.2.470

Fry, A. M., Sampson, J., Shak, C., & Shackleton, S. (2017). Recent advances in pericentriolar material organization: Ordered layers and scaffolding gels. *F1000Research*, *6*(0). https://doi.org/10.12688/f1000research.11652.1

Fu, J., & Glover, D. M. (2012). Structured illumination of the interface between centriole and peri-centriolar material. *Open Biology*, *2*(AUG). https://doi.org/10.1098/rsob.120104

Fu, J., Lipinszki, Z., Rangone, H., Min, M., Mykura, C., Chao-Chu, J., … Glover, D. M. (2016). Conserved molecular interactions in centriole-to-centrosome conversion. *Nature Cell Biology*, *18*(1), 87–99. https://doi.org/10.1038/ncb3274

Gheiratmand, L., Coyaud, E., Gupta, G. D., Laurent, E. M., Hasegan, M., Prosser, S. L., … Pelletier, L. (2019). Spatial and proteomic profiling reveals centrosome-independent features of centriolar satellites. *The EMBO Journal*, *38*(14), 1–22. https://doi.org/10.15252/embj.2018101109

Gibbons, I. R. (2012). *Discovery of dynein and its properties: A personal account*. *Dyneins*. Elsevier. https://doi.org/10.1016/B978-0-12-382004-4.10001-9

Glickstein, M. (2006). Golgi and Cajal: The neuron doctrine and the 100th anniversary of the 1906 Nobel Prize. *Current Biology*, *16*(5), 147–151. https://doi.org/10.1016/j.cub.2006.02.053

Graser, S., Stierhof, Y. D., & Nigg, E. A. (2007). Cep68 and Cep215 (Cdk5rap2) are required for centrosome cohesion. *Journal of Cell Science*, *120*(24), 4321–4331. https://doi.org/10.1242/jcs.020248

Gruss, O. J., Carazo-Salas, R. E., Schatz, C. A., Guarguaglini, G., Kast, J., Wilm, M., … Mattaj, I. W. (2001). Ran induces spindle assembly by reversing the inhibitory effect of importin α on TPX2 activity. *Cell*, *104*(1), 83–93. https://doi.org/10.1016/S0092-

8674(01)00193-3

Guldner, H. H., Lakomek, H. J., & Bautz, F. A. (1984). Human anti-centromere sera recognise a 19.5 kD non-histone chromosomal protein from HeLa cells. *Clinical and Experimental Immunology (Print)*, *58*(1), 13–20.

Gupta, G. D., Coyaud, É., Gonçalves, J., Mojarad, B. A., Liu, Y., Wu, Q., … Pelletier, L. (2015). A Dynamic Protein Interaction Landscape of the Human Centrosome-Cilium Interface. *Cell*, *163*(6), 1483–1499. https://doi.org/10.1016/j.cell.2015.10.065

Hadjihannas, M. V., Brückner, M., & Behrens, J. (2010). Conductin/axin2 and Wnt signalling regulates centrosome cohesion. *EMBO Reports*, *11*(4), 317–324. https://doi.org/10.1038/embor.2010.23

Hajdu, S. I. (2002). The first use of the microscope in medicine. *Annals of Clinical and Laboratory Science*, *32*(3), 309–10. Retrieved from http://www.ncbi.nlm.nih.gov/pubmed/12175096

Hall, E. A., Keighren, M., Ford, M. J., Davey, T., Jarman, A. P., Smith, L. B., … Mill, P. (2013). Acute Versus Chronic Loss of Mammalian Azi1/Cep131 Results in Distinct Ciliary Phenotypes. *PLoS Genetics*, *9*(12). https://doi.org/10.1371/journal.pgen.1003928

Hardy, J. (2016). Fun with "Animicules." Retrieved from https://www.hardydiagnostics.com/wp-content/uploads/2016/05/Leeuwenhoek-Father-of-Microbiology.pdf

Hardy, T., Lee, M., Hames, R. S., Prosser, S. L., Cheary, D. M., Samant, M. D., … Fry, A. M. (2014). Multisite phosphorylation of C-Nap1 releases it from Cep135 to trigger centrosome disjunction. *Journal of Cell Science*, *127*(11), 2493–2506. https://doi.org/10.1242/jcs.142331

Hatori, M., Okano, T., Nakajima, Y., Doi, M., & Fukada, Y. (2006). Lcg is a light-inducible and clock-controlled gene expressed in the chicken pineal gland. *Journal of Neurochemistry*, *96*(6), 1790–1800. https://doi.org/10.1111/j.1471-4159.2006.03712.x

Hayden, J. H., Bowser, S. S., & Rieder, C. L. (1990). Kinetochores capture astral microtubules during chromosome attachment to the mitotic spindle: Direct visualization in live newt lung cells. *Journal of Cell Biology*, *111*(3), 1039–1045. https://doi.org/10.1083/jcb.111.3.1039

He, R., Huang, N., Bao, Y., Zhou, H., Teng, J., & Chen, J. (2013). LRRC45 Is a Centrosome

Linker Component Required for Centrosome Cohesion. *Cell Reports*, *4*(6), 1100–1107. https://doi.org/10.1016/j.celrep.2013.08.005

Heilbrunn, L. V., & Wilbur, K. M. (1937). STIMULATION AND NUCLEAR BREAKDOWN IN THE NEREIS EGG. *The Biological Bulletin*, *73*(3), 557–564. https://doi.org/10.2307/1537615

Hiraki, M., Nakazawa, Y., Kamiya, R., & Hirono, M. (2007). Bld10p Constitutes the Cartwheel-Spoke Tip and Stabilizes the 9-Fold Symmetry of the Centriole. *Current Biology*, *17*(20), 1778–1783. https://doi.org/10.1016/j.cub.2007.09.021

Hori, A., Ikebe, C., Tada, M., & Toda, T. (2014). Msd1/SSX2IP-dependent microtubule anchorage ensures spindle orientation and primary cilia formation. *EMBO Reports*, *15*(2), 175–184. https://doi.org/10.1002/embr.201337929

Hori, A., Morand, A., Ikebe, C., Frith, D., Snijders, A. P., & Toda, T. (2015). The conserved Wdr8-hMsd1/SSX2IP complex localises to the centrosome and ensures proper spindle length and orientation. *Biochemical and Biophysical Research Communications*, *468*(1–2), 39–45. https://doi.org/10.1016/j.bbrc.2015.10.169

Hossain, D., Shih, S. Y. P., Xiao, X., White, J., & Tsang, W. Y. (2020). Cep44 functions in centrosome cohesion by stabilizing rootletin. *Journal of Cell Science*, *133*(4). https://doi.org/10.1242/jcs.239616

Hussain, M. S., Baig, S. M., Neumann, S., Nürnberg, G., Farooq, M., Ahmad, I., … Nürnberg, P. (2012). A truncating mutation of CEP135 causes primary microcephaly and disturbed centrosomal function. *American Journal of Human Genetics*, *90*(5), 871–878. https://doi.org/10.1016/j.ajhg.2012.03.016

Inanc, B., Putz, M., Lalor, P., Dockery, P., Kuriyama, R., Gergely, F., & Morrison, C. G. (2013). Abnormal centrosomal structure and duplication in Cep135-deficient vertebrate cells. *Molecular Biology of the Cell*, *24*(17), 2645–2654. https://doi.org/10.1091/mbc.E13-03-0149

Inoue, D., Stemmer, M., Thumberger, T., Ruppert, T., Bärenz, F., Wittbrodt, J., & Gruss, O. J. (2017). Expression of the novel maternal centrosome assembly factor Wdr8 is required for vertebrate embryonic mitoses. *Nature Communications*, *8*. https://doi.org/10.1038/ncomms14090

Inoué, S. (1953). Polarization optical studies of the mitotic spindle - I. The demonstration of spindle fibers in living cells. *Chromosoma*, *5*(1), 487–500.

https://doi.org/10.1007/BF01271498

Izquierdo, D., Wang, W. J., Uryu, K., & Tsou, M. F. B. (2014). Stabilization of cartwheel-less centrioles for duplication requires CEP295-mediated centriole-to-centrosome conversion. *Cell Reports*, *8*(4), 957–965. https://doi.org/10.1016/j.celrep.2014.07.022

Jedrzejczak-Silicka, M. (2017). History of Cell Culture. *New Insights into Cell Culture Technology*, 1–42. https://doi.org/10.5772/66905

Jiang, S. T., Chiou, Y. Y., Wang, E., Lin, H. K., Lee, S. P., Lu, H. Y., … Li, H. (2008). Targeted disruption of Nphp1 causes male infertility due to defects in the later steps of sperm morphogenesis in mice. *Human Molecular Genetics*, *17*(21), 3368–3379. https://doi.org/10.1093/hmg/ddn231

Jiang, X., Ho, D. B. T., Mahe, K., Mia, J., Sepulveda, G., Antkowiak, M., … Jao, L.-E. (2021). Condensation of pericentrin proteins in human cells illuminates phase separation in centrosome assembly. *Journal of Cell Science*, *134*(14), 5–24. https://doi.org/10.1242/jcs.258897

Johnson, R. T., & Rao, P. N. (1970). Mammalian Cell Fusion : Induction of Premature Chromosome Condensation in Interphase Nuclei. *Nature*, *226*(5247), 717–722. https://doi.org/10.1038/226717a0

Jordan, M. A., Thrower, D., & Wilson, L. (1992). Effects of vinblastine, podophyllotoxin and nocodazole on mitotic spindles. Implications for the role of microtubule dynamics in mitosis. *Journal of Cell Science*, *102*(3), 401–416. https://doi.org/10.1242/jcs.102.3.401

KANE, R. E. (1965). the Mitotic Apparatus. Physical-Chemical Factors Controlling Stability. *The Journal of Cell Biology*, *25*. https://doi.org/10.1083/jcb.25.1.137

Karakas, B., Weeraratna, A. T., Abukhdeir, A. M., Konishi, H., Gustin, J. P., Vitolo, M. I., … Ben, H. P. (2007). P21 Gene Knock Down Does Not Identify Genetic Effectors Seen With Gene Knock Out. *Cancer Biology and Therapy*, *6*(7), 1025–1030. https://doi.org/10.4161/cbt.6.7.4202

Kato, M., Han, T. W., Xie, S., Shi, K., Du, X., Wu, L. C., … McKnight, S. L. (2012). Cell-free formation of RNA granules: Low complexity sequence domains form dynamic fibers within hydrogels. *Cell*, *149*(4), 753–767. https://doi.org/10.1016/j.cell.2012.04.017

Khodjakov, A., Cole, R. W., Oakley, B. R., & Rieder, C. L. (2000). Centrosome-independent mitotic spindle formation in vertebrates. *Current Biology*, *10*(2), 59–67.

https://doi.org/10.1016/S0960-9822(99)00276-6

Kim, K., Lee, S., Chang, J., & Rhee, K. (2008). A novel function of CEP135 as a platform protein of C-NAP1 for its centriolar localization. *Experimental Cell Research*, *314*(20), 3692–3700. https://doi.org/10.1016/j.yexcr.2008.09.016

King, M. R., & Petry, S. (2020). Phase separation of TPX2 enhances and spatially coordinates microtubule nucleation. *Nature Communications*, *11*(1), 1–13. https://doi.org/10.1038/s41467-019-14087-0

Kirschner, M., & Mitchison, T. (1986). Beyond self-assembly: From microtubules to morphogenesis. *Cell*, *45*(3), 329–342. https://doi.org/10.1016/0092-8674(86)90318-1

Kleylein-Sohn, J., Westendorf, J., Le Clech, M., Habedanck, R., Stierhof, Y. D., & Nigg, E. A. (2007). Plk4-Induced Centriole Biogenesis in Human Cells. *Developmental Cell*, *13*(2), 190–202. https://doi.org/10.1016/j.devcel.2007.07.002

Klinger, M., Wang, W., Kuhns, S., Barenz, F., Drager-Meurer, S., Pereira, G., & Gruss, O. J. (2014). The novel centriolar satellite protein SSX2IP targets Cep290 to the ciliary transition zone. *Molecular Biology of the Cell*, *25*(4), 495–507. https://doi.org/10.1091/mbc.E13-09-0526

Kok, F. O., Shin, M., Ni, C. W., Gupta, A., Grosse, A. S., vanImpel, A., … Lawson, N. D. (2015). Reverse genetic screening reveals poor correlation between morpholino-induced and mutant phenotypes in zebrafish. *Developmental Cell*, *32*(1), 97–108. https://doi.org/10.1016/j.devcel.2014.11.018

Koshizuka, Y., Ikegawa, S., Sano, M., Nakamura, K., & Nakamura, Y. (2001). Isolation, characterization, and mapping of the mouse and human WDR8 genes, members of a novel WD-repeat gene family. *Genomics*, *72*(3), 252–259. https://doi.org/10.1006/geno.2000.6475

Kozminski, K. G., Beech, P. L., & Rosenbaum, J. L. (1995). The Chlamydomonas kinesin-like protein FLA10 is involved in motility associated with the flagellar membrane. *Journal of Cell Biology*, *131*(6 I), 1517–1527. https://doi.org/10.1083/jcb.131.6.1517

Kozminski, K. G., Johnson, K. A., Forscher, P., & Rosenbaum, J. L. (1993). A motility in the eukaryotic flagellum unrelated to flagellar beating (Chlamydomonas/ntrelular movement/ultrastcture). *Proc. Natl. Acad. Sci. USA*, *90*(June), 5519–5523.

Kubo, A., & Tsukita, S. (2003). Non-membranous granular organelle consisting of PCM-1: Subcellular distribution and cell-cycle-dependent assembly/disassembly. *Journal of*

*Cell Science*, *116*(5), 919–928. https://doi.org/10.1242/jcs.00282

Kulaga, H. M., Leitch, C. C., Eichers, E. R., Badano, J. L., Lesemann, A., Hoskins, B. E., … Katsanis, N. (2004). Loss of BBS proteins causes anosmia in humans and defects in olfactory cilia structure and function in the mouse. *Nature Genetics*, *36*(9), 994–998. https://doi.org/10.1038/ng1418

Kurtulmus, B., Wang, W., Ruppert, T., Neuner, A., Cerikan, B., Viol, L., … Pereira, G. (2016). WDR8 is a centriolar satellite and centriole-associated protein that promotes ciliary vesicle docking during ciliogenesis. *Journal of Cell Science*, *129*(3), 621–636. https://doi.org/10.1242/jcs.179713

Ledbetter, M. C., & Porter, K. R. (1963). A "microtubule" in plant cell fine structure. *Journal of Cell Biology*, *19*(1), 239–250. https://doi.org/10.1083/jcb.19.1.239

Lohka, M. I., & Maller, J. L. (1985). Induction of nuclear envelope breakdown, chromosome condensation, and spindle formation in cell-free extracts. *Journal of Cell Biology*, *101*(2), 518–523. https://doi.org/10.1083/jcb.101.2.518

Lohka, M. J., & Masui, Y. (1983). Formation in vitro of sperm pronuclei and mitotic chromosomes induced by amphibian ooplasmic components. *Science*, *220*(4598), 719–721. https://doi.org/10.1126/science.6601299

Luykx, P. (1965). The structure of the kinetochore in meiosis and mitosis in Urechis eggs. *Experimental Cell Research*, *39*(2–3), 643–657. https://doi.org/10.1016/0014-4827(65)90068-6

Mardin, B. R., Isokane, M., Cosenza, M. R., Krämer, A., Ellenberg, J., Fry, A. M., & Schiebel, E. (2013). EGF-Induced Centrosome Separation Promotes Mitotic Progression and Cell Survival. *Developmental Cell*, *25*(3), 229–240. https://doi.org/10.1016/j.devcel.2013.03.012

Mardin, B. R., Lange, C., Baxter, J. E., Hardy, T., Scholz, S. R., Fry, A. M., & Schiebel, E. (2010). Components of the Hippo pathway cooperate with Nek2 kinase to regulate centrosome disjunction. *Nature Cell Biology*, *12*(12), 1166–1176. https://doi.org/10.1038/ncb2120

Masui, Y. (2001). From oocyte maturation to the in vitro cell cycle: The history of discoveries of Maturation-Promoting Factor (MPF) and Cytostatic Factor (CSF). *Differentiation*, *69*(1), 1–17. https://doi.org/10.1046/j.1432-0436.2001.690101.x

Matson, J. P., & Cook, J. G. (2017). Cell cycle proliferation decisions: the impact of single

cell analyses. *FEBS Journal*, *284*(3), 362–375. https://doi.org/10.1111/febs.13898

Matsuo, K., Ohsumi, K., Iwabuchi, M., Kawamata, T., Ono, Y., & Takahashi, M. (2012). Kendrin is a novel substrate for separase involved in the licensing of centriole duplication. *Current Biology*, *22*(10), 915–921. https://doi.org/10.1016/j.cub.2012.03.048

Matsuura, K., Lefebvre, P. A., Kamiya, R., & Hirono, M. (2004). Bld10p, a novel protein essential for basal body assembly in Chlamydomonas: Localization to the cartwheel, the first ninefold symmetrical structure appearing during assembly. *Journal of Cell Biology*, *165*(5), 663–671. https://doi.org/10.1083/jcb.200402022

Mazia, D., Chaffee, R. R., & Iverson, R. M. (1961). ADENOSINE TRIPHOSPHATASE IN THE MITOTIC APPARATUS. *Proceedings of the National Academy of Sciences*, *47*(6), 788–790. https://doi.org/10.1073/pnas.47.6.788

Mazo, G., Soplop, N., Wang, W. J., Uryu, K., & Tsou, M. F. B. (2016). Spatial Control of Primary Ciliogenesis by Subdistal Appendages Alters Sensation-Associated Properties of Cilia. *Developmental Cell*, *39*(4), 424–437. https://doi.org/10.1016/j.devcel.2016.10.006

Mazzarello, P. (1999). A unifying concept: The history of cell theory. *Nature Cell Biology*, *1*(1), E13–E15. https://doi.org/10.1038/8964

Mendez, R., & Richter, J. D. (2001). Translational control by CPEB: A means to the end. *Nature Reviews Molecular Cell Biology*, *2*(7), 521–529. https://doi.org/10.1038/35080081

Mitchison, T., & Kirschner, M. (1984). Dynamic instability of microtubule growth. *Nature*, *312*(5991), 237–242. https://doi.org/10.1038/312237a0

Mohri, H. (1968). Amino-acid composition of “tubulin” constituting microtubules of sperm flagella [18]. *Nature*, *217*(5133), 1053–1054. https://doi.org/10.1038/2171053a0

Morgens, D. W., Deans, R. M., Li, A., & Bassik, M. C. (2016). Systematic comparison of CRISPR/Cas9 and RNAi screens for essential genes. *Nature Biotechnology*, *34*(6), 634–636. https://doi.org/10.1038/nbt.3567

Moritz, M., Braunfeld, M. B., Fung, J. C., Sedat, J. W., Alberts, B. M., & Agard, D. A. (1995). Three-dimensional structural characterization of centrosomes from early Drosophila embryos. *Journal of Cell Biology*, *130*(5), 1149–1159. https://doi.org/10.1083/jcb.130.5.1149

Moritz, M., Zheng, Y., Alberts, B. M., & Oegema, K. (1998). Recruitment of the γ-Tubulin Ring Complex to Drosophila Salt-stripped Centrosome Scaffolds. *Journal of Cell Biology*, *142*(3), 775–786. https://doi.org/10.1083/jcb.142.3.775

Mottier-Pavie, V., & Megraw, T. L. (2009). Drosophila Bld10 Is a Centriolar Protein That Regulates Centriole, Basal Body, and Motile Cilium Assembly. *Molecular Biology of the Cell*, *20*(10), 2605–2614. https://doi.org/10.1091/mbc.e08-11-1115

Moudjou, M., Bordes, N., Paintrand, M., & Bornens, M. (1996). Γ-Tubulin in Mammalian Cells the Centrosomal and the.Pdf, *887*, 875–887.

Mykytyn, K., Mullins, R. F., Andrews, M., Chiang, A. P., Swiderski, R. E., Yang, B., … Sheffield, V. C. (2004). Bardet-Bledl syndrome type 4 (BBS4)-null mice implicate Bbs4 in flagella formation but not global cilia assembly. *Proceedings of the National Academy of Sciences of the United States of America*, *101*(23), 8664–8669. https://doi.org/10.1073/pnas.0402354101

Nasa, I., & Kettenbach, A. N. (2018). Coordination of protein kinase and phosphoprotein phosphatase activities in mitosis. *Frontiers in Cell and Developmental Biology*, *6*(MAR), 1–14. https://doi.org/10.3389/fcell.2018.00030

Oegema, K., Wiese, C., Martin, O. C., Milligan, R. A., Iwamatsu, A., Mitchison, T. J., & Zheng, Y. (1999). Characterization of two related Drosophila γ-tubulin complexes that differ in their ability to nucleate microtubules. *Journal of Cell Biology*, *144*(4), 721–733. https://doi.org/10.1083/jcb.144.4.721

Pagan, J. K., Marzio, A., Jones, M. J. K., Saraf, A., Jallepalli, P. V., Florens, L., … Pagano, M. (2015). Degradation of Cep68 and PCNT cleavage mediate Cep215 removal from the PCM to allow centriole separation, disengagement and licensing. *Nature Cell Biology*, *17*(1), 31–43. https://doi.org/10.1038/ncb3076

Paschal, B. M., Shpetner, H. S., & Vallee, R. B. (1987). MAP 1C is a microtubule-activated ATPase which translocates microtubules in vitro and has dynein-like properties. *Journal of Cell Biology*, *105*(3), 1273–1282. https://doi.org/10.1083/jcb.105.3.1273

Paweletz, N. (2001). Walther Flemming: Pioneer of mitosis research. *Nature Reviews Molecular Cell Biology*, *2*(1), 72–75. https://doi.org/10.1038/35048077

Pazour, G. J., Dickert, B. L., Vucica, Y., Seeley, E. S., Rosenbaum, J. L., Witman, G. B., & Cole, D. G. (2000). Chlamydomonas IFT88 and its mouse homologue, polycystic kidney disease gene Tg737, are required for assembly of cilia and flagella. *Journal of Cell*

*Biology*, *151*(3), 709–718. https://doi.org/10.1083/jcb.151.3.709

Pereira, A. J., & Maiato, H. (2012). Maturation of the kinetochore-microtubule interface and the meaning of metaphase. *Chromosome Research*, *20*(5), 563–577. https://doi.org/10.1007/s10577-012-9298-8

Peretz, L., Besser, E., Hajbi, R., Casden, N., Ziv, D., Kronenberg, N., … Behar, O. (2018). Combined shRNA over CRISPR/cas9 as a methodology to detect off-target effects and a potential compensatory mechanism. *Scientific Reports*, *8*(1), 1–13. https://doi.org/10.1038/s41598-017-18551-z

Piel, M., Meyer, P., Khodjakov, A., Rieder, C. L., & Bornens, M. (2000). The respective contributions of the mother and daughter centrioles to centrosome activity and behavior in vertebrate cells. *Journal of Cell Biology*, *149*(2), 317–329. https://doi.org/10.1083/jcb.149.2.317

Piqué, M., López, J. M., Foissac, S., Guigó, R., & Méndez, R. (2008). A Combinatorial Code for CPE-Mediated Translational Control. *Cell*, *132*(3), 434–448. https://doi.org/10.1016/j.cell.2007.12.038

Pizon, V., Gaudin, N., Poteau, M., Cifuentes-Diaz, C., Demdou, R., Heyer, V., … Azimzadeh, J. (2020). hVFL3/CCDC61 is a component of mother centriole subdistal appendages required for centrosome cohesion and positioning. *Biology of the Cell*, *112*(1), 22–37. https://doi.org/10.1111/boc.201900038

Prosser, S. L., & Pelletier, L. (2020). Centriolar satellite biogenesis and function in vertebrate cells. *Journal of Cell Science*, *133*(1). https://doi.org/10.1242/jcs.239566

Puck, T. T. (1962). Quantitative Colonial Growth of Single Mammalian Cells. *Annals of the New York Academy of Sciences*, *71*(6), 1141–1142. https://doi.org/10.1111/j.1749-6632.1958.tb54675.x

Raff, J. W. (2019). Phase Separation and the Centrosome: A Fait Accompli? *Trends in Cell Biology*, *29*(8), 612–622. https://doi.org/10.1016/j.tcb.2019.04.001

Rellos, P., Ivins, F. J., Baxter, J. E., Pike, A., Nott, T. J., Parkinson, D. M., … Smerdon, S. J. (2007). Structure and regulation of the human Nek2 centrosomal kinase. *Journal of Biological Chemistry*, *282*(9), 6833–6842. https://doi.org/10.1074/jbc.M609721200

Richard Mcintosh, J. (2016). Mitosis. *Cold Spring Harbor Perspectives in Biology*, *8*(9), a023218. https://doi.org/10.1101/cshperspect.a023218

Rieder, C. L., & Alexander, S. P. (1990). Kinetochores are transported poleward along a

single astral microtubule during chromosome attachment to the spindle in newt lung cells. *Journal of Cell Biology*, *110*(1), 81–95. https://doi.org/10.1083/jcb.110.1.81

Rodrigues-Ferreira, S., Di Tommasso, A., Dimitrov, A., Cazaubon, S., Gruel, N., Colasson, H., … Nahmias, C. (2009). 8p22 MTUS1 gene product ATIP3 is a novel anti-mitotic protein underexpressed in invasive breast carcinoma of poor prognosis. *PLoS ONE*, *4*(10). https://doi.org/10.1371/journal.pone.0007239

Roque, H., Wainman, A., Richens, J., Kozyrska, K., Franz, A., & Raff, J. W. (2012). Drosophila Cep135/Bld10 maintains proper centriole structure but is dispensable for cartwheel formation. *Journal of Cell Science*, *125*(23), 5881–5886. https://doi.org/10.1242/jcs.113506

Ryu, J. H., Essner, R., Ohta, T., & Kuriyama, R. (2000). Filamentous polymers induced by overexpression of a novel centrosomal protein, Cep135. *Microscopy Research and Technique*, *49*(5), 478–486. https://doi.org/10.1002/(SICI)1097-0029(20000601)49:5<478::AID-JEMT10>3.0.CO;2-J

Sauter, A., Roosen-Runge, F., Zhang, F., Lotze, G., Feoktystov, A., Jacobs, R. M. J., & Schreiber, F. (2015). On the question of two-step nucleation in protein crystallization. *Faraday Discussions*, *179*, 41–58. https://doi.org/10.1039/c4fd00225c

Sawin, K. E., LeGuellec, K., Philippe, M., & Mitchison, T. J. (1992). Mitotic spindle organization by a plus-end-directed microtubule motor. *Nature*, *359*(6395), 540–543. https://doi.org/10.1038/359540a0

Scheer, U. (2014). Historical roots of centrosome research: Discovery of Boveri's microscope slides in Würzburg. *Philosophical Transactions of the Royal Society B: Biological Sciences*, *369*(1650). https://doi.org/10.1098/rstb.2013.0469

Schiff, P. B., Fant, J., & Horwitz, S. B. (1979). Promotion of microtubule assembly in vitro by taxol [19]. *Nature*, *277*(5698), 665–667. https://doi.org/10.1038/277665a0

Schmidt, W. J. (1939). Doppelbrechung der Kernspindel und Zugfasertheorie der Chromosomenbewegung. *Chromosoma*, *1*(1), 253–264. https://doi.org/10.1007/BF01271634

Schwann, T. H. (1993). *Microscopial researches into the accordance in the structure and growth of animals and plants. 1847. Obesity research* (Vol. 1). https://doi.org/10.1002/j.1550-8528.1993.tb00021.x

Shelanski, M. L., Gaskin, F., & Cantor, C. R. (1973). Microtubule assembly in the absence of

added nucleotides. *Proceedings of the National Academy of Sciences of the United States of America*, *70*(3), 765–768. https://doi.org/10.1073/pnas.70.3.765

Shelanski, M. L., & Taylor, E. W. (1967). Isolation of a protein subunit from microtubules. *The Journal of Cell Biology*, *34*(2), 549–554. https://doi.org/10.1083/jcb.34.2.549

Shen, K. F., & Osmani, S. A. (2013). Regulation of mitosis by the NIMA kinase involves TINA and its newly discovered partner, An-WDR8, at spindle pole bodies. *Molecular Biology of the Cell*, *24*(24), 3842–3856. https://doi.org/10.1091/mbc.E13-07-0422

Sherline, P., & Mascardo, R. (1982). Epidermal growth factor-induced centrosomal separation: Mechanism and relationship to mitogenesis. *Journal of Cell Biology*, *95*(1), 316–322. https://doi.org/10.1083/jcb.95.1.316

Sir, J. H., Pütz, M., Daly, O., Morrison, C. G., Dunning, M., Kilmartin, J. V., & Gergely, F. (2013). Loss of centrioles causes chromosomal instability in vertebrate somatic cells. *Journal of Cell Biology*, *203*(5), 747–756. https://doi.org/10.1083/jcb.201309038

Smith, E., Hégarat, N., Vesely, C., Roseboom, I., Larch, C., Streicher, H., … Hochegger, H. (2011). Differential control of Eg5-dependent centrosome separation by Plk1 and Cdk1. *EMBO Journal*, *30*(11), 2233–2245. https://doi.org/10.1038/emboj.2011.120

Smith, T. F., Gaitatzes, C., Saxena, K., & Neer, E. J. (1999). The WD repeat: A common architecture for diverse functions. *Trends in Biochemical Sciences*, *24*(5), 181–185. https://doi.org/10.1016/S0968-0004(99)01384-5

Sonnen, K. F., Schermelleh, L., Leonhardt, H., & Nigg, E. A. (2012). 3D-structured illumination microscopy provides novel insight into architecture of human centrosomes. *Biology Open*, *1*(10), 965–976. https://doi.org/10.1242/bio.20122337

Strnad, P., Leidel, S., Vinogradova, T., Euteneuer, U., Khodjakov, A., & Gönczy, P. (2007). Regulated HsSAS-6 Levels Ensure Formation of a Single Procentriole per Centriole during the Centrosome Duplication Cycle. *Developmental Cell*, *13*(2), 203–213. https://doi.org/10.1016/j.devcel.2007.07.004

Trans, R. L. P., Land, R. S., Sci, R. L. A. J. E., Crust, C., Archaean, H., Evolution, C., & Elsevier, K. C. (1995). Nucleation of microtubule assembly by a y-tubulin-containing ring complex Yixian Zheng *, Mei Lie Wong *, Bruce Alberts * t Be Tim Mitchison t. *Nature*, *378*(December), 578–583.

Tsou, M. F. B., & Stearns, T. (2006). Mechanism limiting centrosome duplication to once per cell cycle. *Nature*, *442*(7105), 947–951. https://doi.org/10.1038/nature04985

Vallee, R. B. (1982). A taxol-dependent procedure for the isolation of microtubules and microtubule-associated proteins (MAPs). *Journal of Cell Biology*, *92*(2), 435–42. https://doi.org/10.1083/jcb.92.2.435

Vasquez-Limeta, A., & Loncarek, J. (2021). Human centrosome organization and function in interphase and mitosis. *Seminars in Cell and Developmental Biology*, *117*(April), 30–41. https://doi.org/10.1016/j.semcdb.2021.03.020

Verde, F., Berrez, J. M., Antony, C., & Karsenti, E. (1991). Taxol-induced microtubule asters in mitotic extracts of Xenopus eggs: Requirement for phosphorylated factors and cytoplasmic dynein. *Journal of Cell Biology*, *112*(6), 1177–1187. https://doi.org/10.1083/jcb.112.6.1177

Villalba, A., Coll, O., & Gebauer, F. (2011). Cytoplasmic polyadenylation and translational control. *Current Opinion in Genetics and Development*, *21*(4), 452–457. https://doi.org/10.1016/j.gde.2011.04.006

Viol, L., Hata, S., Pastor-Peidro, A., Neuner, A., Murke, F., Wuchter, P., … Pereira, G. (2020). Nek2 kinase displaces distal appendages from the mother centriole prior to mitosis. *Journal of Cell Biology*, *219*(3). https://doi.org/10.1083/JCB.201907136

Vlijm, R., Li, X., Panic, M., Rüthnick, D., Hata, S., Herrmannsdörfer, F., … Schiebel, E. (2018). STED nanoscopy of the centrosome linker reveals a CEP68-organized, periodic rootletin network anchored to a C-Nap1 ring at centrioles. *Proceedings of the National Academy of Sciences of the United States of America*, *115*(10), E2246–E2253. https://doi.org/10.1073/pnas.1716840115

Wang, G., Jiang, Q., & Zhang, C. (2014). The role of mitotic kinases in coupling the centrosome cycle with the assembly of the mitotic spindle. *Journal of Cell Science*, *127*(19), 4111–4122. https://doi.org/10.1242/jcs.151753

Wang, W. J., Soni, R. K., Uryu, K., & Tsou, M. F. B. (2011). The conversion of centrioles to centrosomes: Essential coupling of duplication with segregation. *Journal of Cell Biology*, *193*(4), 727–739. https://doi.org/10.1083/jcb.201101109

Wang, X., Yang, Y., Duan, Q., Jiang, N., Huang, Y., Darzynkiewicz, Z., & Dai, W. (2008). sSgo1, a major splice variant of Sgo1, functions in centriole cohesion where it is regulated by Plk1. *Developmental Cell*, *14*(3), 331–341. https://doi.org/10.1016/j.devcel.2007.12.007

Warren, J. C., Rutkowski, A., & Cassimeris, L. (2006). Infection with Replication-deficient

Adenovirus Induces Changes in the Dynamic Instability of Host Cell Microtubules. *Molecular Biology of the Cell*, *17*(8), 3557–3568. https://doi.org/10.1091/mbc.e05-09-0850

Watanabe, K., Takao, D., Ito, K. K., Takahashi, M., & Kitagawa, D. (2019). The Cep57-pericentrin module organizes PCM expansion and centriole engagement. *Nature Communications*, *10*(1), 1–13. https://doi.org/10.1038/s41467-019-08862-2

Watson, M. R., & Hopkins, J. M. (1962). Isolated cilia from Tetrahymena pyriformis. *Experimental Cell Research*, *28*(2), 280–295. https://doi.org/10.1016/0014-4827(62)90284-7

Weisenberg, R. C. (1972). Microtubule formation in vitro in solutions containing low calcium concentrations. *Science*, *177*(4054), 1104–1105. https://doi.org/10.1126/science.177.4054.1104

Weisenberg, R. C., Borisy, G. G., & Taylor, E. W. (1968). The Colchicine-Binding Protein of Mammalian Brain and Its Relation to Microtubules. *Biochemistry*, *7*(12), 4466–4479. https://doi.org/10.1021/bi00852a043

Wells, W. A. (2005). Microtubules get a name. *Journal of Cell Biology*, *168*(6), 852. https://doi.org/10.1083/jcb1686fta1

Wilson, J. W. (1947). Virchow's contribution to the cell theory. *Journal of the History of Medicine and Allied Sciences*, *2*(2), 163–178. https://doi.org/10.1093/jhmas/II.2.163

Woodruff, J. B., Ferreira Gomes, B., Widlund, P. O., Mahamid, J., Honigmann, A., & Hyman, A. A. (2017). The Centrosome Is a Selective Condensate that Nucleates Microtubules by Concentrating Tubulin. *Cell*, *169*(6), 1066–1077.e10. https://doi.org/10.1016/j.cell.2017.05.028

Woodruff, J. B., Wueseke, O., & Hyman, A. A. (2014). Pericentriolar material structure and dynamics. *Philosophical Transactions of the Royal Society B: Biological Sciences*, *369*(1650). https://doi.org/10.1098/rstb.2013.0459

Woodruff, J. B., Wueseke, O., Viscardi, V., Mahamid, J., Ochoa, S. D., Bunkenborg, J., … Hyman, A. A. (2015). Regulated assembly of a supramolecular centrosome scaffold in vitro. *Science*, *348*(6236), 808–812. https://doi.org/10.1126/science.aaa3923

Xia, Y., Huang, N., Chen, Z., Li, F., Fan, G., Ma, D., … Teng, J. (2018). CCDC102B functions in centrosome linker assembly and centrosome cohesion. *Journal of Cell Science*, *131*(23), 1–12. https://doi.org/10.1242/jcs.222901

Yukawa, M., Ikebe, C., & Toda, T. (2015). The Msd1-Wdr8-Pkl1 complex anchors microtubule minus ends to fission yeast spindle pole bodies. *Journal of Cell Biology*, *209*(4), 549–562. https://doi.org/10.1083/jcb.201412111

Zwicker, D., Decker, M., Jaensch, S., Hyman, A. A., & Jülicher, F. (2014). Centrosomes are autocatalytic droplets of pericentriolar material organized by centrioles. *Proceedings of the National Academy of Sciences of the United States of America*, *111*(26). https://doi.org/10.1073/pnas.1404855111

# 7 Appendices

## 7.1 Abbreviation

| | |
|---|---|
| ADP | Adenosine diphosphate |
| APC/C | Anaphase-promoting complex |
| ARL13B | ADP-ribosylation factor-like protein 13B |
| ATP | Adenosine triphosphate |
| C-Nap1 | Centrosomal Nek2-associated protein 1 |
| CDK | Cyclin-dependent kinase 1 |
| CDK5RAP2 | Cdk5 regulatory subunit associated protein 2 |
| Cep135 | Centrosomal protein of 135kDa |
| CP110 | Centriolar coiled-coil protein of 110 kDa |
| CPAP | Centrosomal P4.1-associated protein |
| CSF | Cytostatic Factor |
| DA | Distal Appendage |
| DAPI | 4'6-diamidino-2-phenylindole |
| DMSO | Dimethyl sulfoxide |
| DNA | deoxyribonucleic acid |
| dNTP | deoxynucleosid 5´- triphosphate |
| EDTA | ethylene glycol-bis tetraacetic acid |
| EM | Electron Microscopy |
| ER | Endoplasmic reticulum |
| G1 phase | Growth phase 1 |
| G2 phase | Growth phase 2 |
| GDP | Guanosine diphosphate |
| GFP | green fluorescent protein |
| GTP | Guanosine triphosphate |
| GVBD | Germinal vesicle break down |
| IFT | Introflagellar transport |
| KT-fibers | Kinetochore-fibers |
| MA | spindle apparatus |
| MAP | Microtubule associated protein |

| | |
|---|---|
| MI | Meiosis I |
| MII | Meiosis II |
| MPF | Maturation promoting factor |
| MT | Microtubule |
| Nek2 | NIMA-related kinase 2 |
| NIMA | Never in mitosis A |
| NLS | Nuclear localisation signal |
| OFD2 | Oral-Facial-Digital Syndrome 1 |
| PBS | Phosphate-buffered saline |
| PCM | Pericentrosomal material |
| PFA | paraformaldehyde |
| R-point | Restriction point |
| RanGAP | Ran GTPase-activating protein |
| RanGEF | Guanine Nucleotide Exchange factor |
| RCC1 | Regulator of chromosome condensation |
| RPE-1 | retinal pigment epithelial 1 |
| S phase | Synthesis phase |
| SAC | Spindle Assembly Checkpoint |
| SDA | subDistal Appendage |
| SDS | sodium dodecyl sulphate |
| SSX2IP | SSX Family Member 2 Interacting Protein |
| WDR8 | WD Repeat Containing , Antisense to TP73 |
| WDR47 | WD Repeat Domain 47 |
| γ-TURC | γ-Tubulin Ring Complex |

Nucleotides:

| | |
|---|---|
| A | adenine |
| G | guanine |
| C | cytosine |
| T | thymine |
| U | uracil |

Amino acids:

| | |
|---|---|
| A | Alanine |
| C | Cysteine |

| | |
|---|---|
| D | Aspartate |
| E | Glutamate |
| F | Phenylalanine |
| G | Glycine |
| H | Histidine |
| I | Isoleucine |
| K | Lysine |
| L | Leucine |
| Y | Tyrosine |
| M | Methionine |
| N | Asparagine |
| P | Proline |
| Q | Glutamine |
| R | Arginine |
| S | Serine |
| T | Threonine |
| V | Valine |
| W | Trypthophane |

## 7.2 List of figures and tables

# 7.3 Supplemental tables

Table1: Whole list of wdr8 IP MS results in *Xenopus* egg extract.

| accession No | MW (kDa) | protein annotation | Exclusive Unique Spectrum Count | |
|---|---|---|---|---|
| | | | IgG | WDR8_91 |
| A0A1L8F8M2_XENLA | 101 kDa | non-ribosomal peptide synthase/polyketide synthase | | 150 |
| A0A1L8FLB0_XENLA | 70 kDa | glucuronokinase 1 | | 98 |
| Q5EAX3_XENLA | 52 kDa | wdr8 | | 36 |
| A0A1L8GFF7_XENLA | 65 kDa | Ssx2ip | | 35 |
| A0A1L8HN47_XENLA | 122 kDa | regulator of nonsense transcripts 1 | | 30 |
| Q6INT0_XENLA | 179 kDa | TOP2A – DNA topoisomerase II alpha | | 23 |
| A0A1L8HU26_XENLA | 136 kDa | cep135 | | 20 |
| A0A1L8EKZ2_XENLA | 70 kDa | embryonic polyadenylate-binding protein A | | 20 |
| A0A1L8G3M7_XENLA | 100 kDa | proteasome 26S subunit ubiquitin receptor, non-ATPase 2 L homeolog | | 20 |
| A0A1L8GR71_XENLA | 34 kDa | nucleophosmin1: centrosome duplication | | 17 |
| A0A1L8FKQ9_XENLA | 79 kDa | protein phosphatase Slingshot homolog | | 10 |
| A0A1L8HEX9_XENLA | 117 kDa | helicase MOV-10 isoform X1 | 1 | 10 |
| A0A1L8HJY0_XENLA | 27 kDa | RPS3 – ribosomal protein S3 | | 10 |
| A0A1L8HTV4_XENLA | 147 kDa | microtubule-associated tumor suppressor 1 homolog (MTUS1) | | 9 |
| A0A1L8F2B5_XENLA | 30 kDa | ribosomal protein S4 X-linked | | 8 |
| A0A1L8HF67_XENLA | 87 kDa | DDX20 – DEAD-box helicase 20 | 0 | 7 |
| A0A1L8F3K2_XENLA | 31 kDa | receptor of activated protein C kinase 1 | | 7 |
| A0A1L8GGG0_XENLA | 31 kDa | 60S ribosomal protein L5-A | | 6 |
| A0A1L8FPV6_XENLA | 130 kDa | AGAP1 – ArfGAP with GTPase domain, ankyrin repeat and PH domain 1 | | 6 |
| A0A1L8G3T0_XENLA | 102 kDa | proteasome 26S subunit, non-ATPase 1 S homeolog | | 5 |
| A0A1L8H6Z2_XENLA | 26 kDa | 60S ribosomal protein L10a | | 5 |
| A0A1L8H4P1_XENLA | 38 kDa | Y-box binding protein 1 | | 4 |
| A3KMH8_XENLA | 73 kDa | FMR1 autosomal homolog 1 | 0 | 4 |
| A0A1L8I1W4_XENLA | 30 kDa | ribosomal protein L6 S | | 4 |
| A0A1L8G5E7_XENLA | 25 kDa | 40S ribosomal protein S7 isoform X2 | | 4 |
| A0A1L8I062_XENLA | 34 kDa | ribosomal protein lateral stalk subunit P0 | | 4 |
| A0A1L8FJK3_XENLA | 235 kDa | myoferlin-like | 0 | 3 |
| A0A1L8GFP2_XENLA | 24 kDa | ribosomal protein S8 | | 3 |
| A0A1L8FWH1_XENLA | 16 kDa | 60S ribosomal protein L14 | | 3 |
| A0A1L8F5R3_XENLA | 18 kDa | ribosomal protein L12 S homeolog | | 3 |
| A0A1L8FZ13_XENLA | 13 kDa | RPS20 – ribosomal protein S20 | | 3 |
| A0A1L8HFU5_XENLA | 20 kDa | 60S ribosomal protein L11-like isoform X1 | | 3 |
| A0A1L8FJC7_XENLA | 26 kDa | nucleoplasmin-3 | | 3 |
| A0A1L8H8B8_XENLA | 18 kDa | 60S ribosomal protein L24 | | 3 |
| A0A1L8FIZ6_XENLA | 135 kDa | WDR11 | | 2 |

| | | | | |
|---|---|---|---|---|
| A0A1L8FNQ9_XENLA | 23 kDa | 40S ribosomal protein S9 | | 2 |
| A0A1L8FQ30_XENLA | 94 kDa | queuosine salvage protein isoform | | 2 |
| A0A1L8F956_XENLA | 60 kDa | PAF1 homolog, Paf1/RNA polymerase II complex component | | 2 |
| A0A1L8END4_XENLA | 18 kDa | 40S ribosomal protein S11 | | 2 |
| A0A1L8FPT5_XENLA | 34 kDa | rRNA 2'-O-methyltransferase fibrillarin | | 2 |
| A0A1L8H6H2_XENLA | 28 kDa | RPL8 – ribosomal protein L8 | | 2 |
| A0A1L8ETY8_XENLA | 16 kDa | 60S ribosomal protein L27 | | 2 |
| Q08B25_XENLA | 96 kDa | RBM25 – RNA binding motif protein 25 | | 2 |
| A0A1L8GV48_XENLA | 17 kDa | 60S ribosomal protein L26-like 1 | | 2 |
| A0A1L8EWC9_XENLA | 34 kDa | protein activator of interferon induced protein kinase EIF2AK2 | | 2 |

Table2: Whole list of cep135 IP MS results in *Xenopus* egg extract.

| accession No | MW (kDa) | protein annotation | Exdlusive Unique Spectrum Count | | |
|---|---|---|---|---|---|
| | | | IgG | Cep135 P2 | Cep135 P3 |
| XELAEV_18022892mg | 203 kDa | vitellogenin-B1 precursor | | | 26 |
| XELAEV_18022891mg | 202 kDa | vitellogenin-A2 | | | 7 |
| vtga2 | 202 kDa | vitellogenin A2 | | | 40 |
| XELAEV_18006769mg | 201 kDa | RNA exonuclease 1 homolog isoform X3 | | 12 | |
| XELAEV_18025047mg | 193 kDa | vitellogenin-A2-like | | | 7 |
| A0A1L8H0J0_XENLA | 192 kDa | cep152 | | 6 | |
| Q6INT0_XENLA | 179 kDa | top2a | | 119 | |
| A0A1L8FDS0_XENLA | 167 kDa | EIF3A | | | 32 |
| XELAEV_18016912mg | 164 kDa | Gemin5 | | | 4 |
| XELAEV_18029713mg | 151 kDa | TRAF2 and NCK interacting kinase S homeolog isoform X10 | | | 7 |
| XELAEV_18012803mg | 146 kDa | myb-binding protein 1A-like protein | | 8 | |
| fam83h | 145 kDa | family with sequence similarity 83 member H | | 11 | |
| mink1 | 144 kDa | misshapen like kinase 1 | | | 47 |
| rrp12 | 144 kDa | ribosomal RNA processing 12 homolog | | 3 | |
| XELAEV_18023142mg | 141 kDa | SCL-interrupting locus protein homolog | | | 7 |
| XELAEV_18034144mg | 140 kDa | cleavage and polyadenylation specificity factor subunit 1 isoform X1 | | | 32 |
| dhx38 | 138 kDa | DEAH-box helicase 38 | | | 3 |
| XELAEV_18021901mg | 137 kDa | liprin-alpha-1 isoform X5 | | 1 | |
| A0A1L8HX81_XENLA | 136 kDa | structural maintenance of chromosomes 2 | | 4 | |
| A0A1L8HU26_XENLA | 136 kDa | cep135 | | 46 | 23 |
| A0A1L8F3F9_XENLA | 134 kDa | symplekin | | | 48 |
| XELAEV_18047119mg | 132 kDa | plakophilin 4 S homeolog isoform X1 | | | 21 |
| NAT10 | 130 kDa | N-acetyltransferase 10 | | 6 | |

| | | | | | |
|---|---|---|---|---|---|
| XELAEV_18044603mg | 130 kDa | plakophilin-4 isoform X3 | | | 6 |
| XELAEV_18039657mg | 125 kDa | WD repeat and HMG-box DNA-binding protein 1 | | 13 | |
| tsc1 | 124 kDa | TSC complex subunit 1 | | | 25 |
| wdr6 | 124 kDa | WD repeat domain 6 | | 5 | |
| XELAEV_18009735mg | 122 kDa | regulator of nonsense transcripts 1 | | 32 | |
| XELAEV_18029489mg | 120 kDa | zinc finger protein 451 S homeolog isoform X1 | | 32 | |
| XELAEV_18036889mg | 120 kDa | kinesin-like protein KIF11-B | | 14 | |
| otud4 | 118 kDa | OTU deubiquitinase 4 | | | 15 |
| XELAEV_18012344mg | 117 kDa | helicase MOV-10 isoform X1 | | 18 | |
| cnksr2 | 117 kDa | connector enhancer of kinase suppressor of Ras 2 | | | 7 |
| tsga10 | 107 kDa | testis specific 10 | | | 10 |
| XELAEV_18025501mg | 103 kDa | wdr47 | | | 6 |
| XELAEV_18025501mg | 102 kDa | wdr47 | | | 4 |
| XELAEV_18021339mg | 101 kDa | kinesin-like protein KIF20A isoform X2 | | 4 | |
| XELAEV_18039228mg | 101 kDa | ATP-binding cassette sub-family F member 1 | | 16 | |
| XENTR_v900264382mg | 100 kDa | eukaryotic translation initiation factor 3 subunit C | | | 18 |
| XELAEV_180268731mg | 100 kDa | CCAAT enhancer binding protein zeta L homeolog | | 9 | |
| XELAEV_18021535mg | 99 kDa | matrin-3 | | | 4 |
| XELAEV_18014468mg | 99 kDa | periodic tryptophan protein 2 homolog isoform X1 | | 10 | |
| XELAEV_18021470mg | 94 kDa | heat shock protein family A (Hsp70) member 4 S homeolog | | 22 | |
| arhgef7 | 93 kDa | Rho guanine nucleotide exchange factor 7 | | 12 | |
| rbm28 | 92 kDa | RNA binding motif protein 28 | | 6 | |
| XELAEV_18045528mg | 92 kDa | transducin (beta)-like 3 L homeolog | | 7 | |
| XELAEV_18041000mg | 90 kDa | vacuolar fusion protein MON1 homolog B isoform X7 | | | 14 |
| cul1 | 90 kDa | cullin 1 | | 6 | |
| noc2l | 90 kDa | NOC2 like nucleolar associated transcriptional repressor | | 5 | |
| cul3 | 89 kDa | CUL3 – cullin 3 | | 25 | |
| XELAEV_18039304mg | 89 kDa | SH3KBP1-binding protein 1 isoform X2 | | 4 | |
| ddx20 | 87 kDa | DEAD-box helicase 20 | | | 8 |
| XELAEV_18028315mg | 85 kDa | trifunctional enzyme subunit alpha, mitochondrial-like | | 8 | |
| XELAEV_18041315mg | 84 kDa | cleavage and polyadenylation specificity factor subunit 2 | | | 29 |
| XELAEV_18035836mg | 84 kDa | tripartite motif containing 28 L homeolog isoform X1 | | 14 | |
| nsf | 83 kDa | N-ethylmaleimide sensitive factor, vesicle fusing ATPase | | | 5 |
| XELAEV_18011679mg | 82 kDa | ARF GTPase-activating protein GIT1-like isoform X2 | | 7 | |
| nop2 | 82 kDa | NOP2 nucleolar protein | | 8 | |
| XELAEV_18007483mg | 81 kDa | G protein-coupled receptor kinase interacting ArfGAP 2 L homeolog | | 15 | |

| | | | | | |
|---|---|---|---|---|---|
| XELAEV_18030252mg | 81 kDa | trifunctional enzyme subunit alpha, mitochondrial-like | | 36 | |
| mphosph10 | 81 kDa | M-phase phosphoprotein 10 | | 4 | |
| XELAEV_18019105mg | 80 kDa | ssx2ip | | | 5 |
| nol11 | 80 kDa | nucleolar protein 11 | | 8 | |
| eif3b | 80 kDa | eukaryotic translation initiation factor 3 subunit B | | | 18 |
| prc1 | 78 kDa | protein regulator of cytokinesis 1 | | 17 | |
| XELAEV_18025208mg | 78 kDa | kinesin-like protein KIF2C | | | 16 |
| cpsf3 | 78 kDa | cleavage and polyadenylation specific factor 3 | | | 25 |
| XELAEV_18017717mg | 78 kDa | G2 and S-phase expressed 1 L homeolog | | | 3 |
| utp4 | 77 kDa | UTP4 small subunit processome component | | 7 | |
| XELAEV_18031895mg | 76 kDa | THO complex 1 protein L homeolog | | | 4 |
| XELAEV_18029577mg | 76 kDa | nucleolin S homeolog | | 12 | |
| XELAEV_18008122mg | 76 kDa | nucleolin S homeolog | | 49 | |
| XELAEV_18015366mg | 75 kDa | regulator of MON1-CCZ1 complex | | | 17 |
| XELAEV_18015131mg | 75 kDa | thyroid hormone receptor associated protein 3 S homeolog | | | 4 |
| XGB | 74 kDa | x globin | | 4 | |
| XELAEV_18043094mg | 73 kDa | kelch-like protein 11 | | 10 | |
| XELAEV_18034897mg | 73 kDa | calcium/calmodulin-dependent protein kinase type II subunit gamma isoform X1 | | | 13 |
| wdr43 | 73 kDa | WD repeat domain 43 | | 12 | |
| XELAEV_18006841mg | 73 kDa | pum 3 pumilio RNA binding family member | | 21 | |
| XELAEV_18012485mg | 72 kDa | serine/arginine-rich splicing factor 6-like isoform X1 | | | 8 |
| utp6 | 71 kDa | UTP6 small subunit processome component | | 5 | |
| btrc | 69 kDa | beta-transducin repeat containing E3 ubiquitin protein ligase | | | 5 |
| XELAEV_18009547mg | 68 kDa | protein regulator of cytokinesis 1, gene 2 S homeolog | | 65 | |
| XELAEV_18043370mg | 67 kDa | vesicle-fusing ATPase | | | 42 |
| eif3l | 67 kDa | eukaryotic translation initiation factor 3 subunit L | | | 21 |
| XELAEV_18016113mg | 66 kDa | regulator of chromosome condensation (RCC1) and BTB (POZ) domain containing protein 1 S homeolog | | 4 | |
| igf2bp3 | 66 kDa | insulin like growth factor 2 mRNA binding protein 3 | | 11 | 19 |
| XELAEV_18009057mg | 65 kDa | factor interacting with PAPOLA and CPSF1 S homeolog isoform X1 | | | 11 |
| XELAEV_18025046mg | 65 kDa | afadin- and alpha-actinin-binding protein A (ssx2ip) | | | 13 |
| eif3d | 64 kDa | eukaryotic translation initiation factor 3 subunit D | | | 12 |
| fmr1 | 64 kDa | FMRP translational regulator 1 | | 1 | 7 |
| cpeb1 | 63 kDa | cytoplasmic polyadenylation element binding protein 1 | | | 10 |
| XELAEV_18018637mg | 62 kDa | ATP-dependent RNA helicase DDX56 dead box | | 8 | |

| | | | | | |
|---|---|---|---|---|---|
| XELAEV_18047504mg | 62 kDa | ribosomal L1 domain-containing protein 1 isoform X1 | | 4 | |
| cbs | 62 kDa | cystathionine beta-synthase | | | 18 |
| snw1 | 61 kDa | SNW domain containing 1 | | | 4 |
| hic2 | 61 kDa | HIC ZBTB transcriptional repressor 2 | | 4 | |
| XELAEV_18027946mg | 60 kDa | cep63 isoform X2 | | 19 | |
| XELAEV_180076812mg | 60 kDa | hypermethylated in cancer 2 L homeolog isoform X2 | | 27 | |
| XELAEV_18043948mg | 60 kDa | RNA binding motif protein 39 L homeolog isoform X1 | | | 8 |
| cpsf6 | 59 kDa | cleavage and polyadenylation specific factor 6 | | | 9 |
| XELAEV_18004907mg | 59 kDa | T-complex protein 1 subunit eta | | | 5 |
| XELAEV_18043784mg | 59 kDa | UTP18 small subunit processome component L homeolog isoform X2 | | 5 | |
| XELAEV_18021858mg | 57 kDa | ADP-ribosylation factor GTPase-activating protein 2-like isoform X1 | | 21 | |
| zbtb2 | 57 kDa | zinc finger and BTB domain containing 2 | | 4 | |
| gps1 | 55 kDa | G protein pathway suppressor 1 | | 17 | |
| XELAEV_18036152mg | 54 kDa | cytohesin-2 | | | 6 |
| ddx6 | 54 kDa | DEAD-box helicase 6 | | | |
| XELAEV_18047360mg | 53 kDa | nucleolar protein 58 | | 8 | |
| cstf-64-prov | 53 kDa | cleavage stimulation factor, 3' pre-RNA, subunit 2 | | | 18 |
| wrap73 | 52 kDa | wrap73 | | | 7 |
| XELAEV_18020612mg | 52 kDa | COP9 signalosome complex subunit 2 | 1 | 34 | 3 |
| dcaf13 | 51 kDa | DDB1 and CUL4 associated factor 13 | | 6 | |
| ruvbl2 | 51 kDa | RuvB like AAA ATPase 2 | | 4 | 1 |
| cops3 | 48 kDa | Constitutive Photomorphogenic complex subunit | | 35 | |
| cops3 | 48 kDa | Constitutive Photomorphogenic complex subunit | | 8 | |
| XELAEV_18025701mg | 47 kDa | casein kinase I isoform X1 | | 6 | 12 |
| psmd11 | 47 kDa | proteasome 26S subunit, non-ATPase 11 | | 6 | 4 |
| cops4 | 46 kDa | Constitutive Photomorphogenic complex subunit | 1 | 39 | 2 |
| XELAEV_18046367mg | 46 kDa | casein kinase II subunit alpha | | 4 | 5 |
| lsm14b | 46 kDa | LSM family member 14B | | 7 | |
| rpl3 | 46 kDa | ribosomal protein L3 | 1 | 19 | 1 |
| XELAEV_18043190mg | 46 kDa | RNA-binding protein 34 | | 5 | |
| rpl4 | 45 kDa | ribosomal protein L4 | | 1 | |
| XELAEV_18018266mg | 44 kDa | homer protein homolog 2-like | | 9 | |
| map2k1 | 44 kDa | mitogen-activated protein kinase kinase 1 | | 4 | 7 |
| XELAEV_18038116mg | 43 kDa | ZW10 interactor | | | 11 |
| csnk2a2 | 41 kDa | casein kinase 2 alpha 2 | | 8 | 2 |
| rcl1 | 41 kDa | RNA terminal phosphate cyclase like 1 | | 8 | |
| XELAEV_18016577mg | 41 kDa | serine/threonine kinase receptor associated protein L homeolog | | | 8 |
| rfc3 | 40 kDa | replication factor C subunit 3 | 1 | 34 | 1 |

| | | | | | |
|---|---|---|---|---|---|
| atxn3 | 40 kDa | ataxin 3 | | 7 | |
| rfc4 | 40 kDa | replication factor C subunit 4 | | 23 | |
| XELAEV_18012800mg | 40 kDa | replication factor C subunit 2 isoform X1 | | 20 | |
| XELAEV_18011028mg | 39 kDa | ribosome biogenesis protein BRX1 homolog | | 5 | |
| XELAEV_18041436mg | 39 kDa | aminolevulinate dehydratase L homeolog | | 13 | |
| csnk1a1 | 39 kDa | casein kinase 1 alpha 1 | | 7 | |
| XELAEV_18045683mg | 39 kDa | THO complex subunit 6 homolog | | | 5 |
| eif3h | 38 kDa | eukaryotic translation initiation factor 3 subunit H | 1 | | 29 |
| XELAEV_18010694mg | 38 kDa | replication factor C subunit 5 S homeolog | | 25 | |
| cops5 | 38 kDa | COP9 signalosome subunit 5 | | 26 | 2 |
| ppp1cc | 37 kDa | protein phosphatase 1 catalytic subunit gamma | | | 16 |
| thoc3 | 36 kDa | THO complex 3 | | | 5 |
| decr1 | 35 kDa | 2,4-dienoyl-CoA reductase 1 | | 9 | |
| eif3g | 34 kDa | eukaryotic translation initiation factor 3 subunit G | | | 13 |
| thg1l | 34 kDa | tRNA-histidine guanylyltransferase 1 like | | | 18 |
| cpsf4l | 31 kDa | cleavage and polyadenylation specific factor 4 like | | | 15 |
| cpsf4 | 30 kDa | cleavage and polyadenylation specific factor 4 | | | 2 |
| XELAEV_18042638mg | 30 kDa | gem-associated protein 2 | | | 9 |
| XELAEV_18047771mg | 30 kDa | 40S ribosomal protein S2 | | | 8 |

# Acknowledgements

I want to give my biggest thank to my supervisor Professor Dr. Oliver Gruss. Five years ago, with the idea that to get to know the variety knowledge of science, I joined Gruss lab. Now, not only I get to know variety aspects of science in cell line and *Xenopus* egg extract, I also get to know how to perform a project independently. Thank my supervisor who give me enough time and suggestions for my project and personal growth. Prof. Dr Gruss is also very open-minded and gave trust to me. Without these, I couldn't finish my Ph.D. I also want to give my thanks to my lab members (Gerd Landsberg, Linda Förster, Xin Chen, Ling Na Jin et al.). We has a very pleasant time together. Also thanks to people in Wikter lab (Pietro for discussing my MS results, Micheal for sharing T7 cut method to check crispr efficiency and Christine for helping me with flow cytometry machine and the other lab members). Great thanks to my committee members Prof. Dr. Walter Witke, Prof. Dr. Gabriel Schaaf and Prof. Dr. Ulrike Endesfelder. Thank them for spending time reading my thesis and joining my oral defense.

I also want to thank the supports from my family. For these years I studied abroad and didn't spent too much time with my family and only want to connect them when I need their comforts. They never pushed me with everything. I also want to thank some of my friends who give me ideas when I am in dilemma situations and supported me when I wanna quit. Thanks all the people who had helped me before